Direct instantons, topological charge screening, and QCD glueball sum rules

Hilmar Forkel

IFT - Universidade Estadual Paulista, Rua Pamplona, 145, 01405-900 São Paulo, SP, Brazil
Institut für Theoretische Physik, Universität Heidelberg, D-69120 Heidelberg, Germany

Nonperturbative Wilson coefficients of the operator product expansion (OPE) for the spin-0 glueball correlators are derived and analyzed. A systematic treatment of the direct instanton contributions is given, based on a realistic instanton size distribution and renormalization at the operator scale. In the pseudoscalar channel, topological charge screening is identified as an additional source of (semi-) hard nonperturbative physics. The screening contributions are shown to be vital for consistency with the anomalous axial Ward identity, and previously encountered pathologies (positivity violations and the disappearance of the 0^{-+} glueball signal) are traced to their neglect. On the basis of the extended OPE, a comprehensive quantitative analysis of eight Borel-moment sum rules in both spin-0 glueball channels is then performed. The nonperturbative OPE coefficients turn out to be indispensable for consistent sum rules and for their reconciliation with the underlying low-energy theorems. The topological short-distance physics strongly affects the sum rule results and reveals a rather diverse pattern of glueball properties. New predictions for the spin-0 glueball masses and decay constants and an estimate of the scalar glueball width are given, and several implications for glueball structure and experimental glueball searches are discussed.

I. INTRODUCTION

Among exotic hadrons, i.e., those which evade classification according to the constituent quark model, glueballs [1–3] occupy an extreme position. In fact, they contain no valence quarks at all and are the only hadrons which would persist in a world without quarks. Even the exclusion of sea quarks from QCD, as in quenched lattice simulations, is not expected to alter their properties drastically.[1] Hence glueball structure provides a unique source of information on nonperturbative gluon dynamics and may even shed light on the often elusive gluonic component of the light classical hadrons (and potentially hybrids). A suggestive way to access this information is to investigate the role of known coherent gluon fields, with instantons as the most prominent example, in glueball structure.

The operator product expansion (OPE) [4] of glueball correlation functions provides an effective analytical framework for such investigations. In fact, it exhibits several exceptional features of the gluonium channels already at the qualitative level. The probably most instructive one is directly associated with the defining characteristic of the OPE, i.e., its factorization of the short-distance correlators into contributions from hard and soft field modes. Indeed, since the glueball's gluon content should be mostly nonperturbative, one might expect it to manifest itself primarily in the soft contributions, i.e., in the gluon condensates. Surprisingly, this is not the case: the condensate contributions are unusually weak [5–7] and cannot fully reflect the nonperturbative nature of low-lying gluonia. This suggests

that a major part of the nonperturbative physics is relatively hard and thus resides in the Wilson coefficients. The present paper contains a detailed analysis of such contributions and a comprehensive study of their impact on spin-0 glueball properties.

Indications for the onset of nonperturbative physics in the scalar glueball correlator at unusually short distances, and the ensuing departure from asymptotic freedom, date back to the pioneering days of the QCD sum rule approach [8]. The prototypical candidates for such hard, nonperturbative physics, direct instantons, describe tunneling processes which rearrange the QCD vacuum topology [9] in localized space-time regions small enough to affect the x dependence of the correlators over distances $|x| \ll \Lambda_{QCD}^{-1}$. Although this physics enters the Wilson coefficients, it was until recently ignored in glueball (and other) sum rules, with the exception of an early exploratory estimate in Ref. [10].

The development of instanton "liquid" models [9] allowed several bulk properties of the instanton size distribution in the vacuum to be estimated, and the emerging scales were later supported by lattice simulations [11,12]. On the basis of these scales, the mentioned exploration of instanton contributions to a 0^{++} glueball sum rule [10] found them to be of considerable size and indicated their potential for improving the consistency with the underlying low-energy theorem. However, the involved approximations and especially the neglect of the crucial instanton-induced continuum contributions did not allow for reliable estimates of glueball properties.

Only recently, the exact direct instanton contributions to the spin-0 glueball OPE (to leading order in $\hbar$) were obtained and the instanton-induced continuum contribu-

---

[1]From the perspective of hadronic gluon dynamics, mesons built out of heavy quarks are an opposite extreme in which gluons mainly produce weak Abelian-type Coulomb binding.

tions derived [13]. On the basis of the resulting "instanton-improved OPE" (IOPE) the first quantitative QCD sum rule analysis of direct instanton effects in scalar glueballs became possible. This analysis resolved long-standing consistency problems of the 0^{++} sum rules with purely perturbative Wilson coefficients and led to new predictions for the scalar glueball mass and "decay constant" f_S [13]. In particular, the direct instanton contributions were found to increase the value of f_S about threefold and supported earlier indications for an exceptionally small scalar glueball size [14,15]. They also suggested a prominent role of instantons in the binding of the 0^{++} glueball and generated scaling relations between its main properties and bulk features of the instanton size distribution [13]. A subsequent analysis of the related Gaussian sum rules [16], based on the same instanton contributions, confirmed some of these results and studied more detailed parametrizations of the phenomenological correlator representation.

Previous implementations of direct instanton contributions to hadron correlators, including those in the 0^{++} glueball channel, relied on several standard approximations. However, there are reasons to suspect that these approximations may cause artifacts in the sum rule results. We therefore provide a more thorough and systematic treatment of the direct instanton sector below. Our subsequent comprehensive sum rule analysis will indeed reveal a significant impact of these improvements on the predicted glueball properties. In addition, we will extend the study of nonperturbative Wilson coefficients to other glueball channels. While nonperturbative short-distance contributions are small in the tensor channel (mainly due to the absence of leading instantons corrections), they turn out to generate a rather complex pattern of new physics in the pseudoscalar channel. The analysis of this physics and the ensuing predictions for 0^{-+} glueball properties are further central objectives of our investigation and will provide additional insights into the role of (semi-) hard nonperturbative physics in glueball structure.

The paper is structured as follows: In Sec. II we discuss pertinent general features of the glueball correlators and qualitative aspects of the instanton contributions. We also set up the Borel sum rule framework. In the following Sec. III, we start our discussion of the IOPE by summarizing the known perturbative contributions to the Wilson coefficients. The next section, IV, contains a detailed derivation and analysis of the direct instanton contributions to both spin-0 glueball channels. Here we also implement for the first time realistic instanton size distributions, and we explicitly renormalize the ensuing Wilson coefficients at the operator scale. The exceptional strength of the direct instanton contributions to the spin-0 glueball correlators provides an ideal testing ground for these improvements, which we expect to be useful in other hadron channels as well. (Previous work on direct instanton contributions in

the classical meson and baryon channels, and, in particular, the program starting with Ref. [17], treated all instantons as being of the same size.)

In Sec. V we identify and implement new contributions to the IOPE coefficients in the 0^{-+} glueball correlator. As the instantons, these contributions are of nonperturbative origin and associated with the topology of the gluon fields. They arise from the screening of topological charge in the QCD vacuum and can be derived almost model independently by requiring consistency with the axial anomaly [18]. We present compelling evidence for the screening contributions to be an indispensable complement to the direct instanton contributions.

In Sec. VI, we embark on a comprehensive quantitative analysis of the developed IOPE, including perturbative, direct instanton, and screening contributions. We start by discussing several characteristic features of its Borel moments and their relevance for predicting glueball properties. Subsequently, we study the origin and role of the various subtraction constants (which appear in the lowest-moment sum rules) as well as their impact on the sum rule analysis. We then match the IOPE Borel moments to their phenomenological counterparts, which include both perturbative and instanton contributions to the duality continuum and either one or two isolated, narrow resonances. The eight ensuing Borel sum rules are analyzed numerically, the predictions for 0^{++} and 0^{-+} glueball properties are obtained and their significance for glueball structure and experimental glueball searches is discussed. Finally, in Sec. VII, we summarize our main results and conclusions.

II. GLUEBALL CORRELATION FUNCTIONS

The QCD correlations functions in the main glueball channels are

$$\Pi_G(x) = \langle 0|TO_G(x)O_G(0)|0\rangle, \tag{1}$$

where the local, composite operators O_G with $G \in \{S, P, T\}$ are the standard gluonic interpolating fields, i.e., those with the lowest mass dimension which carry the quantum numbers of the scalar (0^{++}), pseudoscalar (0^{-+}), and tensor (2^{++}) glueballs:

$$O_S(x) = \alpha_s G^a_{\mu\nu}(x)G^{a\mu\nu}(x), \tag{2}$$

$$O_P(x) = \alpha_s G^a_{\mu\nu}(x)\tilde{G}^{a\mu\nu}(x), \tag{3}$$

$$O_T(x) = \Theta^a_{\mu\nu}(x). \tag{4}$$

Here $\Theta^a_{\mu\nu}$ is the energy-momentum stress tensor of QCD and $\tilde{G}$ is the dual of the (Minkowski) gluon field strength,

$$\tilde{G}_{\mu\nu} \equiv \frac{i}{2}\varepsilon_{\mu\nu\rho\sigma}G^{\rho\sigma}. \tag{5}$$

Note that O_S (O_P) is proportional to the Yang-Mills action density (topological charge density[2]) of the gluon fields. The interpolators create vacuum disturbances with the appropriate quantum numbers whose propagation properties we will study below in the framework of a short-distance expansion. The factors of α_s ensure renormalization group (RG) invariance [at least to leading order[3] in $\alpha_s = g_s^2/(4\pi)$]. The corresponding Fourier transforms will be written as

$$\Pi_G(Q^2) = i \int d^4x e^{iqx} \langle 0|TO_G(x)O_G(0)|0\rangle, \qquad (6)$$

with $Q^2 \equiv -q^2$. The above expressions (and the following ones, if not stated otherwise) refer to Minkowski space-time.

A. Low-energy theorems

The zero-momentum limits of both spin-0 glueball correlators are governed by low-energy theorems (LETs) which provide additional first-principle information and useful consistency checks for IOPE and sum rule analysis. In the scalar channel, the LET belongs to a class which was derived by Shifman, Vainshtein, and Zakharov on the basis of renormalization group and scaling arguments [19]. These "dilatation" theorems apply to the zero-momentum limit of the correlators

$$\Pi_{\mathcal{O}}(-q^2) = i \int d^4x e^{iqx} \langle TO_S(x)\mathcal{O}(0)\rangle_{\text{npert}}, \qquad (7)$$

where $\mathcal{O}$ is an arbitrary local color-singlet operator. The subscript refers to UV regularization by subtraction of the high-frequency (perturbative) contributions, i.e.,

$$\Pi_{\mathcal{O}}(0) = \frac{1}{\pi} \int_0^\infty \frac{ds}{s} [\text{Im}\Pi_{\mathcal{O}}(s) - \text{Im}\Pi_{\mathcal{O}}^{\text{high-freq}}(s)]. \quad (8)$$

The associated low-energy theorems read

$$\Pi_{\mathcal{O}}(0) = \frac{8\pi d_{\mathcal{O}}}{b_0} \langle \mathcal{O} \rangle, \qquad (9)$$

where $d_{\mathcal{O}}$ is the canonical dimension of $\mathcal{O}$ and $b_0 = 11N_c/3 - 2N_f/3$ is the lowest-order coefficient in the perturbative expansion of the QCD β function.

This general class includes as a special case with $\mathcal{O} = O_S$ the LET which governs the low-energy behavior of the scalar glueball correlator:

$$\Pi_S(Q^2 = 0) = \frac{32\pi}{b_0} \langle \alpha_s G^2 \rangle. \qquad (10)$$

The appearance of the gluon condensate and the sizeable factor in front render the numerical value of $\Pi_S(0)$ both large and rather uncertain. The present range of values for the gluon condensate is about $\langle \alpha_s G^2 \rangle \sim$ 0.25–0.75 GeV^4. With the value $\langle \alpha_s G^2 \rangle \equiv (0.07 \pm 0.01)$ GeV^4 used in [7], for example, one obtains an upper limit $\Pi_S(0) \simeq 11.17 \langle \alpha_s G^2 \rangle = 0.78$ GeV^4 while $\Pi_S(0) \simeq 0.4 - 0.6$ GeV^4 is probably more realistic. In the whole range of acceptable values, however, the low-energy theorem provides by far the largest soft contribution to the $k = -1$ scalar glueball sum rule (see below).

The zero-momentum limit of the pseudoscalar glueball correlator is likewise governed by a low-energy theorem, although of a rather different nature.[4] It is usually stated for the zero-momentum limit of the correlator of the topological charge density

$$Q(x) = \frac{\alpha_s}{8\pi} G_{\mu\nu}^a \tilde{G}^{a,\mu\nu} = \frac{1}{8\pi} O_P(x), \qquad (11)$$

i.e., for the topological susceptibility

$$\chi_t = i \int d^4x \langle 0|TQ(x)Q(0)|0\rangle = \frac{1}{(8\pi)^2} \Pi_P(Q^2 = 0). \qquad (12)$$

In QCD with three light flavors and $m_{u,d} \ll m_s$, the low-energy theorem then reads [21]

$$\chi_t = \frac{m_u m_d}{m_u + m_d} \langle \bar{q}q \rangle. \qquad (13)$$

This expression is based on the chiral Ward identities for the (anomalous) flavor-singlet and -octet axial currents and generalizes the classic large-N_c result of Di Vecchia and Veneziano [18]. As a consequence, we have

$$\Pi_P(Q^2 = 0) = (8\pi)^2 \frac{m_u m_d}{m_u + m_d} \langle \bar{q}q \rangle, \qquad (14)$$

which reduces to $\Pi_P(0) = 0$ in the chiral limit. In Sec. VI (and VI C in particular) we will analyze the consistency of IOPE and glueball sum rule results with the LETs (10) and (14).

B. Qualitative aspects of instanton contributions

Two properties of the spin-0 glueball correlators indicate on general grounds that they will receive relatively large direct instanton contributions: (i) the underlying spin-0 interpolators (2) and (3) couple exceptionally strongly to

---

[2]In mathematical terms, this is the Pontryagin density or second Chern class associated with the principle fibre bundle in which the gauge fields (i.e., connections) live.

[3]RG invariance of O_S to all orders in α_s can be achieved with the help of the QCD β function by defining $O_S(x) = -4\pi^2\beta(\alpha_s)/(\alpha_s b_0)G_{\mu\nu}^a(x)G^{a\mu\nu}(x)$ (with $b_0 = 11N_c/3 - 2N_f/3$ and for massless quarks), from which our interpolator is recovered to leading order in the perturbative expansion of $\beta(\alpha_s) = -b_0\alpha_s^2/(2\pi)^2 + O(\alpha_s^3)$.

[4]In Ref. [20] a somewhat heuristic attempt was made to generalize the above type of low-energy theorem to the pseudoscalar sector in pure Yang-Mills theory. Since we are working within full QCD, whose three light quark flavors alter the behavior of the 0^{-+} correlator drastically, we have no use for these results here.

instantons [8], and (ii) the leading-order (in $\hbar$) instanton contributions are enhanced by inverse powers of the strong coupling [cf. Eq. (65)].

In addition, the instanton contributions show a strong dependence on spin and parity of the glueball correlator. This is reminiscent of the situation encountered in light meson and baryon correlators, where the remarkable topological, chiral, flavor, and spin-color structure of the quark zero modes [22] in the instanton background generates a characteristic channel dependence pattern [23,24] (which is difficult to reproduce even in more sophisticated quark models [25]). Although the zero modes and quarks in general play a much smaller role in the glueball correlators, an equally (if not more) distinctive channel dependence exists among them, too. It is rooted in the (anti-) self-duality of the (anti-) instanton's field strength,

$$G^{(I,\bar{I})}_{\mu\nu} = \pm \tilde{G}^{(I,\bar{I})}_{\mu\nu}, \tag{15}$$

(in Euclidean space-time) and therefore of purely gluonic nature. (Anti-) self-dual gluon fields have color-electric and -magnetic fields of equal size, $E^a_i = \pm B^a_i$. As a consequence of the Bianchi identity, they form a subset of all solutions of the Euclidean Yang-Mills equation.

The impact of self-duality on the glueball correlators is twofold, as can be read off directly from the interpolating fields (2)–(4). First, during continuation to Minkowski space the Euclidean self-duality Eq. (15) picks up a factor of i, so that

$$O^{(I,\bar{I})}_P(x) = \pm i O^{(I,\bar{I})}_S(x). \tag{16}$$

Therefore, direct instanton (or, more generally, self-dual) contributions to the pseudoscalar glueball correlator are equal in size and opposite in sign to those of the scalar correlator. This property provides a strong link between the IOPEs of both channels, with far-reaching consequences for our analysis. Moreover, self-duality implies that instanton-induced power corrections (condensates) to the IOPE of both 0^{++} and 0^{-+} correlators are restricted to a few terms and cancel in their sum [5]. Double-counting of soft instanton physics in both Wilson coefficients and condensates of the IOPE is therefore excluded (with a few potential exceptions to be discussed below). Furthermore, since direct-instanton-induced interactions turn out to be attractive in the scalar glueball channel, they must be repulsive in the pseudoscalar channel.

Another obvious property of self-dual fields is that their energy, proportional to $E^2 + B^2$, is zero (as expected for vacuum fields). Hence their energy-momentum tensor vanishes, i.e.,

$$O^{(I,\bar{I})}_T(x) = 0. \tag{17}$$

This implies the absence of leading direct instanton contributions to the tensor glueball correlator. As a consequence, we have nothing to add to the standard sum rule analyses (with solely perturbative Wilson coefficients) in

the 2^{++} channel [7,8,26], except for a comment: the soft (i.e., condensate) contributions to the tensor correlator are conspicuously small, higher-dimensional power corrections vanish [27], and instanton-induced power corrections are absent [6]. Nonperturbative contributions to the IOPE of this correlator should therefore primarily reside in the Wilson coefficients of higher-dimensional operators (starting with the gluon condensate). However, direct instanton (and other hard, nonperturbative) contributions, although not forbidden by self-duality, are suppressed by minimally four factors of $\Lambda_{\text{QCD}}/Q \sim 0.2$ where $Q \sim 1$ GeV is the typical momentum scale in sum rule analyses. Nonperturbative contributions to the IOPE coefficients are therefore expected to be small, too, perhaps related to the relatively weak binding in the tensor channel observed on the lattice [28]. In fact, the hierarchy of interactions induced by self-dual gluon fields (i.e., attractive, absent, and repulsive in the 0^{++}, 2^{++}, and 0^{-+} channels, respectively) agrees with the level ordering among the lowest-lying glueball states in the quenched lattice spectrum [15,28].

C. Spectral representation, Borel moments and sum rules

In order to make contact with the glueball information in the IOPE, we match it to the spectral representation of the correlators, i.e., we construct sum rules. The spectral representation in the hadronic basis is conveniently written in the form of a dispersion relation,

$$\Pi_G(Q^2) = \frac{1}{\pi} \int_0^\infty ds \frac{\text{Im}\Pi_G(-s)}{s + Q^2}, \tag{18}$$

where $\text{Im}\Pi_G(-s)$ is the imaginary part of the correlator at timelike momenta and where the necessary number of subtractions is implied but not written explicitly. Among the lowest-lying on-shell intermediate states which contribute to the spectral function $\rho_G(s) \equiv \text{Im}\Pi_G(-s)/\pi$ are the lightest glueball in the G channel (probably with admixtures of light quarkonium) and possibly light mesons with the same quantum numbers and sufficiently strong couplings to the gluonic interpolators. Beyond the isolated resonances, the multihadron continuum will set in at a threshold s_t. We therefore write the phenomenological representation of the spectral function as

$$\text{Im}\Pi^{(\text{ph})}_G(-s) = \text{Im}\Pi^{(\text{res})}_G(-s) + \text{Im}\Pi^{(\text{cont})}_G(-s). \tag{19}$$

A simple and efficient description of most hadronic spectral functions, which is particularly suited for QCD sum rule applications (and beyond, e.g., for the parametrization and interpretation of lattice data [29,30]) can be achieved with one or two narrow resonances and a duality continuum [31]. For the IOPE sum rules in the spin-0 glueball channels, we will limit ourselves to maximally two isolated resonances which we describe in zero-width approximation, i.e., as poles

$$\mathrm{Im}\Pi_G^{(\mathrm{res})}(-s) = \pi f_{G1}^2 m_{G1}^4 \delta(s - m_{G1}^2)$$
$$+ \pi f_{G2}^2 m_{G2}^4 \delta(s - m_{G2}^2), \quad (20)$$

with $\langle 0|O_G(0)|Gi(k)\rangle = f_{Gi}m_{Gi}^2$. Invoking local parton-hadron duality, the hadronic continuum is replaced by its quark-gluon counterpart. [A different description of the resonance region, in terms of Goldstone-boson pairs, can be found in Ref. [32]. The resonance region is then roughly estimated by integrating the Goldstone-boson continuum (with the perturbative continuum-subtracted) up to the bound imposed by the low-energy theorem (10).] The duality continuum is obtained from the discontinuities of the IOPE by analytical continuation to timelike momenta, i.e.,

$$\mathrm{Im}\Pi_G^{(\mathrm{cont})}(-s) = \theta(s - s_0)\mathrm{Im}\Pi_G^{(\mathrm{IOPE})}(-s). \quad (21)$$

The step function ensures that the continuum is restricted to the invariant-mass region where it is dual to higher-lying resonance and multihadron contributions. This duality region starts at the effective threshold s_0.

For accurate QCD sum rules it is generally insufficient to match phenomenological and IOPE representations of the correlators directly in momentum space. However, substantial improvement can be achieved by a Borel transform [31]

$$[\hat{B}\Pi(Q^2)](\tau) = \lim_{n,Q^2\to\infty} \frac{(Q^2)^{n+1}}{n!}\left(\frac{-d}{dQ^2}\right)^n \Pi(Q^2),$$
$$\frac{Q^2}{n} \equiv \tau^{-1} \quad (22)$$

(in the convention of Ref. [33]) on both sides of the sum rules. The Borel transform improves the "convergence" of the IOPE, eliminates subtraction terms and, most importantly, implements an exponential continuum suppression which puts more emphasis on the glueball states. For the quantitative analysis of the spin-0 glueball channels one usually considers a family of sum rules, based on the Borel moments

$$\mathcal{L}_{G,k}(\tau) = \hat{B}[(-Q^2)^k\Pi_G(Q^2)](\tau), \qquad k \in \{-1, 0, 1, 2\}. \quad (23)$$

The selection of these four moments, which differ in their weighting of the intermediate-state spectrum, has practical reasons: higher powers $k > 2$ reduce the sum rule reliability (e.g., by shrinking the fiducial regions, see Sec. IV D) without yielding much further information, while $k < -1$ would introduce additional subtraction constants which are not determined by the low-energy theorems. (The new subtraction term in the $k = -2$ sum rule of the 0^{-+} glueball channel is proportional to the derivative of the topological charge correlator at $Q^2 = 0$ and, as argued in Ref. [34], may play a role in determining the proton's spin content (cf. Sec. VI E). The Borel moments satisfy the

recurrence relation

$$\mathcal{L}_{G,k+1}(\tau) = -\frac{\partial}{\partial\tau}\mathcal{L}_{G,k}(\tau). \quad (24)$$

By applying the operator in Eq. (23) to the dispersion relation (18) with the spectral function (19), we obtain the phenomenological representation of the Borel moments as

$$\mathcal{L}_{G,k}^{(\mathrm{ph})}(\tau; m_{Gi}, f_{Gi}, s_0) = f_{G1}^2 m_{G1}^{4+2k}e^{-m_{G1}^2\tau}$$
$$+ f_{G2}^2 m_{G2}^{4+2k}e^{-m_{G2}^2\tau} - \delta_{k,-1}\Pi_G^{(\mathrm{ph})}(0)$$
$$+ \frac{1}{\pi}\int_{s_0}^\infty ds s^k\mathrm{Im}\Pi_G^{(\mathrm{IOPE})}(-s)e^{-s\tau}. \quad (25)$$

In order to determine the hadronic parameters m_{Gi}, f_{Gi} and s_0, one matches these moments to their IOPE counterparts $\mathcal{L}_{G,k}^{(\mathrm{IOPE})}$ (to be calculated below) in the fiducial τ region where both sides are expected to be reliable. This leads to the sum rules

$$\mathcal{L}_{G,k}^{(\mathrm{IOPE})}(\tau) = \mathcal{L}_{G,k}^{(\mathrm{ph})}(\tau; m_{Gi}, f_{Gi}, s_0). \quad (26)$$

After the standard renormalization group improvement, these sum rules are conveniently rewritten in terms of the continuum-subtracted Borel moments of the IOPE,

$$\mathcal{R}_{G,k}(\tau; s_0) \equiv -\delta_{k,-1}\Pi_G^{(\mathrm{IOPE})}(0)$$
$$+ \frac{1}{\pi}\int_0^{s_0} ds s^k\mathrm{Im}\Pi_G^{(\mathrm{IOPE})}(-s)e^{-s\tau}. \quad (27)$$

The subtraction constants $\Pi_G^{(\mathrm{IOPE})}(0)$ are generated by the nonperturbative contributions to the Wilson coefficients (see below). In terms of the $\mathcal{R}_{G,k}$, the glueball sum rules attain their final form

$$\mathcal{R}_{G,k}(\tau; s_0) = -\delta_{k,-1}\Pi_G^{(\mathrm{ph})}(0) + f_{G1}^2 m_{G1}^{4+2k}e^{-m_{G1}^2\tau}$$
$$+ f_{G2}^2 m_{G2}^{4+2k}e^{-m_{G2}^2\tau}, \quad (28)$$

which isolates the glueball contributions, the subtraction term for $k = -1$, and possibly an additional resonance on the right-hand side.

The values of the subtraction constants $\Pi_G^{(\mathrm{ph})}(0)$ are determined by the low-energy theorems (10) and (14). (The perturbative UV contributions to the IOPE are, as in Eq. (8), removed by renormalization of the perturbative Wilson coefficients, cf. Sec. III A.) The large constant $\Pi_S^{(\mathrm{ph})}(0)$ is known to dominate the scalar $k = -1$ sum rule with purely perturbative Wilson coefficients [6]. This leads to a much slower decay with τ than in the $k \geq 0$ sum rules and thus to a much smaller glueball mass prediction (well below 1 GeV). The direct instanton contributions [13] overcome this mutual inconsistency which had plagued the 0^{++} glueball sum rules since their inception.

We will further elaborate on the role of the subtraction constants in Sec. VI C.

III. IOPE 1: PERTURBATIVE WILSON COEFFICIENTS

Our main tool for the QCD-based calculation of the spin-0 glueball correlators at short distances is the instanton-improved operator product expansion. The general expression for the IOPE at large, spacelike momenta $Q^2 \equiv -q^2 \gg \Lambda_{\text{QCD}}$,

$$\Pi_G(Q^2) = \sum_{d=0,4,\dots} \tilde{C}_d^{(G)}(Q^2;\mu)\langle \hat{O}_d \rangle_\mu, \qquad (29)$$

exhibits the characteristic factorization of contributions from hard and soft field modes at the operator renormalization scale μ: hard modes with momenta $|k| > \mu$ contribute to the momentum-dependent Wilson coefficients $\tilde{C}_d(Q^2;\mu)$ while soft modes with $|k| \leq \mu$ contribute to the vacuum expectation values ("condensates") of the operators $\hat{O}_d$ of dimension d which are renormalized at μ.

The perturbative contributions to the Wilson coefficients constitute the conventional OPE and will be discussed in the present section. In addition, the Wilson coefficients receive crucial nonperturbative contributions from direct instantons, i.e., those with sizes $\rho \lesssim \mu^{-1}$.[5] Their evaluation is the subject of Sec. IV. Additional hard and nonperturbative contributions to the IOPE of the 0^{-+} correlator, due to topological charge screening, are identified and evaluated in Sec. V.

A. Perturbative OPE coefficients

In this section we summarize what is known about the perturbative contributions to the Wilson coefficients $\tilde{C}_d^{(S,P)}(Q^2)$ of the scalar and pseudoscalar glueball correlators. At present, perturbative contributions are available up to maximally three loops, and for operators up to dimension $d = 8$. The accordingly truncated OPE has the form

$$\Pi_G^{(\text{pc})}(Q^2) \simeq \tilde{C}_0^{(G)} + \tilde{C}_4^{(G)}\langle \hat{O}_4 \rangle + \tilde{C}_6^{(G)}\langle \hat{O}_6 \rangle + \tilde{C}_8^{(G)}\langle \hat{O}_8 \rangle, \qquad (30)$$

where $G = S, P$ denotes the $(0^{++}, 0^{-+})$ glueball channel.

Up to $O(\alpha_s^2)$ (i.e., up to three loops—the two powers of α_s from the interpolating fields are not counted here), the

---

[5]In studies of the OPE at large orders d, instantons of a different type were employed as a tool for assessing the impact of near-origin singularities on the asymptotic OPE behavior [35]. (In the context of an operational, OPE-based definition of quark-hadron duality such effects are referred to as "local-duality violations.")

coefficient of the unit operator has the generic Q^2 dependence

$$\tilde{C}_0^{(G)} = Q^4 \ln\left(\frac{Q^2}{\mu^2}\right)\left[A_0^{(G)} + A_1^{(G)} \ln\left(\frac{Q^2}{\mu^2}\right) + A_2^{(G)}\ln^2\left(\frac{Q^2}{\mu^2}\right)\right], \qquad (31)$$

were we have omitted irrelevant subtraction polynomials in Q^2. Since the next-to-next-to-leading order [N²LO, i.e., $O(\alpha_s^2)$] corrections are known only for the unit-operator coefficients $\tilde{C}_0^{(G)}$, strict compliance with the perturbative expansion would require their exclusion. Nevertheless, due to their exceptional size, the power suppression of their higher-dimensional counterparts $\tilde{C}_{d\geq 4}^{(G)}$, and their special role in the duality continuum, they are usually taken into account.

The radiative corrections to the gluon condensate coefficient $\tilde{C}_4$ are known up to $O(\alpha_s)$. The NLO corrections are of particular importance in $\tilde{C}_4$ since the leading $O(\alpha_s^0)$ term is momentum independent and therefore contributes only to the lowest ($k = -1$) Borel-moment sum rule. The overall Q^2 dependence of $\tilde{C}_4$ is

$$\tilde{C}_4^{(G)}\langle \hat{O}_4 \rangle = B_0^{(G)} + B_1^{(G)} \ln\left(\frac{Q^2}{\mu^2}\right). \qquad (32)$$

The 3-gluon condensate term has the generic form

$$\tilde{C}_6^{(G)}\langle \hat{O}_6 \rangle = \frac{1}{Q^2}\left[C_0^{(G)} + C_1^{(G)} \ln\left(\frac{Q^2}{\mu^2}\right)\right], \qquad (33)$$

while the 4-gluon condensates produce a term of the form

$$\tilde{C}_8^{(G)}\langle \hat{O}_8 \rangle = D_0^{(G)} \frac{1}{Q^4}. \qquad (34)$$

Collecting all four contributions, we arrive at the general expression for the Q^2 dependence of the OPE with perturbative Wilson coefficients in both spin-0 glueball correlators,

$$\Pi_G^{(\text{pc})}(Q^2) \simeq \left[A_0^{(G)} + A_1^{(G)} \ln\left(\frac{Q^2}{\mu^2}\right) \right.$$
$$\left. + A_2^{(G)}\ln^2\left(\frac{Q^2}{\mu^2}\right)\right]Q^4 \ln\left(\frac{Q^2}{\mu^2}\right) + B_0^{(G)}$$
$$+ B_1^{(G)} \ln\left(\frac{Q^2}{\mu^2}\right) + \left[C_0^{(G)} + C_1^{(G)} \ln\left(\frac{Q^2}{\mu^2}\right)\right]\frac{1}{Q^2}$$
$$+ D_0^{(G)} \frac{1}{Q^4}. \qquad (35)$$

During renormalization group improvement in Sec. III B the coefficients $A_i - D_i$ will acquire a logarithmic Q^2 dependence due to the presence of the running coupling α_s (and of the anomalous dimension γ_{3g} in the case of the C_i).

In view of potentially large quarkonium admixtures to physical glueball states we emphasize that the perturbative

Wilson coefficients receive explicit quark loop contributions, both from radiative corrections and through the perturbative β function during RG improvement. Especially in the scalar channel[6] the perturbative N_f dependence (N_f is the number of light-quark flavors with $m_q \lesssim \Lambda_{QCD}$) can be significant [see also Eq. (10)]. The soft quark contributions to the condensates and their N_f dependence are very likely larger but more difficult to estimate.

1. 0^{++} channel

At present, the most accurate perturbative coefficients of the unit operator, renormalized in the $\overline{MS}$ scheme and with threshold effects included, can be found in Refs. [16,38]. For three light-quark flavors (i.e., $N_c = N_f = 3$) they read

$$A_0^{(S)} = -2\left(\frac{\alpha_s}{\pi}\right)^2\left[1 + \frac{659}{36}\frac{\alpha_s}{\pi} + 247.480\left(\frac{\alpha_s}{\pi}\right)^2\right], \quad (36)$$

$$A_1^{(S)} = 2\left(\frac{\alpha_s}{\pi}\right)^3\left[\frac{b_0}{4} + 65.781\frac{\alpha_s}{\pi}\right], \quad (37)$$
$$A_2^{(S)} = -10.1250\left(\frac{\alpha_s}{\pi}\right)^4.$$

In addition to the rather recently calculated $O(\alpha_s^2)$ contributions, these expressions contain several corrections to the $O(\alpha_s)$ contributions which were implemented in older sum rules analyses. In Ref. [39], the quark loop contributions were omitted (corresponding to $N_f = 0$) and $A_0^{(S)}$ contained a small error [40] which was later corrected [41] and implemented into $A_0^{(S)}$ [7]. The $O(\alpha_s)$ contribution to $A_0^{(S)}$ was corrected once more in Ref. [38]. As a consequence, the numerical coefficient given above is about 25% larger than the one used in Ref. [7].

The coefficients B_i of the lowest-dimensional nontrivial operator, i.e., the gluon condensate, receive important radiative corrections which were calculated in Ref. [39] for $N_f = 0$. Including the quark loop contributions for $N_f = 3$ [16], they become

$$B_0^{(S)} = 4\alpha_s\left[1 + \frac{175}{36}\frac{\alpha_s}{\pi}\right]\langle\alpha_s G^2\rangle, \quad (38)$$
$$B_1^{(S)} = -\frac{\alpha_s^2 b_0}{\pi}\langle\alpha_s G^2\rangle$$

($\langle\alpha_s G^2\rangle \equiv \langle\alpha_s G_{\mu\nu}^a G^{a\mu\nu}\rangle$). As a consequence, the $O(\alpha_s)$ contribution to B_0 is about 20% larger than the one used in Ref. [7]. Note that the $O(1)$ coefficient is Q^2 independent.

_____

[6] In Ref. [36] it has been argued that the results of the standard-OPE sum rules (without direct instanton contributions) for the pseudoscalar glueball for $N_f = 0$ is close to that of full QCD ($N_f = 3$) because the leading perturbative Wilson coefficient has a weak N_f dependence (weaker than in the scalar channel) and since mixing with quarkonium seems to be smaller in the 0^{-+} than in the 0^{++} sector [37].

Hence, the leading power correction will enter all but the lowest Borel-moment (i.e., $\mathcal{R}_{S,-1}$) sum rules solely via radiative corrections.

The 3-gluon condensate term, again including $O(\alpha_s)$ radiative corrections, was first calculated for $N_f = 0$ [39] and adapted to $N_f = 3$ in Ref. [16], with the result

$$C_0^{(S)} = 8\alpha_s^2\langle gG^3\rangle, \qquad C_1^{(S)} = 0 \quad (39)$$

($\langle gG^3\rangle \equiv \langle gf_{abc}G_{\mu\nu}^a G_\rho^{b\nu}G^{c\rho\mu}\rangle$). Both Refs. [7,39] use the $N_f = 0$ value $C_1^{(S)} = -58\alpha_s^3\langle gG^3\rangle$ [39] instead. (Ref. [7] otherwise sets $N_f = 3$.) Up to $O(\alpha_s)$, there is no explicit N_f dependence in $C_0^{(S)}$.

The contributions from the highest-dimensional ($d = 8$) operators appear in the combination

$$\langle\alpha_s^2 G^4\rangle_S := 14\langle(\alpha_s f_{abc}G_{\mu\rho}^b G_\nu^{\rho c})^2\rangle - \langle(\alpha_s f_{abc}G_{\mu\nu}^b G_{\rho\lambda}^c)^2\rangle, \quad (40)$$

of 4-gluon condensates and were calculated to leading order in the pioneering paper [5]:

$$D_0^{(S)} = 8\pi\alpha_s\langle\alpha_s^2 G^4\rangle_S. \quad (41)$$

Estimates of the numerical value of $\langle\alpha_s^2 G^4\rangle$ are customarily based on the vacuum factorization approximation [5],

$$\langle\alpha_s^2 G^4\rangle_S \simeq \frac{9}{16}\langle\alpha_s G^2\rangle^2. \quad (42)$$

The uncertainty in this estimate does barely affect the quantitative sum rule analysis since the impact of the coefficient (41) is almost negligible.

2. 0^{-+} channel

The lowest-order perturbative contributions to the unit-operator coefficient of the 0^{-+} correlator were first obtained in Ref. [5]. Subsequently, the calculation was extended to $O(\alpha_s)$ [36] and augmented by the 3-loop corrections [38] in Ref. [42] (where also an error in the $O(\alpha_s)$ contribution was corrected). The result is

$$A_0^{(P)} = -2\left(\frac{\alpha_s}{\pi}\right)^2\left[1 + 20.75\frac{\alpha_s}{\pi} + 305.95\left(\frac{\alpha_s}{\pi}\right)^2\right], \quad (43)$$

$$A_1^{(P)} = 2\left(\frac{\alpha_s}{\pi}\right)^3\left[\frac{9}{4} + 72.531\frac{\alpha_s}{\pi}\right], \quad (44)$$
$$A_2^{(P)} = -10.1250\left(\frac{\alpha_s}{\pi}\right)^4.$$

[Ref. [36] contains a misprint of the sign of the $\ln^2$ term in its Eq. (2).] The leading order contributions to $A_{0,1}$ agree, as expected, with those of the scalar glueball correlator. The NLO corrections of Ref. [38] affect A_0 only weakly but increase A_1 by almost a factor of 4. The N²LO contribution increases A_0 by about a factor of 2. Finally, $A_2 \sim 10^{-3}$ for $\alpha/\pi \sim 0.1$ and thus is practically negligible compared to A_0 and A_1.

The gluon condensate contribution was calculated to lowest-order in Ref. [5] and up to $O(\alpha_s)$ in Ref. [36], with the result

$$B_0^{(P)} = 4\pi \frac{\alpha}{\pi} \langle \alpha_s G^2 \rangle, \qquad B_1^{(P)} = 9\pi \left(\frac{\alpha_s}{\pi} \right)^2 \langle \alpha_s G^2 \rangle. \quad (45)$$

(The sign of the LO contribution to B_0 is corrected and the NLO contribution is not determined by the renormalization group [36].)

The $\langle gG^3 \rangle$ term was calculated to lowest-order in Ref. [5]. The 2-loop contribution was first obtained for $N_f = 0$ [36] and later for $N_f = 3$ [42], with the result

$$C_0^{(P)} = -8\pi^2 \left(\frac{\alpha_s}{\pi} \right)^2 \langle gG^3 \rangle, \qquad C_1^{(P)} = 0. \quad (46)$$

(For $N_f = 0$ one has $C_1^{(P)} = 58\pi^2 (\alpha_s/\pi)^3 \langle gG^3 \rangle$ instead [36].)

For the $d = 8$ contributions, which is associated with the combination

$$\langle g^4 G^4 \rangle_P = 2g_s^4 f^{abc} f^{ade} \langle G_{\mu\nu}^b G_{\alpha\beta}^c G^{d,\mu\nu} G^{e,\alpha\beta} + 10 G_{\mu\alpha}^b G^{c,\alpha\nu} G^{d,\mu\beta} G_{\beta\nu}^e \rangle, \quad (47)$$

of 4-gluon condensates, one finds [5]

$$D_0^{(P)} = \frac{1}{4} \frac{\alpha_s}{\pi} \langle g_s^4 G^4 \rangle_P, \quad (48)$$

which is [explicitly and to the given $O(\alpha_s)$] N_f independent. (Ref. [42] contains a typographical error in the definition of $\langle g_s^4 G^4 \rangle_P$.) As in the scalar case, the condensate $\langle g_s^4 G^4 \rangle_P$ is conventionally factorized [5] according to

$$\langle (f^{abc} G_{\mu\nu}^b G_{\alpha\beta}^c)^2 \rangle \simeq \frac{5}{16} \langle G_{\mu\nu}^a G^{a,\mu\nu} \rangle^2, \quad (49)$$

$$\langle (f^{abc} G_{\mu\alpha}^b G^{c,\alpha\nu})^2 \rangle \simeq \frac{1}{16} \langle G_{\mu\nu}^a G^{a,\mu\nu} \rangle^2, \quad (50)$$

so that

$$\langle g^4 G^4 \rangle_P = 30\pi^2 \langle \alpha_s G^2 \rangle^2, \quad (51)$$

and thus finally

$$D_0^{(P)} = \frac{15\pi}{2} \alpha_s \langle \alpha_s G^2 \rangle^2. \quad (52)$$

As in the scalar case, the uncertainty in D_0 has practically no impact on the quantitative sum rule analysis.

We note in passing that the perturbative contributions to $\tilde{C}_0$ increase in both spin-0 glueball correlators with the order of α_s. The size ratios of the $O(\alpha_s^0):O(\alpha_s^1):O(\alpha_s^2)$ corrections to $A_0^{(P)}$ are about 1:2:3, for example (at $\alpha_s/\pi \simeq 0.1$). This type of behavior is often encountered in QCD perturbation series and might foreshadow the approach to the asymptotic regime.

B. Borel moments, continuum subtraction, and RG improvement

The perturbative Wilson coefficients enter the glueball sum rules (28) through their contributions to the continuum-subtracted Borel moments (27). In this section we outline the calculation of these moments in the dispersive representation. The unit-operator coefficients contain the strongest UV divergences and therefore require the maximal number of subtractions, which turns out to be three (see below):

$$\Pi_G^{(\text{cont})}(Q^2) = \Pi_G(0) - Q^2 \Pi_G'(0) + \frac{1}{2} Q^4 \Pi_G''(0) - \frac{Q^6}{\pi} \int_{s_0}^\infty ds \frac{\text{Im}\Pi_G(-s)}{s^3(s + Q^2)}. \quad (53)$$

The further evaluation of the continuum contributions requires explicit expressions for the imaginary parts of the perturbative Wilson coefficients at timelike momenta. Those are obtained from the coefficients of the last section whose q dependence resides in a combination of powers $(q^2)^n$ and logarithms $\ln(-q^2/\mu^2)$. The imaginary parts of the pure power corrections (i.e., the B_0, C_0, and D_0 terms) are concentrated at $s = 0$ and thus do not contribute to the duality continuum, while the logarithms acquire an imaginary part $-\pi$ at timelike momenta. For $s > 0$ we therefore find

$$\text{Im}\Pi_G^{(\text{pc})}(-s) = -\pi \left[A_0^{(G)} s^2 + 2A_1^{(G)} s^2 \ln\left(\frac{s}{\mu^2} \right) \right. + A_2^{(G)} s^2 \left(3\ln^2\left(\frac{s}{\mu^2} \right) - \pi^2 \right) + B_1^{(G)} - \left. \frac{C_1^{(G)}}{s} \right]. \quad (54)$$

The next step is to calculate the Borel moments of $\Pi_G^{(\text{pc})}(Q^2)$ according to Eq. (23) and to subtract the continuum contributions, which leads to

$$\mathcal{L}_{G,k}^{(\text{pc})}(\tau; s_0) = \mathcal{L}_{G,k}^{(\text{pc})}(\tau) - \frac{1}{\pi} \int_{s_0}^\infty ds s^k \text{Im}\Pi_G^{(\text{pc})}(-s) e^{-\tau s}. \quad (55)$$

After inserting the imaginary part, Eq. (54), the perturbative continuum can be evaluated explicitly. The resulting, final expressions for $\mathcal{L}_{G,k}(\tau; s_0)$ are conventionally written in terms of the partial sums

$$\rho_k(x) = e^{-x} \sum_{n=0}^k \frac{x^n}{n!}, \quad (56)$$

and the exponential integral

$$E_1(x) = \int_1^\infty dt \frac{e^{-xt}}{t}. \quad (57)$$

They can be found in Appendix A.

Before implementing the continuum-subtracted Borel moments into the sum rules (28), one still has to perform the standard renormalization group improvement. Using the leading order perturbative β function, RG improvement amounts to the replacements [5]

$$\mu^2 \to \frac{1}{\tau}, \tag{58}$$

$$\alpha \to \bar{\alpha}_s(1/\tau) = \frac{-4\pi}{b_0 \ln(\Lambda^2 \tau)}, \tag{59}$$

$$\langle gG^3 \rangle \to \left(\frac{\bar{\alpha}_s(1/\tau)}{\bar{\alpha}_s(\mu^2)} \right)^{7/11} \langle gG^3 \rangle. \tag{60}$$

[Formally, the inclusion of NLO corrections to the β function would be more consistent for the evolution of the $O(\alpha_s^2)$ contributions to the unit-operator coefficients. However, their impact is negligible in the kinematical region relevant for the sum rules.] Following the notation of Eq. (27), the resulting Borel moments will be renamed $\mathcal{R}_{G,k}^{(pc)}(\tau, s_0)$. (It is common practice to perform the RG improvement after the Borel transform, i.e., after the subtraction terms are eliminated. Interchanging this order leads to the same results, up to corrections of higher order in α_s.)

The final expressions for the continuum-subtracted Borel moments, as generated by the perturbative IOPE coefficients, are ($\gamma = 0.5772$ is Euler's constant and the small contributions from the A_2 coefficients are omitted):

$$\mathcal{R}_{G,-1}^{(pc)}(\tau, s_0) = -\frac{A_0(\tau)}{\tau^2}[1 - \rho_1(s_0\tau)] + \frac{2A_1(\tau)}{\tau^2}[\gamma - 1$$
$$+ E_1(s_0\tau) + e^{-\tau s_0} + \ln(s_0\tau)\rho_1(s_0\tau)]$$
$$- B_0(\tau) + B_1(\tau)[\gamma + E_1(s_0\tau)]$$
$$- C_0(\tau)\tau + C_1(\tau)\tau\bigg[\gamma - 1$$
$$- \frac{e^{-\tau s_0}}{\tau s_0} + E_1(s_0\tau)\bigg] - \frac{D_0(\tau)}{2}\tau^2, \tag{61}$$

$$\mathcal{R}_{G,0}^{(pc)}(\tau, s_0) = -\frac{2A_0}{\tau^3}[1 - \rho_2(s_0\tau)] + \frac{4A_1}{\tau^3}\bigg[\gamma - \frac{3}{2}$$
$$+ E_1(s_0\tau) + \rho_0(s_0\tau) + \frac{1}{2}\rho_1(s_0\tau)$$
$$+ \ln(s_0\tau)\rho_2(s_0\tau)\bigg] - \frac{B_1}{\tau}\bigg[1 - \rho_0(s_0\tau)\bigg]$$
$$+ C_0 - C_1[\gamma + E_1(s_0\tau)] + D_0\tau, \tag{62}$$

$$\mathcal{R}_{G,1}^{(pc)}(\tau, s_0) = -\frac{6A_0}{\tau^4}[1 - \rho_3(s_0\tau)] + \frac{12A_1}{\tau^4}\bigg[\gamma - \frac{11}{6}$$
$$+ E_1(s_0\tau) + \rho_0(s_0\tau) + \frac{1}{2}\rho_1(s_0\tau)$$
$$+ \frac{1}{3}\rho_2(s_0\tau) + \ln(s_0\tau)\rho_3(s_0\tau)\bigg]$$
$$- \frac{B_1}{\tau^2}[1 - \rho_1(s_0\tau)]$$
$$+ \frac{C_1}{\tau}[1 - \rho_0(s_0\tau)] - D_0, \tag{63}$$

$$\mathcal{R}_{G,2}^{(pc)}(\tau, s_0) = -\frac{24A_0}{\tau^5}[1 - \rho_4(s_0\tau)] + \frac{48A_1}{\tau^5}\bigg[\gamma - \frac{25}{12}$$
$$+ E_1(s_0\tau) + \rho_0(s_0\tau) + \frac{1}{2}\rho_1(s_0\tau)$$
$$+ \frac{1}{3}\rho_2(s_0\tau) + \frac{1}{4}\rho_3(s_0\tau)$$
$$+ \ln(s_0\tau)\rho_4(s_0\tau)\bigg] - \frac{2B_1}{\tau^3}[1 - \rho_2(s_0\tau)]$$
$$+ \frac{C_1}{\tau^2}[1 - \rho_1(s_0\tau)]. \tag{64}$$

We conclude this section with a comment on the perturbative N_f dependence and the choice $N_f = 3$ adopted above. At present, the identification of all experimental glueball candidates remains controversial [2,3] and lattice simulations including light quarks are still limited to relatively small lattices and poor statistics [43]. Hence, quenched lattice calculations [28] are currently the most reliable source for information on the glueball spectrum. One might therefore be tempted to argue that setting $N_f = 0$ in the perturbative Wilson coefficients would allow for a more accurate comparison with the quenched lattice results.

However, the values of all nonperturbative input parameters, i.e., the condensates, the subtraction constants, and the bulk scales of the instanton size distribution, are deduced more or less directly from observables and therefore refer to the physical world with three active flavors. The N_f dependence of all these quantities, furthermore, is not known well enough to allow for a reliable extrapolation to $N_f = 0$. The realistic case $N_f = 3$, besides being physically more relevant and allowing for quarkonium mixing effects, is therefore the only consistent choice for the perturbative Wilson coefficients.

IV. IOPE 2: DIRECT INSTANTONS

We now turn to our main objective, the analysis of nonperturbative contributions to the Wilson coefficients.

In the present section we study their prototype, direct instantons[7] (with sizes $\rho < \mu^{-1}$) [24], which mediate fast tunneling rearrangements of the vacuum. Direct instanton contributions to the scalar glueball correlators and Borel sum rules were evaluated in Ref. [13] and found to be instrumental in resolving mutual inconsistencies among the sum rules and with the underlying low-energy theorem. Moreover, they generate more stable and reliable sum rules, scaling relations between glueball and instanton properties and new predictions for the fundamental glueball properties.

After a few introductory remarks on direct instantons and the semiclassical approximation, we will discuss pertinent aspects of the instanton size distribution $n(\rho)$ in the QCD vacuum. In particular, we comment on the shortcomings of the "spike" approximation to $n(\rho)$ which underlied all previous studies of direct instanton effects, and then improve upon it by implementing a realistic finite-width size distribution which embodies all essential features revealed by instanton liquid model and lattice simulations.

Armed with the improved size distribution, we then embark on the calculation of direct instanton contributions to both spin-0 correlators, starting from x space, and discuss their properties in some detail. In the course of this discussion we derive several new expressions for the instanton contributions. We also outline the derivation of the instanton-induced continuum contributions [13] and obtain the continuum-subtracted Borel moments for general instanton size distributions. Next we discuss, on the basis of some analytical results, generic effects of finite-width distributions and their impact on IOPE and sum rules. Finally, we renormalize the direct-instanton-induced Wilson coefficients at the operator scale μ (which was ignored in previous studies of direct instanton effects).

To start with, let us recall some basic features of the semiclassical expansion which underlies the evaluation of the direct instanton contributions. (For an introduction to direct instantons and more details see Ref. [24].) To leading order in $\hbar$, the (Euclidean) functional integrals representing the correlation functions are evaluated at the relevant action minima, i.e., the instanton and anti-instanton solutions closest to the space-time points linked by the correlator, with field strength (in nonsingular Lorentz gauge) [45]

---

[7]By now there exists a rather large body of work on direct instanton contributions to IOPE and Borel sum rules in classical hadron channels [24] which uncovered important new instanton effects in hadron structure (in the nucleon channel, e.g., the stabilization of the chirally-odd nucleon sum rule [17], the emergence of a new, stable sum rule for the nucleon magnetic moments, the reconciliaton of sum rule and chiral perturbation theory predictions for the neutron-proton mass difference, a nonperturbative dynamical mechanism of isospin violation [44], etc.).

$$G_{\mu\nu}^{(I),a}(x) = \frac{-4\rho^2}{g_s} \frac{\eta_{a\mu\nu}}{[(x - x_0)^2 + \rho^2]^2},\qquad(65)$$

(x_0 and ρ are position and size of the instanton, respectively, and $\eta_{a\mu\nu}$ is the 't Hooft symbol [22]). The functional integrals then reduce to integrals over the collective coordinates of the saddle points, i.e., over $x_{0,\mu}$, ρ and the color orientation U. Quantum effects break the conformal symmetry of classical Yang-Mills theory and thereby generate a nontrivial measure $n(\rho)$, i.e., the instanton size distribution, for the integral over ρ. The factor g_s^{-1} in Eq. (65) enhances the direct instanton contributions to the correlators (6) by a factor α_s^{-2} compared to the leading perturbative contributions. Since $\alpha_s/\pi \sim 0.1$ at typical sum rule momenta $Q \sim 1$ GeV, this enhancement is substantial and partially explains the important role of direct instantons in the spin-0 glueball channels.

The restriction of the semiclassical approximation to the saddle points associated with the nearest (anti-) instanton is justified by the hierarchy of IOPE and instanton scales. The distances $|x| \sim |Q^{-1}| \lesssim 0.2 - 0.3$ fm $\ll \Lambda_{\text{QCD}}^{-1}$ accessible to the IOPE, in particular, are much smaller than the average instanton separation $\bar{R} \sim 1$ fm (which is inferred from to the instanton density $\bar{n}_{I+\bar{I}} \sim 1$ fm^{-4} in the vacuum, see below). The relative diluteness of the instanton medium, characterized by the ratio $\bar{\rho}/\bar{R} \sim 0.3$, further reduces the impact of multi-instanton correlations. Multi-instanton corrections were calculated explicitly in the pseudoscalar meson channel (which strongly couples to instantons) in Ref. [46] and indeed found to be negligible. Nevertheless, we will discover a unique exception to this rule, generated by short-range correlations among topological charges (including those carried by instantons) in the QCD vacuum, in Sec. V.

A. Instanton size distribution

As alluded to above, the evaluation of direct instanton contributions to the IOPE coefficients requires the instanton (and anti-instanton) size distribution $n_{I,\bar{I}}(\rho)$ as an input. By definition, $n_I(\rho)$ specifies the average number $d^5 N_I = n_I(\rho)d\rho d^4 x_0$ of instantons with sizes between ρ and $\rho + d\rho$ and positions between x_0 and $x_0 + dx_0$ in the vacuum, i.e.,

$$n_I(\rho) = \frac{d^5 N_I}{d\rho d^4 x_0}.\qquad(66)$$

Integrating over ρ, one obtains the instanton density

$$\bar{n}_I = \int_0^\infty d\rho \, n_I(\rho) = \frac{d^4 N_I}{d^4 x_0} \sim \frac{N_I}{V_4},\qquad(67)$$

where V_4 is the space-time volume. Since the vacuum (in the thermodynamic limit) contains on average equal numbers of instantons and anti-instantons, the same relations hold for the anti-instanton size distribution $n_{\bar{I}}(\rho)$ and den-

sity $\bar{n}_{\bar{I}}$. We therefore omit the subscripts $I, \bar{I}$ and define

$$n(\rho) \equiv n_I(\rho) = n_{\bar{I}}(\rho), \qquad (68)$$

which implies $\bar{n} = \bar{n}_I = \bar{n}_{\bar{I}}$. As a consequence, the total number of pseudoparticles (instantons *and* anti-instantons) in a vacuum volume V_4 is $2\bar{n}V_4$.

In the IOPE context, the status of the size distribution $n(\rho)$ is analogous to that of the condensates: both are generated mostly by long-wavelength physics and characterize universal (i.e., hadron-channel independent) bulk properties of the vacuum. Hence the associated scales have to be imported from other sources (e.g., from phenomenology or the lattice). Because of their definition in terms of QCD amplitudes this is unambiguously possible, and due to their small number and universal character the IOPE's predictive power is only moderately affected.

The main scales of $n(\rho)$ are set by its two leading moments, i.e., the overall instanton density

$$\bar{n} = \int_0^\infty d\rho\, n(\rho), \qquad (69)$$

and the average instanton size

$$\bar{\rho} = \frac{1}{\bar{n}} \int_0^\infty d\rho\, \rho\, n(\rho). \qquad (70)$$

A large body of successful phenomenology in the instanton liquid model [9] has settled on the benchmark values $\bar{\rho} \simeq 0.33$ fm and $\bar{n} \simeq 0.5$ fm^4 which were (inside errors) confirmed by lattice simulations [11,12,47] and which we will use throughout the paper. These scales imply a mean separation $\bar{R} \sim 1$ fm between instantons, i.e., much larger than the average instanton size. This allows the individual instantons to retain their identity.

The simplest parametrization which is able to embody these scales is the spike distribution $n_{\mathrm{sp}}(\rho) = \bar{n}\delta(\rho - \bar{\rho})$ [10]. Since the IOPE coefficients are not expected to be particularly sensitive to details of $n(\rho)$, the spike approximation has so far been exclusively relied upon in evaluating direct instanton contributions. Nevertheless, it is clearly an oversimplification and produces several artifacts, as we will see below. Moreover, additional features of $n(\rho)$, beyond the mentioned moments $\bar{n}$ and $\bar{\rho}$, appear now well enough settled to be implemented, too. Indeed, first-principle information on the behavior of $n(\rho)$ at small ρ is available from perturbation theory in the instanton background [22,48] and implies the power-law behavior

$$n(\rho) \overset{\rho \to 0}{\longrightarrow} A\rho^{b_0 - 5} \qquad (71)$$

(where $b_0 = 11N_c/3 - 2N_f/3$). Furthermore, lattice results and instanton vacuum model arguments [9,12,49–51] agree on a Gaussian falloff of the large-ρ tail,

$$n(\rho) \overset{\rho \to \infty}{\longrightarrow} Be^{-C(\rho/\bar{\rho})^2}. \qquad (72)$$

Note, incidentally, that this strong suppression of large

instantons (with sizes $\rho \gg \bar{\rho}$) is in marked contrast to earlier dilute-gas assumptions [48] which proved inconsistent (i.e., IR unstable).

In the rest of the present section, we are going to construct the finite-width (Gaussian-tail) distribution which incorporates all currently known information about the size distribution, as summarized above. It is fully determined by the behavior at small and large ρ and by the two leading moments $\bar{n}$ and $\bar{\rho}$. As will be demonstrated below, additional details of $n(\rho)$ have no significant impact on the IOPE coefficients. Before discussing the Gaussian-tail distribution, we briefly recall the essential features of the traditional spike approximation and introduce an approximate finite-width distribution which will be useful later (although its exponential tail fails to satisfy the constraint (72) and makes it unsuitable for quantitative analyses). Finally, we anticipate that the finite-width distribution has an additional benefit: it affords a simple and gauge-invariant way to implement the operator renormalization scale μ, as will be shown in Sec. IV F.

1. Spike-distribution

Before discussing finite-width distributions, we mention a few obvious properties of the simplest approximation to the instanton size distribution, the zero-width or spike distribution

$$n_{\mathrm{spk}}(\rho) = \bar{n}\delta(\rho - \bar{\rho}), \qquad (73)$$

which sets the sizes of all instantons equal to their average value $\bar{\rho}$ and has up to now been exclusively used in evaluating direct instanton contributions. Its two lowest moments determine this distribution uniquely. Moreover, it becomes exact in the large-N_c limit of instanton liquid vacuum models.

Most other features of the spike distribution, however, differ qualitatively from the finite-width distribution: the median is equal to its mean, all higher (centralized) moments, including the variance

$$\langle (\rho - \bar{\rho})^2 \rangle = 0, \qquad (74)$$

vanish identically, and the support both at small and large ρ is exactly zero. As we will see in Secs. IV E and VI, these properties induce several artifacts, including unphysical oscillations in the instanton-induced spectral functions at timelike momenta.

2. Exponential-tail distribution

In order to estimate the sensitivity of our glueball predictions to the detailed shape of the size distribution and to allow for some analytical estimates, we now introduce an approximate size distribution with power-law behavior at small ρ and an exponential decay at large ρ,

$$n_{\exp}(\rho) = \frac{(n+1)^{n+1}}{n!} \frac{\bar{n}}{\bar{\rho}} \left(\frac{\rho}{\bar{\rho}}\right)^n \exp\left[-(n+1)\frac{\rho}{\bar{\rho}}\right]. \qquad (75)$$

Although the exponential large-ρ tail is inconsistent with the behavior (72), this distribution is nevertheless useful because it allows the ρ integral in the instanton-induced spectral function to be done analytically. The resulting expressions provide a convenient benchmark for analyzing generic effects of finite-width distributions.

For $N_f = 3$, instanton background perturbation theory fixes the power of the small-ρ behavior at $n = 4$ [cf. Eq. (71)], i.e.,

$$n_{\exp}(\rho) = \frac{5^5}{2^3 3} \frac{\bar{n}}{\bar{\rho}} \left(\frac{\rho}{\bar{\rho}}\right)^4 \exp\left(-\frac{5\rho}{\bar{\rho}}\right) \quad \text{for } N_f = 3. \quad (76)$$

The variance of the exponential-tail distribution,

$$\langle (\rho - \bar{\rho})^2 \rangle = \frac{1}{\bar{n}} \int n_{\exp}(\rho) \rho^2 d\rho - \bar{\rho}^2 = \frac{1}{5} \bar{\rho}^2, \quad (77)$$

implies a half-width of about $0.7\bar{\rho}$, similar to lattice and instanton liquid results [9,12]. This is reassuring since the width of $n_{\exp}$ is not an independent parameter but determined by $\bar{\rho}$. The maximum of the distribution is reached at

$$\rho_{\text{peak}} = \frac{4\bar{\rho}}{5}, \quad (78)$$

(i.e., $\rho_{\text{peak}} \simeq 4/3 \text{ GeV}^{-1}$ for the standard value $\bar{\rho} \simeq 1/3$ fm). A parametrization for $n(\rho)$ with a similar exponential tail,

$$n(\rho) = \frac{N}{\rho} \exp\left(-\frac{\alpha}{\rho} - \beta\rho\right), \quad (79)$$

has been used in a study of the asymptotic OPE behavior [35]. As the distribution (76), it allows relevant ρ integrals to be done analytically. However, it fails to reproduce the power-law behavior at small ρ and cannot be made to reproduce both $\bar{n}$ and $\bar{\rho}$.

3. Gaussian-tail distribution

We now turn to the size distribution which incorporates all known features discussed above, including the power behavior (71) at small ρ and the Gaussian tail (72) at large ρ. It is obtained from the general form

$$n(\rho) = N\rho^n \exp\left(-A\frac{\rho^2}{\bar{\rho}^2}\right), \quad (80)$$

by requiring the two lowest moments to satisfy Eqs. (69) and (70). This determines A and N uniquely, with the result

$$n_g(\rho) = 2\frac{\bar{n}}{\bar{\rho}} \left(\frac{\rho}{\bar{\rho}}\right)^n \frac{[\Gamma(\frac{n+2}{2})]^{n+1}}{[\Gamma(\frac{n+1}{2})]^{n+2}} \exp\left[-\left(\frac{\Gamma(\frac{n+2}{2})}{\Gamma(\frac{n+1}{2})}\right)^2 \left(\frac{\rho}{\bar{\rho}}\right)^2\right]. \quad (81)$$

As already mentioned, a Gaussian tail is found in the instanton liquid model (ILM) [50] as well as in other approaches [9,49,51,52]. Moreover, it is confirmed by lattice data [12]. In the ILM, for example, one finds [50]

$$n_{\text{ILM}}(\rho) = C\rho^{b_0-5} \exp\left(-\frac{b_0 - 4}{2} \frac{\rho^2}{\bar{\rho}^2}\right), \quad (82)$$

($b_0 = 11N_c/3 - 2N_f/3$) which approaches the spike approximation at large N_c,

$$\lim_{N_c \to \infty} n_{\text{ILM}}(\rho) \propto \delta(\rho - \bar{\rho}). \quad (83)$$

At $N_c = N_f = 3$ it becomes

$$n_{\text{ILM}}(\rho) = C\rho^4 \exp\left(-\frac{5}{2} \frac{\rho^2}{\bar{\rho}^2}\right), \quad (84)$$

to be compared with our distribution (81) for $n = 4$,

$$n_g(\rho) = \frac{2^{18}}{3^6 \pi^3} \frac{\bar{n}}{\bar{\rho}} \left(\frac{\rho}{\bar{\rho}}\right)^4 \exp\left(-\frac{2^6}{3^2 \pi} \frac{\rho^2}{\bar{\rho}^2}\right), \quad (N_f = 3). \quad (85)$$

The width of the ILM distribution is about 10% larger. Equation (85) is the size distribution on which all our quantitative calculations and results below will be based.

The distribution (85) has the variance

$$\langle (\rho - \bar{\rho})^2 \rangle = \left(\frac{3^2 5\pi}{2^7} - 1\right)\bar{\rho}^2 \simeq \frac{1}{10}\bar{\rho}^2, \quad (86)$$

which corresponds to a half-width of about $\bar{\rho}/2$, somewhat smaller than the half-width of the exponential-tail distribution (76). The position of the peak lies at

$$\rho_{\text{peak}} = \frac{3}{4}\sqrt{\frac{\pi}{2}}\bar{\rho} \simeq 0.94\bar{\rho}. \quad (87)$$

Since n_g is more symmetric than $n_{\exp}$, its ρ_{peak} is somewhat larger. Moreover, due to its enhanced large-ρ decay, $n_g(\rho)$ contains a larger number of intermediate-size instantons with $\rho \sim \bar{\rho}$. It affects the IOPE coefficients somewhat more strongly since only instantons with $\rho \lesssim \mu^{-1} \sim 2\bar{\rho}$ (where μ is the operator renormalization scale) contribute to them.

B. Direct-instanton contributions in x space

In this section we derive, to leading order in the semi-classical expansion, the direct instanton contributions to the IOPE coefficients $\tilde{C}_0^{(S,P)}$ of the spin-0 glueball correlators. We also comment on contributions of higher orders in $\hbar$ and on coefficients of higher-dimensional operators. The calculations, as well as the discussion of the singularity structure and of the pointlike-instanton limit, are best performed in Euclidean space-time, the instanton's natural habitat.

As outlined above, the semiclassical contributions from instanton-induced saddle points to the functional integral of the glueball correlators are obtained by evaluating their Wick expansion in the instanton background, e.g., by means of the gluon background-field propagator of Ref. [53]. Adding up the contributions from the nearest

instanton and anti-instanton one finds, to leading order in $\hbar$,

$$\Pi_S^{(I+\bar{I})}(x^2) = \sum_{I,\bar{I}} \int d\rho\, n(\rho) \int d^4x_0 \langle T O_S(x) O_S(0)\rangle_{I+\bar{I}}$$

$$(88)$$

$$= \frac{2^9 3^2}{\pi^2} \int d\rho\, n(\rho) \int d^4x_0 \frac{\rho^8}{[(x-x_0)^2+\rho^2]^4[x_0^2+\rho^2]^4}.$$

$$(89)$$

We recall that it suffices to perform all calculations in the scalar channel since the pseudoscalar correlator receives, due to self-duality, identical instanton contributions (in Euclidean space-time). A convenient analytical expression for the above x_0 integral in terms of a hypergeometric function [54],

$$\int d^4x_0 \frac{\rho^{12}}{[(x-x_0)^2+\rho^2]^4[x_0^2+\rho^2]^4}$$
$$= \frac{\pi^2}{42} {}_2F_1\left(4,6,\frac{9}{2},-\frac{x^2}{4\rho^2}\right),$$

$$(90)$$

is derived in Appendix B.

The singularity structure of the instanton contributions at fixed instanton size ρ can then be read off from

$$\Pi_S^{(I+\bar{I})}(x^2;\rho) = \frac{2^8 3}{7} \frac{1}{\rho^4} {}_2F_1\left(4,6,\frac{9}{2},-\frac{x^2}{4\rho^2}\right),$$

$$(91)$$

by recalling the well-known analyticity properties of the hypergeometric functions [54]: Eq. (91) has no singularities inside a circle of radius 2ρ around $x = 0$, but it has cuts emerging from the two branch points $x = \pm 2i\rho$. [These singularities have their origin in the (partially gauge-dependent) denominators of the instanton's field strength (65).] Contributions from these branch points dominate the Fourier transform of Eq. (91) at large momentum transfer (see next section). The final result for the instanton contributions is obtained by integrating Eq. (91) over all instanton sizes with the weight $n(\rho)$:

$$\Pi_S^{(I+\bar{I})}(x^2) = \int d\rho\, n(\rho) \Pi_S^{(I+\bar{I})}(x^2;\rho)$$
$$= \frac{2^8 3}{7} \int d\rho \frac{n(\rho)}{\rho^4} {}_2F_1\left(4,6,\frac{9}{2},-\frac{x^2}{4\rho^2}\right). \quad (92)$$

Note that the ρ integration over physically reasonable instanton size distributions, with the power-law behavior (71) at small ρ and $N_f \leq 3$, does not produce singularities of Eq. (92) at $x^2 = 0$. This implies, in particular, that the $x^2 \to 0$ limit is finite (see below). From ${}_2F_1(a,b,c,0) = 1$ one obtains

$$\Pi_S^{(I+\bar{I})}(x^2=0) = \frac{2^8 3}{7} \int d\rho \frac{n(\rho)}{\rho^4}. \quad (93)$$

The x dependence of Eq. (91) shows that the instanton-induced correlations are maximal at $x^2 = 0$ and strongly decay ($\propto |x|^{-8}$ at fixed ρ) for $|x| \gg 2\rho$, i.e., when the arguments of the correlator cease to lie both within the bulk of the instanton's localized action density. Note, furthermore, that the x dependence of the fixed-size instanton contribution reduces to a delta function in the small-ρ limit,

$$\lim_{\rho\to 0}\Pi_S^{(I+\bar{I})}(x^2;\rho) = \frac{2^8 3}{7} \lim_{\rho\to 0}\frac{1}{\rho^4} {}_2F_1\left(4,6,\frac{9}{2},-\frac{x^2}{4\rho^2}\right)$$
$$= 2^7 \pi^2 \delta^4(x). \quad (94)$$

This pointlike-instanton approximation will be useful below.

Technically, the result (92) provides the leading non-perturbative contributions to the IOPE coefficient $\tilde{C}_0^{(S)}(x)$ of the unit operator in the scalar glueball channel. (Strictly speaking, soft-mode contributions, in particular, those due to large instantons with $\rho > \mu^{-1}$, should still be excluded cf. Sec. IV F.) Of course, the coefficients of higher-dimensional operators receive direct instanton contributions as well. The coefficient $\tilde{C}_4^{(S)}$ of the lowest-dimensional condensate $\langle \alpha G^2\rangle$, for example, gets a correction from the process in which one of the gluon fields emanating from the interpolator (2) is soft and turns into a gluon condensate while the other one is hard and propagates in the instanton background. The general form of this contribution is

$$\Pi_{G,\langle\alpha G^2\rangle}^{(I+\bar{I})}(x^2) \propto \langle\alpha_s G^2\rangle \int d\rho\, n(\rho)$$
$$\times \int d^4x_0 \frac{\rho^4}{[(x-x_0)^2+\rho^2]^4}. \quad (95)$$

Relative to the unit-operator term, this correction is suppressed by four powers of $\varepsilon \equiv |x|\Lambda_{QCD} \lesssim 0.2$. More generally, power corrections associated with d-dimensional operators are parametrically suppressed by a factor ε^d and also by the relatively large glueball mass scale (cf. Sec. VI). Therefore, we neglect such contributions in the following.[8]

The IOPE coefficients also receive instanton corrections from higher orders in the semiclassical expansion. To $O(\hbar)$, these corrections arise from Gaussian quantum fluctuations around the instanton fields [9] and have the form

$$\Pi_{G,O(\hbar)}^{(I+\bar{I})}(x^2) \propto \alpha_s^2 \langle G_{\mu\nu}^{(I),a}(x)$$
$$\times [D_\mu^x D_\rho^y D_{\nu\sigma}(x,y)]^{ab} G_{\rho\sigma}^{(I),b}(y)\rangle|_{y=0} + ... \quad (96)$$

---

[8]In the IOPE of the pseudoscalar meson correlator, analogous instanton-enhanced power corrections are associated with chiral-symmetry breaking operators and therefore turn out to be important [55].

where D_μ^x is the covariant derivative in the adjoint representation and $D_{\nu\beta}$ is the gluon propagator in the instanton background. Radiative corrections of this sort are suppressed by at least two powers of α_s. Moreover, the average instanton is small on the QCD scale, $\bar{\rho}\Lambda_{\rm QCD} \ll 1$, and the instanton action $S_I(\bar{\rho}) \sim 10\hbar$ consequently large compared to the action of the quantum corrections. We therefore do not expect such corrections to have significant impact on our analysis and do not consider them further.

Finally, it is instructive to compare our result (92) with direct instanton contributions to pseudoscalar meson correlators [46,55,56]. The latter arise mostly from quarks propagating in the zero-mode states of the gauge-covariant Dirac operator in the instanton background [22]. (The nonzero modes can normally be approximated by plane waves.) In the meson sector, the distinct topological, chiral, flavor, and spin-color properties of these zero modes are responsible for most features of the direct instanton contributions, including their strong channel dependence. Clearly, the instanton-induced physics in the glueball correlators is quite different in this respect. (It does not require, incidentally, to account for ambient soft vacuum fields in the gluon propagators which, in contrast, rather strongly affect the quark-zero-mode propagation.)

C. Borel moments

The next step in our program is to calculate the Borel moments (23) associated with the direct instanton contributions (92). This is best done by first transforming to (Euclidean) momentum space,

$$\Pi_S^{(I+\bar{I})}(Q^2) = \int d^4x\, e^{iQx}\Pi_S^{(I+\bar{I})}(x^2), \qquad (97)$$

or, more explicitly,

$$\Pi_S^{(I+\bar{I})}(Q^2) = \frac{2^{10}3\pi^2}{7}\int d\rho\,\frac{n(\rho)}{\rho^4}$$
$$\times \int_0^\infty dr\, r^3 \frac{J_1(Qr)}{Qr}\,{}_2F_1\!\left(4, 6, \frac{9}{2}, -\frac{r^2}{4\rho^2}\right) \qquad (98)$$

$$= 2^5\pi^2 \int d\rho\, n(\rho)(Q\rho)^4 K_2^2(Q\rho), \qquad (99)$$

where $J_1(z)$ and $K_2(z)$ are Bessel and McDonald functions [54]. In the last equation we have made use of the integral [57]

$$\int_0^\infty dr\, r^2 J_1(Qr)\,{}_2F_1\!\left(4, 6, \frac{9}{2}, -\frac{r^2}{4\rho^2}\right) = \frac{7}{2^5 3}Q^5\rho^8 K_2^2(Q\rho). \qquad (100)$$

[An alternative calculation of Eq. (99), which agrees with the expression first obtained in [6], can be found in Appendix B.]

It is instructive to examine the limits of $\Pi_S^{(I+\bar{I})}(Q^2)$. Using for simplicity the spike distribution (73) and the asymptotic behavior of the McDonald functions [54], one finds

$$\Pi_S^{(I+\bar{I})}(Q^2) \overset{Q^2\to\infty}{\longrightarrow} 2^4\pi^3\bar{n}(Q\bar{\rho})^3 e^{-2Q\bar{\rho}}. \qquad (101)$$

The exponential decay of the integrand at large Q is expected since $\Pi_S^{(I+\bar{I})}(x^2; \rho)$ is analytic in the circle $|x| < 2\rho$ around $x^2 = 0$. Its scale is set by the singularities nearest to the real axis, i.e., the branch points at $x = \pm 2i\rho$. Physically, this can be understood as the phase-space suppression encountered when distributing the hard momentum Q over multiple soft modes of the coherent instanton field with size ρ. While the fixed-size instanton contribution (91) contains no asymptotic power corrections (due to the absence of singularities at $x^2 = 0$), integration over the instanton size does produce inverse powers of Q. However, they start with Q^{-5} [the power is determined by the small-ρ behavior (71) of $n(\rho)$] and therefore do not interfere with the power corrections of the truncated IOPE [cf. Eq. (35)].

In the opposite limit, i.e., for $Q^2 \to 0$, the instanton contributions turn into

$$\Pi_S^{(I+\bar{I})}(Q^2 = 0) = 2^7\pi^2 \int d\rho\, n(\rho), \qquad (102)$$

which is independent of any details of the instanton size distribution and could as well have been obtained from the pointlike approximation (94). This term plays a key role, as an instanton-induced subtraction constant, in the lowest (i.e., $k = -1$) Borel moments and in the associated spin-0 sum rules (cf. Sec. VI C). The obligatory removal of soft contributions from instanton-induced Wilson coefficients (cf. Secs. IV F and VI C) deemphasizes contributions from multi-instantons and other soft vacuum fields [not taken into account in Eq. (92)] and should thereby improve the nearest-instanton approximation. Although the latter is strictly valid only for $|x| \ll \bar{R}$, it often seems to work over larger distances (as long as cluster decomposition does not become an issue [9]), due to the strong localization and small packing fraction of the instantons.[9] Nevertheless, one should not expect Eq. (102) to be a complete representation of the correlator at $Q = 0$, as can be seen, for example, from the one-instanton approximation to the gluon condensate,

$$\langle \alpha G^2 \rangle_{I+\bar{I}} = 16\pi \int d\rho\, n(\rho), \qquad (103)$$

---

[9]This conclusion is supported by quark and gluon condensate estimates on the basis of the one-instanton approximation which are not far from the phenomenological values, and by the fact that their multi-instanton corrections (evaluated in the ILM) are typically of the order of 10%−20%. (I thank Sasha Dorokhov for interesting discussions on this point.)

which, when multiplied by $32\pi/b_0$, yields only about half of Eq. (102) and therefore does not saturate the low-energy theorem (10). The inconsistency with the low-energy theorem (14) in the pseudoscalar channel, incidentally, is far more dramatic and can be overcome only by additional nonperturbative physics (cf. Secs. V and VI C).

According to the general definition (23), the Borel moments of the direct instanton contributions are

$$\mathcal{L}_{S,k}^{(I+\bar{I})}(\tau) = \hat{B}[(-Q^2)^k \Pi_S^{(I+\bar{I})}(Q^2)] \qquad (104)$$

(for $k \in \{-1, 0, 1, 2\}$). In order to calculate these moments explicitly, it is convenient to rewrite Eq. (99) in terms of an integral representation for the McDonald function before applying the Borel operator (22). In Appendix B we outline this calculation for $k = -1$, which results in [13]

$$\mathcal{L}_{S,-1}^{(I+\bar{I})}(\tau) = -2^6\pi^2 \int d\rho n(\rho)\xi^2 e^{-\xi}\Big[(1 + \xi)K_0(\xi)$$
$$+ \Big(2 + \xi + \frac{2}{\xi}\Big)K_1(\xi)\Big]. \qquad (105)$$

Above we have introduced the dimensionless variable $\xi = \rho^2/2\tau$. From the lowest, "generating" Borel moment all higher moments are obtained by differentiation with respect to $-\tau$,

$$\mathcal{L}_{S,k+1}^{(I+\bar{I})}(\tau) = -\frac{\partial}{\partial\tau}\mathcal{L}_{S,k}^{(I+\bar{I})}(\tau), \qquad (k \geq -1), \qquad (106)$$

and explicitly read

$$\mathcal{L}_{S,0}^{(I+\bar{I})}(\tau) = 2^8\pi^2 \int d\rho \frac{n(\rho)}{\rho^2}\xi^5 e^{-\xi}\Big[K_0(\xi)$$
$$+ \Big(1 + \frac{1}{2\xi}\Big)K_1(\xi)\Big], \qquad (107)$$

$$\mathcal{L}_{S,1}^{(I+\bar{I})}(\tau) = -2^9\pi^2 \int d\rho \frac{n(\rho)}{\rho^4}\xi^7 e^{-\xi}\Big[\Big(2 - \frac{9}{2\xi}\Big)K_0(\xi)$$
$$+ \Big(2 - \frac{7}{2\xi} - \frac{3}{2\xi^2}\Big)K_1(\xi)\Big], \qquad (108)$$

$$\mathcal{L}_{S,2}^{(I+\bar{I})}(\tau) = 2^{10}\pi^2 \int d\rho \frac{n(\rho)}{\rho^6}\xi^9 e^{-\xi}\Big[\Big(4 - \frac{44}{2\xi} + \frac{51}{2\xi^2}\Big)K_0(\xi)$$
$$+ \Big(4 - \frac{40}{2\xi} + \frac{32}{2\xi^2} + \frac{12}{2\xi^3}\Big)K_1(\xi)\Big]. \qquad (109)$$

For $\tau \to 0$, at fixed ρ, all instanton-induced Borel moments vanish exponentially. This is a direct reflection of the exponential large-Q suppression in Eq. (101) and renders these moments practically negligible for $\tau \lesssim 0.2$ GeV^{-2} (at $\rho = \bar{\rho}$). More specifically, if $\bar{\xi} = \bar{\rho}^2/2\tau \gg 1$ and if $n(\rho)$ is replaced by the spike approximation (73), Eqs. (105)–(109) reduce to

$$\mathcal{L}_{S,k}^{(I+\bar{I})}(\tau) \overset{\tau\to 0}{\to} (-1)^k 2^4 \pi^{5/2} \bar{n}\bar{\rho}^{7+2k} \frac{e^{-\bar{\rho}^2/\tau}}{\tau^{(9+4k)/2}}\Big[1 + O\Big(\frac{\tau}{\bar{\rho}^2}\Big)\Big]. \qquad (110)$$

In the case of $k = 0$, for instance, Eq. (110) is reliable when $\tau \lesssim 0.4$ GeV^{-2} but it underestimates the maximum at $\tau \sim 0.6$ GeV^{-2} and has the wrong decay power at larger τ (about twice the correct one, see below). The estimate of the instanton contributions to the $k = -1$ sum rule in Ref. [10] were based on the approximation (110). Because of the wrong decay behavior and the missing continuum contributions, however, it is unsuitable for reliable glueball mass and coupling estimates. In fact, after subtracting the associated continuum contributions [as in Eq. (55), see next section], the exponential suppression (110) will turn into an enhancement and generate increasing instanton contributions down to $\tau = 0$.

At intermediate τ ($\tau \gtrsim 0.2$ GeV^{-2}), $\mathcal{L}_{S,-1}^{(I+\bar{I})}(\tau)$ rises quite steeply towards its maximum. The associated, fast variations of its slope generate large oscillations in the higher Borel moments [due to the τ derivative in Eq. (106)] which would increasingly impede reliable sum rule fits. Again, this problem is overcome by subtracting the crucial instanton-induced continuum contributions, which transforms the oscillations into a monotonic decay. In the opposite limit, i.e., for $\tau \gg \bar{\rho}^2/2$, the $k \geq 0$ Borel moments approach zero from above while $\mathcal{L}_{S,-1}^{(I+\bar{I})}$ reaches the negative subtraction constant $-\Pi_S^{(I+\bar{I})}(0)$. The general decay behavior of the instanton contributions for large τ is an inverse power law. This continues to hold for fairly general $n(\rho)$ [including (76) and (85)] as long as $\tau \gg \rho_c^2/2$ where ρ_c is roughly the maximal size at which $n(\rho)$ has appreciable support. More explicitly, one has

$$\mathcal{L}_{S,k}^{(I+\bar{I})}(\tau) \overset{\tau\to\infty}{\to} -\delta_{k,-1}\Pi_S^{(I+\bar{I})}(0) + \frac{a_k}{\tau^{k+3}} \int d\rho \frac{n(\rho)}{\rho^{2(k+1)}}$$
$$+ O(\tau^{-k-4}), \qquad (111)$$

with positive coefficients a_k. As a consequence, the instanton-induced Borel moments decay as fast as their leading perturbative counterparts for $\tau \to \infty$, and faster than all power corrections (cf. Sec. III B). (Of course, this limit is not physical since the short-distance expansion breaks down for $\tau \to \infty$.)

D. Imaginary part and instanton-induced continuum

The discontinuities of the IOPE at timelike momenta generate the duality continuum (21). In the spin-0 glueball channels, the instanton-induced continuum contributions were first obtained in Ref. [13] and shown to have crucial impact on consistency and predictions of the 0^{++}-glueball sum rules. In the following, we outline their calculation and analyze some of their pertinent properties. Besides providing new insight into the structure of the instanton contributions, this analysis will prove useful in assessing

the effects of realistic instanton size distributions in subsequent sections. Finally, we assemble the instanton-induced, continuum-subtracted Borel moments which enter the spin-0 glueball sum rules.

The imaginary part of the instanton contributions is obtained by analytically continuing Eq. (99) in the complex $s = q^2 = -Q^2 + i\varepsilon$ plane. The behavior of the McDonald functions under analytical continuation can be expressed as [54]

$$K_\nu(z) = \begin{cases} \frac{i\pi}{2} e^{i\pi\nu/2} H_\nu^{(1)}(ze^{i\pi/2}) & \text{for } -\pi < \arg z \le \frac{\pi}{2} \\ \frac{-i\pi}{2} e^{-i\pi\nu/2} H_\nu^{(1)}(ze^{-i\pi/2}) & \text{for } \frac{\pi}{2} < \arg z \le \pi \end{cases} \tag{112}$$

where $H_\nu^{(1)}$ is the Hankel function of the first kind,

$$H_\nu^{(1)}(z) = J_\nu(z) + iY_\nu(z). \tag{113}$$

From the cut structure of the Hankel functions [54] one then finds

$$\text{Im} K_2^2(-i\sqrt{s}\rho) = -\frac{\pi^2}{2} J_2(\sqrt{s}\rho)Y_2(\sqrt{s}\rho) - \frac{2\pi}{\rho^2}\delta(s), \tag{114}$$

which leads to [13]

$$\text{Im}\Pi_S^{(I+\bar{I})}(-s) = -2^4\pi^4 s^2 \int d\rho n(\rho)\rho^4 J_2(\sqrt{s}\rho)Y_2(\sqrt{s}\rho). \tag{115}$$

Several qualitative and quantitative features can be readily deduced from this expression. First of all, for $s \to 0$ (i.e., $s \ll \bar{\rho}^{-2}$) it reduces to

$$\text{Im}\Pi_S^{(I+\bar{I})}(-s) \overset{s \ll \bar{\rho}^{-2}}{\to} 2^3\pi^3 s^2 \int d\rho n(\rho)\rho^4$$
$$\times \left[1 + \frac{1}{6}\rho^2 s + O(s^2)\right], \tag{116}$$

which has the leading s^2 dependence of the free gluon loop. This implies, for example, that the large-τ behavior of the corresponding, continuum-subtracted Borel moments (see below) equals that of the leading perturbative Wilson coefficient. Since the continuum subtraction does not affect the falloff at large τ, it also confirms the decay behavior (111) established in the last section.

A more important property to notice is that the analytical continuation has turned the exponentially small instanton contributions (99) at large Q^2 and fixed ρ into strong oscillations with increasing amplitude at timelike s. This becomes more explicit at large s,

$$\text{Im}\Pi_{S,\text{spk}}^{(I+\bar{I})}(-s) \overset{s \to \infty}{\to} 2^4\pi^3 s^{3/2}\bar{n}\bar{\rho}^3 \cos(2\sqrt{s}\bar{\rho}), \tag{117}$$

where we have used the spike approximation (73). Such a behavior is familiar from the analytical continuation of semiclassical tunneling amplitudes in quantum mechanics and can lead to a selective enhancement of parts of the

amplitude (when crossing Stokes lines) [58]. Potential problems of this sort (including the strong oscillations) will be tamed by finite-width instanton size distributions (cf. Sec. IV E). In any case, the overall growth of the instanton-induced imaginary part $\propto s^{3/2}$ at large s (and fixed ρ) is weaker than that of the free gluon loop [cf. Eq. (54)] and the dispersive integral exists without subtractions, i.e.,

$$\Pi_S^{(I+\bar{I})}(Q^2) = \frac{1}{\pi} \int_0^\infty ds \frac{\text{Im}\Pi_S^{(I+\bar{I})}(-s)}{s + Q^2} \tag{118}$$

$$= -2^4\pi^3 \int d\rho n(\rho)\rho^4 \int_0^\infty ds \frac{s^2 J_2(\sqrt{s}\rho)Y_2(\sqrt{s}\rho)}{s + Q^2}. \tag{119}$$

The analytical evaluation of the s integral indeed reproduces Eq. (99).

As discussed above, the small-Q^2 limit of the correlator (99) lies outside the range of validity of both the nearest-instanton approximation and the IOPE. Usually, this does not cause concern because the sum rules are analyzed at momenta $Q^2 \gtrsim 1 \text{ GeV}^2$ where both approximations should work. However, the lowest Borel moment (with $k = -1$) by design contains the $Q^2 = 0$ limit of the correlator as a subtraction constant. This term is not eliminated by the Borel transform since the latter is applied to $\Pi(Q^2)/Q^2$:

$$\mathcal{L}_{S,-1}^{(I+\bar{I})}(\tau) = \hat{B}\left[-\frac{\Pi_S^{(I+\bar{I})}(0)}{Q^2} + \frac{\Pi_S^{(I+\bar{I})}(Q^2) - \Pi_S^{(I+\bar{I})}(0)}{-Q^2}\right] \tag{120}$$

$$= -\Pi_S^{(I+\bar{I})}(0) + \frac{1}{\pi} \int_0^\infty ds \frac{\text{Im}\Pi_S^{(I+\bar{I})}(-s)}{s} e^{-s\tau}, \tag{121}$$

which of course also follows directly from Eq. (118) with $\hat{B}[Q^{-2}(s + Q^2)^{-1}] = s^{-1}[1 - \exp(-s\tau)]$ and implies both

$$\lim_{\tau \to 0} \mathcal{L}_{S,-1}^{(I+\bar{I})}(\tau) = 0 \tag{122}$$

[cf. Eq. (118) at $Q^2 = 0$] and in the opposite limit

$$\lim_{\tau \to \infty} \mathcal{L}_{S,-1}^{(I+\bar{I})}(\tau) = -\Pi_S^{(I+\bar{I})}(Q^2 = 0) \tag{123}$$

[in agreement with Eq. (111)].

Note that the zero-momentum limit (102) of the correlator can be recovered from the dispersive representation (118) as

$$\Pi_S^{(I+\bar{I})}(Q^2 = 0)$$
$$= -2^4\pi^3 \int d\rho n(\rho)\rho^4 \int_0^\infty ds s J_2(\sqrt{s}\rho)Y_2(\sqrt{s}\rho)$$
$$= 2^7\pi^2 \int d\rho n(\rho), \tag{124}$$

where we have made use of the integral [57]

$$\int_0^\infty ds s J_2(\sqrt{s}\rho)Y_2(\sqrt{s}\rho) = -\frac{8}{\pi\rho^4}. \quad (125)$$

In order to avoid subtraction constants of this type, moments with negative k are usually not considered in sum rule applications. In the spin-0 glueball channels, however, the $k = -1$ moments are particularly useful because the subtraction terms on the phenomenological side [cf. Eq. (28)] are determined by the low-energy theorems of Sec. II A. As shown above, the implementation of this additional first-principle information comes at the price of dealing with the IOPE-induced subtraction constants, too. Their interpretation, treatment, and role in the $k = -1$ sum rules will be the subject of Sec. VI C.

The dispersive representation of the higher Borel moments follows from Eq. (121) by taking the appropriate number of τ derivatives, according to the recursion (106). This results in

$$\mathcal{L}_{S,k}^{(I+\bar{I})}(\tau) = -\delta_{k,-1}\Pi_S^{(I+\bar{I})}(Q^2 = 0)$$
$$+ \frac{1}{\pi}\int_0^\infty ds s^k \mathrm{Im}\Pi_S^{(I+\bar{I})}(-s)e^{-s\tau} \quad (126)$$

$$= -2^7\pi^2\delta_{k,-1}\int d\rho\, n(\rho)$$
$$- 2^4\pi^3\int d\rho\, n(\rho)\rho^4\int_0^\infty ds s^{k+2}J_2(\sqrt{s}\rho)Y_2(\sqrt{s}\rho)e^{-s\tau}. \quad (127)$$

Note that the UV convergence of the dispersion integrals is ensured by the Laplace kernel and that Eq. (127) is often easier to handle than the individual integrated expressions (105)–(109). Moreover, the subtraction of the instanton-induced continuum [cf. Eq. (27)],

$$\mathcal{R}_{S,k}^{(I+\bar{I})}(\tau;s_0) = \mathcal{L}_{S,k}^{(I+\bar{I})}(\tau) - \frac{1}{\pi}$$
$$\times \int_{s_0}^\infty ds s^k \mathrm{Im}\Pi_S^{(I+\bar{I})}(-s)e^{-s\tau}, \quad (128)$$

provides now immediately a compact expression for the instanton contributions to all 0^{++} glueball sum rules:

$$\mathcal{R}_{S,k}^{(I+\bar{I})}(\tau;s_0) = -2^7\pi^2\delta_{k,-1}\int d\rho\, n(\rho) - 2^4\pi^3\int d\rho\, n(\rho)\rho^4$$
$$\times \int_0^{s_0} ds s^{k+2}J_2(\sqrt{s}\rho)Y_2(\sqrt{s}\rho)e^{-s\tau}. \quad (129)$$

[These contributions are not affected by perturbative (one-loop) RG improvement since the anomalous dimension of the interpolating field $O_S(x)$ vanishes to this order.]

Depending on the choice for $n(\rho)$, the size of the instanton-induced Borel moments (129) is either significantly larger or comparable to the size of their perturbative counterparts (61)–(64). The instanton continuum turns out to be indispensable for the sum rules to match at intermediate and small τ [13] since the perturbative continuum

cannot smoothly extend the exponentially vanishing instanton contributions (127) towards $\tau \to 0$ [cf. Eq. (110)].

E. Analytical results for specific instanton size distributions

In order to learn more about the impact of finite-width distributions $n(\rho)$ on the spectral function (115) and the derived Borel moments, it will prove useful to carry out the integration over the instanton size analytically. As mentioned in Sec. IV A, this becomes possible when specializing to the exponential-tail distribution (76). First, however, we are going to establish the point of reference for later comparison by briefly reviewing the results for the spike distribution (73). Inserting it into the instanton-induced spectral function (115) results in

$$\mathrm{Im}\Pi_{S,\mathrm{spk}}^{(I+\bar{I})}(-s) = -2^4\pi^4\bar{n}\bar{\rho}^4 s^2 J_2(\sqrt{s}\bar{\rho})Y_2(\sqrt{s}\bar{\rho}), \quad (130)$$

which was used in [13] and subsequent work. The plot of this expression in Fig. 1(a) shows, besides the expected rather violent oscillations with increasing amplitude (note the scale), a strong violation of positivity for $s \gtrsim 4$ GeV^2. (We use the standard instanton scales $\bar{n} = 0.75 \times 10^{-3}$ GeV^{-4} and $\bar{\rho} = 1.69$ GeV^{-1} throughout the paper.) At small s, the spike-induced imaginary part starts out quadratically,

$$\mathrm{Im}\Pi_{S,\mathrm{spk}}^{(I+\bar{I})}(-s) \overset{s\to 0}{\to} 2^3\pi^3\bar{n}(\bar{\rho}^2 s)^2. \quad (131)$$

At large s the rise becomes slightly weaker and gets modulated by a harmonic oscillation [cf. Eq. (117)]. The direct instanton contributions to the continuum-subtracted Borel moments simplify to

$$\mathcal{R}_{S,k,\mathrm{spk}}^{(I+\bar{I})}(\tau) = -2^7\pi^2\bar{n}\delta_{k,-1}$$
$$- 2^4\pi^3\bar{n}\bar{\rho}^4\int_0^{s_0} ds s^{k+2}J_2(\sqrt{s}\bar{\rho})Y_2(\sqrt{s}\bar{\rho})e^{-s\tau}. \quad (132)$$

Now we derive the analogous results on the basis of the more realistic finite-width distribution (76) with exponential large-ρ tail. Although a Gaussian falloff is favored by instanton liquid and lattice simulations (cf. Sec. IV A) and modifies the detailed behavior of the instanton-induced imaginary part at $s \lesssim \bar{\rho}^{-2}$, the resulting expressions will be a useful benchmark for assessing qualitative effects of realistic $n(\rho)$ (and for evaluating them numerically). The exponential-tail distribution (76) specializes the imaginary part (115) to

$$\mathrm{Im}\Pi_{S,\mathrm{exp}}^{(I+\bar{I})}(-s) = -\frac{2\cdot 5^5\pi^4}{3}\frac{\bar{n}}{\bar{\rho}^5}s^2$$
$$\times \int_0^\infty d\rho\, \rho^8 J_2(\sqrt{s}\rho)Y_2(\sqrt{s}\rho)e^{-5\rho/\bar{\rho}}. \quad (133)$$
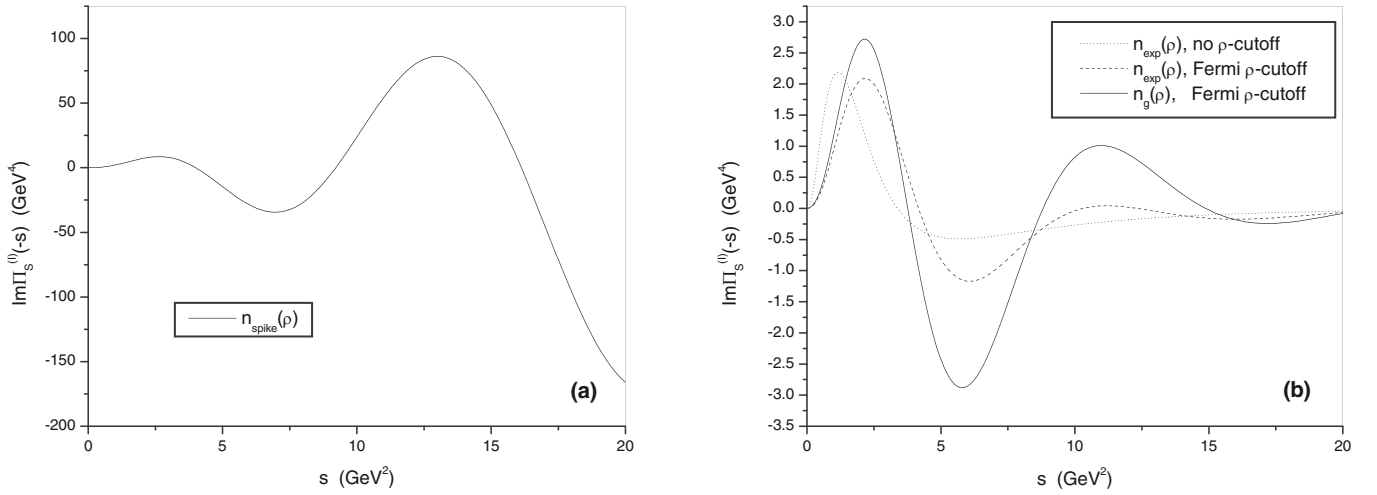
FIG. 1. Direct-instanton-induced imaginary part of the 0^{++} glueball correlator, $\mathrm{Im}\Pi_S^{(I+\bar{I})}(-s)$, obtained on the basis of (a) the spike and (b) finite-width instanton size distributions. In (b) the results for the exponential-tail distribution without (dotted line) and with (dashed line) large-ρ cutoff as well as for the Gaussian-tail distribution with large-ρ cutoff (solid line) are plotted. Note the difference in scale between (a) and (b).

A somewhat lengthy but essentially straightforward calculation shows that the ρ integral can be expressed as a combination of three hypergeometric functions,

$$\mathrm{Im}\Pi_{S,\exp}^{(I+\bar{I})}(-s) = \frac{5^5\pi^4}{2^{22}3}\frac{\bar{n}}{\bar{\rho}^9}s^{-9/2}\left\{3^45^27^211\left[2^7s^2\bar{\rho}^4{}_2F_1\left(\frac{9}{2},\frac{13}{2},5,-\frac{25}{4s\bar{\rho}^2}\right) + 3\cdot5\cdot13\left(-2^53s\bar{\rho}^2{}_2F_1\left(\frac{11}{2},\frac{15}{2},6,-\frac{25}{4s\bar{\rho}^2}\right)\right.\right.$$
$$\left.\left. + 5^311{}_2F_1\left(\frac{13}{2},\frac{17}{2},7,-\frac{25}{4s\bar{\rho}^2}\right)\right)\right]\right\}. \tag{134}$$

This spectral function is plotted in Fig. 1(b). Comparison with its counterpart (130) in Fig. 1(a) reveals that the finite-width distribution has turned the problematic, spike-induced oscillations into a monotonic falloff at large s.

More specifically, owing to ${}_2F_1(a, b, c, 0) = 1$, the first and leading term in (134) decays as

$$\mathrm{Im}\Pi_{S,\exp}^{(I+\bar{I})}(-s)\stackrel{s\to\infty}{\to}\frac{3^35^77^211\pi^4}{2^{15}}\frac{\bar{n}}{\bar{\rho}^5}s^{-5/2}. \tag{135}$$

The damping of the large-s oscillations is a generic effect of finite-width distributions. Nevertheless, the imaginary part (134) still changes sign once, due to the interference among the individual terms. The associated positivity violations are much milder than those in Eq. (130), however, and their impact on the Borel moments in the relevant τ region is strongly reduced. Moreover, the imaginary part of the full IOPE is now nonnegative for all s, as it should be. We therefore expect that extended size distributions will improve the consistency of the Borel sum rules.

At small s, Eq. (134) becomes

$$\mathrm{Im}\Pi_{S,\exp}^{(I+\bar{I})}(-s)\stackrel{s\to0}{\to}\frac{2^73\cdot7\pi^3}{5^3}\bar{n}(\bar{\rho}^2s)^2. \tag{136}$$

It is instructive to compare the above behavior to the $s\to0$ limit (131) of the spike distribution: the quadratic s depen-

dence is maintained but Eq. (136) is about 3 times larger. This enhancement can be traced to the large-ρ tail of $n_{\exp}(\rho)$ by expressing the small-s behavior of the instanton-induced spectral function for general $n(\rho)$ as

$$\mathrm{Im}\Pi_S^{(I+\bar{I})}(-s)\stackrel{s\ll\bar{\rho}^{-2}}{\to}2^3\pi^3\bar{n}\langle\rho^4\rangle s^2, \tag{137}$$

where $\langle\rho^4\rangle$ is the fourth moment of the instanton size distribution. Comparison with Eq. (131) or direct evaluation via Eq. (76) shows that

$$\langle\rho^4\rangle_{\exp} = \frac{2^43\cdot7}{5^3}\bar{\rho}^4, \tag{138}$$

which relates the enhancement factor to the increased weight of instantons with $\rho > \bar{\rho}$. We therefore anticipate this factor to be reduced when the large-ρ contributions are excluded from the IOPE coefficients in Sec. IV F.

In view of the rather dramatic enhancement and modulation of the instanton-induced spectral function at large s by the spike distribution, one might wonder how the latter can produce useful approximations to the continuum-subtracted Borel moments (129) at all. The reason is two-fold: first, these moments are essentially Laplace transforms of the spectral function,

$$\mathcal{R}_{S,k}^{(I+\bar{I})}(\tau; s_0) = -2^7\pi^2\delta_{k,-1}\int d\rho n(\rho) - \frac{1}{\pi}$$
$$\times \int_0^{s_0} ds s^k \text{Im}\Pi_S^{(I+\bar{I})}(-s)e^{-s\tau}, \quad (139)$$

which implies that contributions from the $s \gg \tau^{-1}$ region are exponentially suppressed. In addition, the large-s contributions of the spike-induced spectral function

partially cancel each other due to the modulating oscillations. The impact of the large-s behavior on the Borel moments is therefore strongly reduced (except at very small τ which are irrelevant for the sum rule analysis, see below).

In order to explore the effects of finite-width distributions on the τ and s_0 dependence of the Borel moments more quantitatively, we again resort to the exponential-tail distribution which yields

$$\mathcal{R}_{S,k,\exp}^{(I+\bar{I})}(\tau, s_0) = -2^7\pi^2\delta_{k,-1}\int d\rho n_{\exp}(\rho) + \frac{5^5\pi^3}{2^{22}3}\frac{\bar{n}}{\bar{\rho}^9}\int_0^{s_0} ds s^{k-4}e^{-s\tau}\left\{3^4 5^2 7^2 11\left[2^7 s^2 \bar{\rho}^4 {}_2F_1\left(\frac{9}{2},\frac{13}{2},5,-\frac{25}{4s\bar{\rho}^2}\right)\right.\right.$$
$$\left.\left. + 3\cdot 5\cdot 13\left(-2^5 3 s\bar{\rho}^2 {}_2F_1\left(\frac{11}{2},\frac{15}{2},6,-\frac{25}{4s\bar{\rho}^2}\right) + 5^3 11 {}_2F_1\left(\frac{13}{2},\frac{17}{2},7,-\frac{25}{4s\bar{\rho}^2}\right)\right)\right]\right\}. \quad (140)$$

Obviously, all Borel moments reach finite limits for $\tau \to 0$. Towards $\tau \to \infty$ we find from Eq. (137) that the τ dependence of the Borel moments vanishes as

$$\mathcal{R}_{S,k}^{(I+\bar{I})}(\tau, s_0) \overset{\tau\to\infty}{\to} -2^7\pi^2\delta_{k,-1}\int d\rho n(\rho)$$
$$+ 2^3\pi^2(k+2)!\frac{\bar{n}\langle\rho^4\rangle}{\tau^{k+3}}[1-\rho_{k+2}(s_0\tau)], \quad (141)$$

where we have used the definition (56) for the partial sums $\rho_k(x)$. Of course this result holds for all reasonable instanton size distributions: specific choices for $n(\rho)$ do not affect the τ dependence but just the overall magnitude of the moments at $\tau \gg \bar{\rho}^2$.

The impact of finite-width distributions on the s_0 dependence of the Borel moments (which generates the $0^\pm$-channel dependence of the direct instanton contributions) will play an important role in our subsequent discussion. From Eq. (140) we find that in the sum-rule-relevant (τ, s_0) region (specifically for $s_0 \gtrsim 2-4$ GeV^2 and $\tau \gtrsim 0.2$ GeV^{-1}) the magnitude of the instanton contributions decreases more strongly with increasing s_0 if the exponential-tail distribution is employed. The direct instanton contributions to the pseudoscalar glueball sum rule, where s_0 is typically a factor of 2 larger than in the scalar channel, therefore become smaller than those to the scalar sum rule. This reduces the instanton-induced repulsion in the 0^{-+} channel without significantly weakening the important attraction in the 0^{++} channel.

Furthermore, we observe that for sufficiently large s_0 the instanton-induced Borel moments (140) turn negative at small τ. (For the $k=0$ moment this happens if $\tau \lesssim \tau_c \sim 0.3$ GeV^{-2}. For $k>0$, τ_c increases due to the stronger s^k weight of the spectral function at larger s.) This positivity violation (which grows with s_0 and therefore has more impact on the pseudoscalar sum rule) would reduce the fiducial τ domain of the associated Borel sum rules (cf. Sec. VI D) but does not *a priori* prohibit a sum rule

analysis. Nevertheless, it exposes a shortcoming of Eq. (140) which can be traced to the contributions from large instantons. In fact, we will argue in the next section on general grounds that such contributions have to be excluded from the IOPE coefficients. (The discussion of the far more serious instanton-induced positivity violations at *large* τ in the 0^{-+} channel will be the subject of Sec. V.)

Finally, we note that the above results remain qualitatively unchanged when $n_{\exp}(\rho)$ is replaced by the Gaussian-tail distribution (85). Even the quantitative results are generally very similar, as expected from the arguments of Sec. IV A and confirmed by numerical integration of the corresponding ρ integrals.

F. Implementation of the operator renormalization scale

In the exact version of the (I)OPE, contributions to the Wilson coefficients originate exclusively from hard field modes with momenta larger than the operator renormalization scale μ [4,59]. Potential double-counting of soft modes and IR renormalons [60] are thereby excluded from the outset and the μ independence of (RG-invariant) short-distance amplitudes becomes manifest. However, the gauge-invariant implementation of IR cutoffs in the perturbative Wilson coefficients is technically complex and commonly neglected in QCD sum rule applications (with a few exceptions[10]). This "pragmatic" approximation works well since in QCD soft perturbative amplitudes are generally much smaller than their nonperturbative counterparts (which generate the condensates).

However, it is *a priori* unclear whether the pragmatic neglect of IR cutoffs works for nonperturbative Wilson coefficients as well, as tacitly assumed in all previous work on direct instantons. In the following we will argue

---

[10]If IR divergencies are encountered, see, e.g., Refs. [61]

that realistic, finite-width instanton size distributions permit an explicit and straightforward implementation of such IR cutoffs for the direct instanton contributions. This allows us to improve upon the pragmatic treatment of the nonperturbative sector and to assess its conceptual basis and range of validity. (The exceptional strength of the direct instanton contributions makes the spin-0 glueball correlators a particularly suitable testing ground for this renomalization.)

Our implementation of the renormalization scale μ is based on the observation that an instanton of fixed size ρ mainly contributes field modes with momenta $|k| < \rho^{-1}$ to the correlator. The contributions of large instantons with $\rho > \mu^{-1}$ and the fluctuations around them are therefore almost exclusively soft and should be excluded from the Wilson coefficients. This (partial, see below) cutoff procedure is gauge invariant simply because the instanton size is. Since the renormalization scale associated with the conventional condensate values (cf. Sec. VI A) is not very accurately determined, it would not make sense to treat μ^{-1} as a sharp cutoff. Instead, we implement it smoothly by replacing the full instanton size distribution $n(\rho)$ with

$$\tilde{n}_{\mu}(\rho) \equiv \theta_{\beta}(\mu^{-1} - \rho)n(\rho), \qquad (142)$$

where the soft step function θ_{β} can be chosen, e.g., in the form of a Fermi distribution

$$\theta_{\beta}(\mu^{-1} - \rho) = \frac{1}{2}\left\{1 - \tanh\left[\frac{\beta}{2}(\rho - \mu^{-1})\right]\right\}. \quad (143)$$

The "diffuseness" parameter β sets the scale for the width of the transition region. With $\beta \ll \mu$ the cutoff practically ceases to exist, i.e., all instanton sizes are about evenly affected, whereas for $\beta \gg \mu$ a sharp cutoff is reached. For practical calculations we find values $\beta \sim 5\bar{\rho}^{-1} \sim 3$ GeV to be an effective compromise between these extremes. [For $\beta \gtrsim 5$ GeV strong oscillations of the imaginary part set in (even at $s > 20$ GeV^2) while for $\beta \lesssim 2$ GeV the cutoff is already rather ineffective.] Alternatively, we will use

$$\theta_{\beta}(\mu^{-1} - \rho) = \frac{1}{2} - \frac{1}{\pi} \arctan[\beta(\rho - \mu^{-1})], \quad (144)$$

which has a softer transition region and a bigger large-ρ tail for equal values of β, to estimate the sensitivity of the sum rule results to the details of the cutoff procedure.

The physical interpretation of the above μ implementation is very transparent: the modified distribution (142) just excludes non-direct instanton contributions to the IOPE coefficients since those are already included in the condensates.[11] Nevertheless, this does not exclude *all* $|k| < \mu$

modes since even arbitrarily small instantons contain some soft contributions.[12] A complete renormalization would naively amount to replacing

$$G_{\mu}^{(I)}(x) \rightarrow \int_{|k|<\mu} \frac{d^4k}{(2\pi)^4} e^{-ikx} \tilde{G}_{\mu}^{(I)}(k), \qquad (145)$$

where $\tilde{G}_{\mu}^{(I)}$ is the Fourier transform of the instanton field. However, such a procedure is unacceptable since it violates gauge invariance. In fact, devising a gauge-invariant cutoff is a complex task since gauge transformations generally change the momentum content of the fields. This problem is well known in the application of Wilson's renormalization group to gauge fields and has not yet been solved satisfactorily (although it could, at least in principle, be tackled on the lattice by a coarse-graining procedure analogous to spin blocking). Nevertheless, there is reason to believe that our above, simplified renormalization of the direct instanton contributions is sufficiently complete since the overall momentum transfer Q acts as an additional IR cutoff [63], by suppressing field modes with momenta $k \ll Q$.

An interesting question in this context concerns the direct-instanton-induced μ dependence. The μ dependence of both the perturbative coefficients and the condensates (which arise from the anomalous dimensions) is logarithmic (cf. Appendix A) and therefore rather weak.[13] Since mutual cancellations among all contributions are required to render the correlators μ independent, one expects the μ dependence of the nonperturbative coefficients to be similarly weak. This turns out to be indeed the case, mainly because large-ρ contributions are already strongly suppressed by the external momentum scale $Q \gtrsim 1$ GeV in Eq. (99) and by the Gaussian tail (72) of realistic instanton size distributions. Hence the μ^{-1} cutoff does only reduce intermediate-size instanton contributions significantly, implying a relatively weak μ dependence for $\mu < \bar{\rho}^{-1}$ (which holds for $\mu = 0.5$ GeV and $\bar{\rho}^{-1} \simeq 0.6$ GeV adopted below).

---

[11]Note that the large-ρ cutoff affects higher-$O(\hbar)$ corrections as well since it effectively restricts the internal momenta of the quantum fluctuations.

[12]Another way to see that the large-ρ cutoff cannot entirely exclude soft contributions derives from the singularity structure of the direct instanton contributions (92) at $x = 0$, as discussed in Sec. IV B. Indeed, potential instanton-induced power corrections are not removed by the large-ρ cutoff because the small-x singularity structure is not affected by large instantons (for physically sensible $n(\rho)$). (The nucleon correlator IOPE [17] provides a simple example: instanton-induced power corrections are present despite the large-ρ "cutoff" implicit in the spike distribution.) Note, incidentally, that the self-duality (15) of the instanton's field strength severely restricts potential instanton-induced power corrections in quark-based correlators (to at most a few terms) [62].

[13]Additional μ dependence of the condensates due to nonperturbative physics (e.g., due to instantons [64,65]) can of course not be excluded. Our results and general sum rule experience suggest, however, that it should be similarly weak for $\mu/\Lambda_{QCD} \sim 2 - 3$.

One could contemplate, incidentally, to identify $\mu = Q$ in Eq. (142) by analogy with the RG improvement of the perturbative IOPE coefficients. However, avoiding or summing large logarithms is not an issue here. Furthermore, the impact on the sum rules would be limited by the moderate μ dependence, and the additional s dependence in the spectral integrals of Eq. (129) would obscure the comparison with spike distribution results. We will therefore keep μ fixed in the quantitative analysis below.

The implementation of μ has several significant effects. One of them is the reduction of the instanton-induced imaginary part for $s \ll \mu^2$ (where mainly the excluded soft modes had contributed), and a second one is the shift of its leading peak towards larger s. Both features can be understood by noting that

$$\mathrm{Im}\Pi_S^{(I+\bar{I})}(-s) \overset{s \ll \mu^2 < \bar{\rho}^{-2}}{\longrightarrow} 2^3\pi^3\bar{n}s^2$$
$$\times \left[\langle\rho^4\rangle_\mu + \frac{1}{6}\langle\rho^6\rangle_\mu s + O(s^2) \right], \tag{146}$$

for $s \ll \mu^2$, where we have defined the moments of the renormalized size distribution $\tilde{n}(\rho)$ as

$$\langle\rho^k\rangle_\mu = \frac{1}{\bar{n}} \int_0^\infty d\rho\, \rho^k \tilde{n}_\mu(\rho). \tag{147}$$

The reduced magnitude of the imaginary part (146) is obviously due to $\theta_\beta(\mu^{-1} - \rho) < 1$ for all ρ, which implies $\langle\rho^k\rangle_\mu < \langle\rho^k\rangle$. The shift of the peak is caused by the stronger reduction of the higher moments: due to the asymmetry of $n(\rho)$, impressed by its limiting behavior [cf. Eqs. (71) and (72)], $\langle\rho^k\rangle/\bar{\rho}^k$ increases with increasing k. Since this enhancement originates from the large-ρ tail of the distribution, it is strongly reduced by renormalization and the ratio $\langle\rho^k\rangle_\mu/\langle\rho^k\rangle$ therefore decreases with k.

Another significant renormalization effect is the reduction of the number of "active" instantons in the Wilson coefficients, i.e.,

$$\bar{n} = \int_0^\infty d\rho\, n(\rho) \rightarrow \int_0^\infty d\rho\, \tilde{n}_\mu(\rho) \equiv \bar{n}_{\mathrm{dir}} \equiv \zeta\bar{n}, \quad (148)$$

with $\zeta < 1$, where $\bar{n}_{\mathrm{dir}}$ correctly accounts for the density of *direct* instantons. This effect is missed when using the spike distribution since it is normalized to the total instanton density, i.e., large instantons with $\rho > \bar{\rho}$ are not excluded but simply counted as instantons of average size. (This suggests to use $\bar{n}_{\mathrm{dir}}$ instead of $\bar{n}$ to improve direct-instanton calculations on the basis of the spike distribution.) The above reasoning indicates, incidentally, that direct-instanton calculations involving the spike distribution strictly make sense only for $\bar{\rho} < \mu^{-1}$. Although satisfied by the (not very accurately determined) standard values $\mu^{-1} \sim 0.4$ fm and $\bar{\rho} \sim 0.33$ fm, this condition would be violated by larger choices for μ and/or $\bar{\rho}$.

Summarizing the main results of this section, we find the exclusion of nondirect instantons by an explicit large-ρ cutoff to be mandatory when implementing finite-width distributions. However, the pragmatic neglect of μ *together* with the use of the spike distribution (with $\bar{\rho} < \mu^{-1}$) can be useful for an approximate estimate of the Borel moments since large instantons (with $\rho \gg \bar{\rho}$) are rare in the QCD vacuum and since their contributions are bounded by Q^{-1} acting as an additional cutoff. This justifies the tacit assumption underlying earlier implementations of direct instantons. Nevertheless, the renormalization generates several new and important effects, including an effective reduction of the instanton density, which will significantly improve both sum rule consistency and results (see Sec. VI).

V. IOPE 3: TOPOLOGICAL CHARGE SCREENING

The direct instanton contributions to 0^{++} and 0^{-+} glueball correlators differ only in their sign (cf. Secs. II B and IV). As a consequence, the instanton-induced attraction in the scalar channel turns into a strong repulsion in the pseudoscalar channel. Therefore it is hardly surprising that the signal for the pseudoscalar glueball disappears and that even the general positivity requirement is violated [42] when these repulsive contributions are added to the perturbative Wilson coefficients. We demonstrate this by plotting the $k = 0$ Borel moment in the 0^{-+} channel,

$$\mathcal{R}_{P,0}^{(\mathrm{pc}+I)}(\tau; s_0) = \frac{1}{\pi} \int_0^{s_0} ds[\mathrm{Im}\Pi_P^{(\mathrm{pc})}(-s)$$
$$+ \mathrm{Im}\Pi_P^{(I+\bar{I})}(-s)]e^{-s\tau}, \tag{149}$$

obtained from both perturbative and instanton-induced Wilson coefficients [on the basis of the spike distribution (73)], in Fig. 2(a). The sum-rule-relevant s_0 range starts at $s_0 \gtrsim$ 6–8 GeV^2, where the Borel moment indeed becomes negative for $\tau \gtrsim 0.8$ GeV^{-2}, i.e., in the middle of the fiducial domain (cf. Sec. VI). (The negative areas of the Borel moment at smaller s_0 and τ are an artifact of the spike distribution which will be removed by realistic instanton size distributions, cf. Sec. VI.) Moreover, the τ slope becomes positive for $\tau \gtrsim 1$ GeV^{-2}, and both features make a match to the decaying exponential of a resonance [cf. Eq. (28)] impossible. Contrary to lattice results [28,43], the corresponding sum rule would therefore predict the absence of low-lying pseudoscalar glueballs. In addition, we will find below that the low-energy theorem (14) in the 0^{-+} channel would be badly violated.

In search for the origin of these problems one should keep in mind that the (up to the sign) identical expressions for the direct instanton-induced Borel moments (129), involving the same approximations, play a highly beneficial role in the 0^{++} sum rules and enhance their consistency [13]. In fact, this might not be as paradoxical as it first appears: although the moments (129) have the same
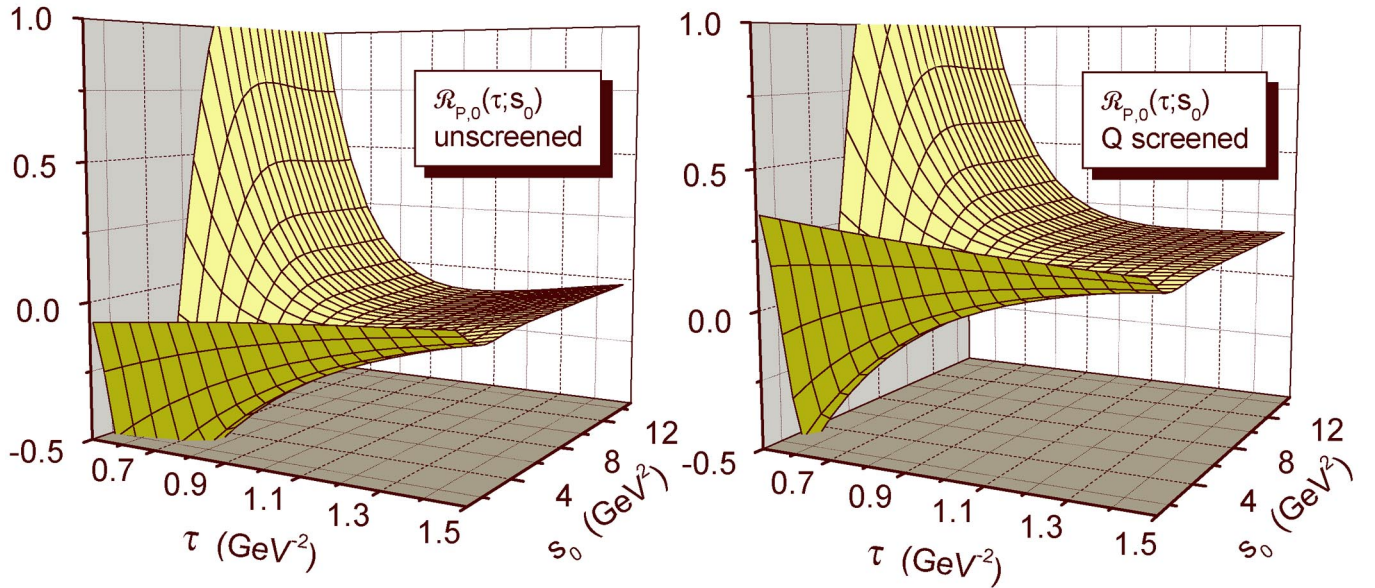
FIG. 2 (color online).   The $k = 0$ continuum-subtracted IOPE Borel moment of the 0^{-+} glueball correlator, calculated on the basis of the spike distribution (a) without (left panel) and (b) with (right panel) topological charge screening contributions.

magnitude in both channels, the direct instanton contributions to the sum rules do not. The difference lies in the value of the duality threshold s_0 which is typically more than twice as large in the 0^{-+} than in the 0^{++} channel. (This is mainly a reflection of the larger 0^{-+} glueball mass.) Their rather strong s_0 dependence thus equips the direct instanton contributions with a certain channel dependence.

As demonstrated above, however, this channel dependence is too weak to resolve the mentioned deficiencies. Yet it is conceivable that the underlying approximations, i.e., the spike distribution and the neglected renormalization, may have underestimated the s_0 dependence. Partly for this reason we have improved upon these standard approximations, by implementing realistic instanton size distributions and the renormalization scale. It turns out that their combined impact indeed mitigates the problems in the 0^{-+} glueball channel, but it is too small to resolve any of them.

Thus we face for the first time the situation that direct instanton contributions seem to worsen the consistency of a set of QCD sum rules and to create serious new problems. Since our treatment of the direct instanton sector leaves not much room for further improvement,[14] one is bound to conclude that essential additional physics is still missing in the IOPE coefficients of the 0^{-+} glueball correlator. Our main guide in the search for this physics, which will be the

subject of the next section, is the fact that it apparently did not show up in other hadron channels: previously considered sum rules were found to be consistent and stable with perturbative and direct-instanton-induced Wilson coefficients only.

A. Topological charge correlations

As argued above, the failure of direct instanton contributions to generate acceptable pseudoscalar glueball sum rules strongly suggests that equally important—and therefore very likely nonperturbative—contributions to the Wilson coefficients are still amiss. Since these contributions should affect almost exclusively the 0^{-+} glueball correlator, one is led to search for a unique property which singles this channel out among other hadron correlators. The result is quite obvious: the interpolating field O_P is proportional to the topological charge density Q,

$$O_P(x) = 8\pi Q(x), \qquad (150)$$

which implies that the 0^{-+} glueball correlator is proportional to the topological charge correlator.[15] Hence it distinguishes in the strongest possible way between instantons and anti-instantons and is highly sensitive to instanton-anti-instanton correlations. [In contrast, $O_S(x)$ is proportional to the gluonic action density and therefore treats instantons and anti-instantons on the same footing.]

---

[14]As discussed in Sec. IV, multi-instanton effects are generally negligible, due to the small instanton packing fraction. In the pseudoscalar meson channel, where direct instanton contributions have exceptional strength [55], this was shown explicitly [46].

[15]As a consequence of the chiral anomaly (see below), the same holds for the correlator of the divergence of the flavor-singlet axial current (with the quantum numbers of the η_0) in the chiral limit. This correlator is thus equally sensitive to topological charge correlations.

The correlations between topological charges are generated by light-quark exchange or, equivalently at low energy, by the exchange of flavor-singlet pseudoscalar mesons. The form of these interactions is dictated by the axial U(1) anomaly [66]

$$\partial_\mu \sum_{i=u,d,s} \bar{q}_i \gamma_\mu \gamma_5 q_i = 2 \sum_{i=u,d,s} m_i \bar{q}_i i \gamma_5 q_i + 2N_f Q. \quad (151)$$

Compliance with the ensuing behavior under $U_A(1)$ transformations requires the lightest pseudoscalar flavor-singlet meson η_0 to couple to the topological charge density as [18]

$$\Delta \mathcal{L} = -i\gamma_{\eta_0} Q(x) \eta_0(x), \quad (152)$$

where the coupling γ_{η_0} is often written as $\gamma_{\eta_0} = \sqrt{2N_f}/f_{\eta_0}$. The form of this interaction and most of its qualitative consequences do not depend on the specific origin of $Q(x)$. Instanton models and lattice simulations indicate that the topological charge density in the QCD vacuum is rather strongly localized and mostly carried by instantons [9,67], however, and we will adopt this picture in some of the developments below. Owing to the coupling (152), η_0 exchange generates strong correlations between topological charges which add to the direct instanton-induced ones (of range $\bar{\rho}$) evaluated in Sec. IV. The quark chiralities entering the anomaly Eq. (151) require the η_0-mediated interactions to be attractive (repulsive) between topological charges of opposite (equal) sign.

Between isolated topological charges these interactions would be of long range since the η_0 would be a light (quasi-) Goldstone boson. In the topological charge ensemble of the QCD vacuum, however, the η_0-exchange forces are screened by the formation of Debye-Hückel clouds [68] in which positive (negative) topological charges surround themselves with negative (positive) ones. This collective mechanism, in turn, renders the η_0-induced interactions short-ranged by generating a screening mass for the η_0[16] (which solves the $U(1)$ problem [69]). Topological charge screening has been discussed in Refs. [70,71] and investigated in ILM [72] as well as unquenched lattice [73,74] simulations. Indirect evidence for strongly localized screening clouds also has been found in the difference-to-sum ratio of the isovector scalar and pseudoscalar ILM correlators [75] where "unquenching" strongly suppresses the instanton-induced spin-flip probability for a propagating quark at short distances.

In order to understand how topological charge screening affects the IOPE, one has to compare the factorization scale μ with the characteristic scale of the screening

mechanism. Since the physical η' mass (i.e., the η_0 mass after $\eta_0 - \eta_8$ mixing is taken into account, see below) is about twice as large as μ, topological charge screening takes place over distances of the order of the screening length

$$\lambda_{\mathrm{scr}} \simeq \frac{1}{m_{\eta'}} \sim 0.2 \text{ fm} < \mu^{-1}, \quad (153)$$

which are small on the IOPE scale. Hence screening contributes mainly to the Wilson coefficients. This also follows directly from the observation that Q screening strongly influences the x dependence of the topological charge correlator at $|x| \lesssim \lambda_{\mathrm{scr}} \ll \Lambda_{\mathrm{QCD}}^{-1}$, which resides exclusively in the Wilson coefficients. And since Q screening is a nonperturbative and collective mechanism originating from the light-quark sector, it obviously cannot be described either by perturbative or by direct instanton contributions. Thus we have reached our objective to uncover nonperturbative contributions to the Wilson coefficients which go beyond the direct instanton approximation and affect almost exclusively the 0^{-+} glueball correlator.

Under the premise that the topological vacuum charge density is mostly associated with instantons, the screening corrections can be identified with multi-instanton effects.[17] In fact, topological charge screening has been observed in instanton vacuum model calculations and found to affect mostly the 0^{-+} glueball and η' channels [9,15]. Even if light-quark-induced interactions and therefore screening effects are neglected, phenomenological and lattice results in the majority of all calculated hadron correlators are well reproduced. However, in the η' and the related 0^{-+} glueball channel (and to a lesser degree in the scalar-isovector a_0 meson channel) this approximation clearly fails and the η' correlator turns negative. Unquenching of the light-fermion sector resolves these problems and generates the η' [76] and 0^{-+} glueball [15] resonances (although neglected interference terms between classical and one-loop effects did not allow to determine 0^{-+} glueball properties in Ref. [15]).

B. Screening contributions

The screening contributions to the topological charge correlator (and therefore to the 0^{-+} glueball correlator) can be calculated from the pertinent low-energy approximation to the (Euclidean) QCD generating functional

---

[16]Note the direct analogy with long-range Coulomb interactions which get screened into short-range Yukawa interactions between the electric charges of an electrolyte or a QED plasma, thereby turning the photon effectively massive.

[17]At first, there seems to be a certain analogy with the effective mass which instanton-induced quark zero modes acquire due to interactions with ambient, soft vacuum fields. This effective mass also goes beyond the isolated-instanton approximation. However, it originates from soft subgraph corrections (of mean field type) to hard subgraphs and therefore does not affect the x dependence of the Wilson coefficients. The topological charge screening corrections, in contrast, have a very pronounced x and channel dependence.

$$Z[\theta] = \int D\{A_\mu, q, \bar{q}\} \exp\left[-S_{\text{QCD}} + i \int d^4x \theta(x) Q(x)\right],$$

(154)

in the presence of a classical source $\theta(x)$. The correlation function of the topological charge density (and the related one for the 0^{-+} glueball) is then obtained by functional differentiation,

$$\langle Q(x)Q(0)\rangle = -Z[0]^{-1} \frac{\delta^2 Z[\theta]}{\delta\theta(x)\delta\theta(0)} \Big|_{\theta=0}.$$

(155)

We now outline the derivation of the appropriate low-energy approximation to $Z[\theta]$. (More details can be found in Refs. [70,71].) To begin with, one integrates over the quark fields and separates the domain of the gluonic integration variable into the underlying multi-instanton background and the nontopological remainder, over which one integrates first. [Of course, in practice this could be done at best approximately, on the lattice, but the part of the result which is relevant in our context will be obtained indirectly from the $U_A(1)$ anomaly (151) and effective field theory arguments.] It remains to sum over all classical multi-instanton configurations and to integrate over their collective coordinates $(U, \rho, x_0)_i$. Integrating over the color orientations U_i and sizes ρ_i turns the ith (anti-) instanton into a colorless lump of topological charge density centered at $x_{0,i}$. Equation (154) then becomes the partition function of a medium of localized topological charges (which we approximate as pointlike), interacting via a multilocal "potential" V:

$$Z[\theta] = \sum_{N_+,N_-} \frac{\bar{n}^{N_++N_-}}{N_+!N_-!} \left(\prod_{i=1}^{N_++N_-} \int d^4x_{0,i}\right)$$
$$\times \exp\left[-V(x_{0,1}...x_{0,N_++N_-}) + i\sum_{i=1}^{N} Q_i\theta(x_{0,i})\right],$$

(156)

where $\bar{n}$ is the average density of either positive or negative topological charges. In order to find an approximate expression for V, we recall that the lowest-lying excitations of the QCD vacuum are the pseudoscalar Goldstone bosons. Since (in the chiral limit) the flavor-singlet η_0 gets its mass from the topological gluon fields over which we did not integrate yet, we expect it at this stage to be part of a degenerate U(3) flavor nonet. At low energies, the interactions V between the topological charges will then be dominantly mediated by η_0 exchange,

$$V(x_{0,1}...x_{0,N_++N_-}) \simeq \sum_{i<j}^{N_++N_-} v_{\eta_0}(x_{0,i}, x_{0,j}),$$

(157)

with the coupling to $Q(x)$ determined by the axial anomaly [cf. Eq. (152)]. Since the η_0 contains a superposition of both quark chiralities with opposite sign, the anomaly implies that equal (opposite) topological charges repel

(attract) each other. We therefore have

$$v_{\eta_0}(x_{0,i}, x_{0,j}) = q_i q_j \int \frac{d^4q}{(2\pi)^4} \frac{\gamma_{\eta_0}^2}{q^2+m_{\text{NG}}^2} \exp[iq(x_{0,i}-x_{0,j})],$$

(158)

where $q_i = \pm 1$ is the topological charge located at $x_{0,i}$ and m_{NG}^2 is the part of the η_0 (Nambu-Goldstone) mass due to finite current quark masses. After absorbing an infinite factor into the renormalization of $\bar{n}$ and performing the remaining sums and integrals in Eq. (156), one ends up with the low-energy approximation

$$Z[\theta] \simeq \mathcal{N} \int D\eta_0 \exp(-S_{\text{eff}}[\eta_0, \theta]),$$

(159)

and the effective action [77]

$$S_{\text{eff}}[\eta_0, \theta] = \int d^4x \left[\frac{1}{2}(\partial\eta_0)^2 + \frac{1}{2}m_{\text{NG}}^2\eta_0^2 + 2\bar{n}\cos(\gamma_{\eta_0}\eta_0 + \theta)\right].$$

(160)

Expanding the action (160) up to $O(\eta_0^2)$ one finds that the interaction between the topological charges in the vacuum has generated the expected screening contribution

$$m_{\text{scr}}^2 = 2\bar{n}\gamma_{\eta_0}^2,$$

(161)

to the η_0 mass, $m_{\eta_0}^2 = m_{\text{NG}}^2 + m_{\text{scr}}^2$, which does not vanish in the chiral limit and solves the U(1) problem. [The tree approximation in Eq. (158) is reliable as long as $\bar{n}\gamma_{\eta_0}^4 \ll 1$ and $\bar{n}/m_{\text{NG}}^4 \gg 1$.] With the help of Eq. (155) we finally obtain the low-energy approximation

$$\langle Q(x)Q(0)\rangle = \frac{\Pi_P(x)}{(8\pi)^2} \simeq 2\bar{n}\delta^4(x) - (2\bar{n}\gamma_{\eta_0})^2\langle\eta_0(x)\eta_0(0)\rangle$$

(162)

to the topological charge correlator. Although we have referred to instantons as the source of the topological charge density $Q(x)$ for definiteness, the above arguments would hold with inessential modifications (e.g., in the set of collective coordinates) for other localized, topological charge carrying gluon fields as well.

The first term in Eq. (162) is just the correlation due to the topological charge "cloud" of a single-instanton in the pointlike limit (which we have adopted above for simplicity). This can be seen explicitly from the direct instanton contribution (92) by implementing the pointlike-instanton limit (94) with the help of the spike distribution for $\bar{\rho} = 0$, i.e., $n_{\text{pl}}(\rho) = \bar{n}\delta(\rho)$. The result

$$\frac{\Pi_{P,\rho\to0}^{(I+\bar{I})}(x)}{(8\pi)^2} = \frac{1}{(8\pi)^2}\int d\rho n_{\text{pl}}(\rho)\Pi_P^{(I+\bar{I})}(x^2; \rho) = 2\bar{n}\delta^4(x)$$

(163)

is indeed identical to the first term in Eq. (162). The second

term in Eq. (162) is the expected Debye screening correction.

C. Singlet-octet mixing, Borel moments and subtraction term

The screening contributions to the topological charge and 0^{-+} glueball correlators in Eq. (162) do not yet contain the $\eta_0 - \eta_8$ mixing corrections which arise from finite light-quark masses. These corrections are rather substantial, however, and should be implemented into the IOPE. This will also allow us to use the experimental η' and η meson masses and mixing angle, instead of extrapolations to the chiral limit. In addition, it is more consistent with our use of the standard condensate values below which were obtained from phenomenology and thus correspond to realistic light-quark masses.[18] The quark-mass dependence of the perturbative Wilson coefficients, on the other hand, originates from (dominantly strange) quark-loop corrections and should be negligible.

The screening contributions to Eq. (162) can be adapted to physical quark masses by expressing them in terms of the η and η' mass eigenstates. These are related to the singlet (η_0) and octet (η_8) flavor eigenstates by

$$\begin{pmatrix} |\eta_0\rangle \\ |\eta_8\rangle \end{pmatrix} = \begin{pmatrix} \cos\varphi & -\sin\varphi \\ \sin\varphi & \cos\varphi \end{pmatrix} \begin{pmatrix} |\eta'\rangle \\ |\eta\rangle \end{pmatrix}, \qquad (164)$$

where φ is the $\eta_0 - \eta_8$ mixing angle. The η_0 correlator therefore becomes

$$\langle \eta_0(x)\eta_0(0)\rangle = \cos^2\varphi\langle\eta'(x)\eta'(0)\rangle + \sin^2\varphi\langle\eta(x)\eta(0)\rangle, \qquad (165)$$

which allows us to rewrite the screening contributions to the topological charge correlator (162) in the form

$$\langle Q(x)Q(0)\rangle_{\text{scr}} = -(2\bar{n}\gamma_{\eta_0})^2[\cos^2\varphi D(m_{\eta'}, x)$$
$$+ \sin^2\varphi D(m_\eta, x)], \qquad (166)$$

where we have used the Euclidean tree-level propagator

$$\langle \eta(x)\eta(0)\rangle = D(m_\eta, x) = \frac{m_\eta}{4\pi^2 x}K_1(m_\eta x), \qquad (167)$$

for η and the analogous one for η'. Diagonalization of the physical Goldstone-boson mass matrix [70,72] relates the screening mass (161) to the physical masses of the pseudoscalar mesons as

$$m_{\text{scr}}^2 = 2\bar{n}\gamma_{\eta_0}^2 = m_{\eta'}^2 + m_\eta^2 - 2m_K^2. \qquad (168)$$

[Note that Eq. (168) reduces to $m_{\text{scr}}^2 = m_{\eta_0}^2 = m_{\eta'}^2$ in the chiral limit.] After continuation to Minkowski space-time, our final expression for the screening contribution to the

---

[18]The calculation of the quark-mass dependence of gluon condensates on the lattice is impeded by small signal-to-noise ratios and problems with reaching physical light-quark masses. The quark-mass dependence is expected to be non-negligible.

IOPE of the pseudoscalar glueball correlator becomes

$$\Pi_P^{(\text{scr})}(x) = F_{\eta'}^2 D(m_{\eta'}, x) + F_\eta^2 D(m_\eta, x), \qquad (169)$$

where $(F_{\eta'}, F_\eta) = 16\pi\bar{n}\gamma_{\eta_0}(\cos\varphi, \sin\varphi)$.

All mass and coupling parameters in Eq. (169) will be fixed at their experimental values. For the η and η' masses and the mixing angle we use $m_\eta = 547.30 \pm 0.12$ MeV, $m_{\eta'} = 957.78 \pm 0.14$ MeV [3], and $\varphi = 22.0° \pm 1.2°$ [78]. The axial anomaly renders even the $Q-\eta_0$ coupling and the overall coupling $2\bar{n}\gamma_{\eta_0}$ experimentally accessible, with the result $(2\bar{n}\gamma_{\eta_0})^2 = 9.732 \times 10^{-4}$ GeV^6 [78]. Alternatively, this coupling could be estimated from the standard value $\bar{n} = 0.5$ fm$^{-4} = 7.53 \times 10^{-4}$ GeV^4 of the instanton density and the experimental pseudoscalar meson masses according to

$$(2\bar{n}\gamma_{\eta_0})^2 = 2\bar{n}(m_{\eta'}^2 + m_\eta^2 - 2m_K^2), \qquad (170)$$

which yields (with $m_{K^0} = 497.67 \pm 0.31$ MeV [3]) the value $(2\bar{n}\gamma_{\eta_0})^2 = 1.086 \times 10^{-3}$ GeV^6. It is reassuring that both estimates are perfectly consistent. We will use the rounded value $(2\bar{n}\gamma_{\eta_0})^2 = 10^{-3}$ GeV^6 in our quantitative analysis below, which implies $F_{\eta'}^2 = 0.543$ GeV^6 and $F_\eta^2 = 0.0886$ GeV^6.

From the Fourier transform of the screening contribution,

$$\Pi_P^{(\text{scr})}(Q) = \frac{F_{\eta'}^2}{Q^2 + m_{\eta'}^2} + \frac{F_\eta^2}{Q^2 + m_\eta^2}, \qquad (171)$$

we finally obtain the Borel moments

$$\mathcal{R}_{P,k}^{(\text{scr})}(\tau) = -\delta_{k,-1}\left(\frac{F_{\eta'}^2}{m_{\eta'}^2} + \frac{F_\eta^2}{m_\eta^2}\right) + F_{\eta'}^2 m_{\eta'}^{2k}e^{-m_{\eta'}^2\tau}$$
$$+ F_\eta^2 m_\eta^{2k}e^{-m_\eta^2\tau}. \qquad (172)$$

The τ-independent term in Eq. (172) is the screening-induced subtraction constant $-\Pi_P^{(\text{scr})}(0)$ which will play a pivotal rule in the $\mathcal{R}_{P,-1}$ sum rule analysis below. Already at this stage, however, its necessity can be seen from yet another inconsistency which one would encounter by restricting the nonperturbative Wilson coefficients exclusively to direct instanton contributions. Indeed, the latter generate a large subtraction constant [cf. Eq. (102)]

$$\Pi_P^{(I+\bar{I})}(0) = -2^7\pi^2\bar{n} \qquad (173)$$

(where we have adopted the spike distribution) which cannot be matched on the phenomenological side of the sum rule since the low-energy theorem (14) dictates the zero-momentum limit of the physical correlator to be of the order of the light current quark masses, i.e., about an order of magnitude smaller. The additional screening contribution from Eq. (172) cancels most of the direct instanton contributions, however, and thereby restores consistency.

The underlying mechanism becomes most transparent in the chiral limit where the low-energy theorem requires the subtraction term to vanish and the cancellation to become complete [cf. Eq. (14)]. Indeed, the zero-quark-mass limit of the screening contribution,

$$\Pi_P^{(\text{scr})}(0) = \frac{F_{\eta'}^2}{m_{\eta'}^2} = \frac{(16\pi\bar{n}\gamma_{\eta_0})^2}{2\bar{n}\gamma_{\eta_0}^2} = 2^7\pi^2\bar{n} \qquad (174)$$

(obtained from the definitions of F_η and $F_{\eta'}$ and the mass relation (168) with $m_\eta = m_K = \varphi = 0$), exactly cancels the direct instanton contribution (173) and thereby restores consistency with the low-energy theorem. The topological charge is totally screened in the chiral limit since the massless Goldstone-boson exchange generates infinite-range interactions. The presence of the screening contributions thus explains how the direct-instanton-induced subtraction terms can be of equal size in both spin-0 channels whereas the low-energy theorems (10) and (14) require the size of their phenomenological counterparts to differ by an order of magnitude. This provides compelling evidence for the vital role of topological charge screening in the IOPE of the 0^{-+} glueball correlator.

Furthermore, the cancellation between the direct instanton- and screening-induced subtraction terms suggests a strategy for implementing the IOPE scale μ into the screening contributions. As shown above, restricting the size of the direct instantons to $\rho < \mu^{-1}$ implies the replacement of $\bar{n}$ in Eq. (173) by $\bar{n}_{\text{dir}} = \zeta\bar{n}$ with $\zeta < 1$ [cf. Eq. (148)]. Compliance with the low-energy theorem then requires the same replacement in the screening contributions (174) and therefore in $\Pi_P^{(\text{scr})}(Q^2)$. This is physically reasonable since only instantons with $\rho < \mu^{-1} \sim O(\lambda_{\text{scr}})$ can take part in the short-range screening mechanism. A conceptually similar restriction has already been implied by using the pointlike (i.e., $\rho = 0$) approximation in deriving Eq. (169).

We conclude this section with a first look at the quantitative impact of the screening contributions on the 0^{-+} Borel moments. To this end, we contrast Fig. 2(a) of the $k = 0$ moment, based on the perturbative and instanton-induced Wilson coefficients as given in Eq. (149), with the same plot but including the screening contributions, in Fig. 2(b) . The previous deficiencies, i.e., both the negative sign and the positive slope of the Borel moment in the $s_0 \gtrsim 7 - 8$ GeV^2 region, are clearly resolved. In particular, $\mathcal{R}_{P,0}$ now decays monotonically and approximately exponentially with τ and thus contains a clear signal for a pseudoscalar glueball resonance (and the η', see below) which will be analyzed quantitatively in Sec. VI. [We recall that the negative regions of the Borel moment at smaller s_0 and τ are an artifact of the spike distribution and will disappear when realistic instanton size distributions are implemented (cf. Fig. 4 below).]

In summary, we have found strong evidence for the direct instanton contributions alone to be a seriously incomplete description of the hard, nonperturbative physics in the 0^{-+} glueball correlator. Sum rules based on this selective choice of contributions [42], i.e., without the screening contributions, are in several ways inconsistent. Reliable sum rules can be obtained only if the complementary physics generated by topological charge screening is properly included.

VI. QUANTITATIVE ANALYSIS OF BOREL MOMENTS AND SUM RULES

We now assemble the various IOPE contributions (61)–(64), (129), and (172) obtained above into our theoretical prediction for the continuum-subtracted Borel moments (27),

$$\mathcal{R}_{G,k}(\tau; s_0) = \mathcal{R}_{G,k}^{(\text{pc})}(\tau, s_0) + \mathcal{R}_{G,k}^{(I+\bar{I})}(\tau; s_0)$$
$$+ \delta_{G,P}\mathcal{R}_{P,k}^{(\text{scr})}(\tau), \qquad (175)$$

which form the left-hand side of the Borel sum rules (28). These moments summarize the microscopic (i.e., quark-gluon level) information contained in the IOPE and the local-duality continuum. Some additional input of a more implicit nature is needed, however, before quantitative glueball properties can be extracted from them by means of a sum rule analysis: a specific parametrization of the resonance sector (i.e., the number of isolated resonances and their shapes and widths), the determination of the duality threshold, the establishment of the "fiducial" τ domain in which all underlying approximations are expected to be reliable, and finally the choice of sum rule optimization criteria.

Before tackling these issues in Sec. VI D, we will make an effort to obtain as much qualitative insight as possible from the IOPE moments alone. The main focus will be on pertinent features of the τ and s_0 dependence as well as the scales which govern it, and an analysis of the various subtraction constants and their impact. The gained insights will help both to select the optimal strategy for the sum rule analysis and to better understand the physics which underlies its predictions.

A. Input parameters and scales

Before embarking on the quantitative analysis, we have to fix the values of the various constants and scales which appear in the IOPE and its moments (175). All of them will be standard (or in their standard range). The dominant soft scale is set by the gluon condensate,

$$\langle \alpha_s G^2 \rangle \equiv \langle \alpha_s G_{\mu\nu}^a G^{a\mu\nu} \rangle \simeq 0.055 \text{ GeV}^4 \qquad (176)$$

(this value lies in the middle of the phenomenologically acceptable range $\langle \alpha_s G^2 \rangle \sim 0.035 - 0.075$ GeV^4 [7,31]), which determines the higher-dimensional gluon conden-

sates as

$$\langle gG^3 \rangle \equiv \langle g f_{abc} G_{\mu\nu}^a G_\rho^{b\nu} G^{c\rho\mu} \rangle \simeq -1.5 \langle \alpha_s G^2 \rangle^{3/2}, \quad (177)$$

$$\langle \alpha_s^2 G^4 \rangle_S \simeq \frac{9}{16} \langle \alpha_s G^2 \rangle^2, \qquad \langle \alpha_s^2 G^4 \rangle_P \simeq \frac{15}{8} \langle \alpha_s G^2 \rangle^2. \quad (178)$$

All condensate values refer to the renormalization scale $\mu \simeq 0.5$ GeV. The lattice estimate for the three-gluon condensate [79] is sometimes replaced by the single-instanton estimate $\langle gG^3 \rangle \sim 0.27$ GeV$^2 \langle \alpha_s G^2 \rangle$. [Adopting different values of the lowest-dimensional condensates (inside their standard range) would affect mainly the predictions of the pseudoscalar $k = -1, 0$ sum rules where the relative impact of the power corrections is largest.] Furthermore, the phenomenological subtraction constant in the pseudoscalar channel, determined by the low-energy theorem (14), contains the quark condensate

$$\langle \bar{q}q \rangle \simeq -(0.24 \text{GeV})^3. \quad (179)$$

For the leading moments of the instanton size distribution we use the canonical values [9]

$$\bar{n} \simeq \frac{1}{2} \text{ fm}^{-4} = 7.53 \times 10^{-4} \text{ GeV}^4, \quad (180)$$

$$\bar{\rho} \simeq \frac{1}{3} \text{ fm} = 1.69 \text{ GeV}^{-1}, \quad (181)$$

which also completely determine the finite-width size distributions discussed in Sec. IV A. Our quantitative predictions are based on the realistic Gaussian-tail distribution (85) with the soft cutoff (143) at $\beta = 3$ GeV. The corresponding direct instanton fraction ζ, defined in Eq. (148), is

$$\zeta_g \equiv \frac{\bar{n}_{\text{dir},g}}{\bar{n}} = \frac{1}{\bar{n}} \int_0^\infty d\rho \, n_g(\rho) \theta_\beta(\mu^{-1} - \rho) \simeq 0.66, \quad (182)$$

which implies that about two thirds of all instantons are direct, i.e., small enough to affect the Wilson coefficients. (The ζ values from the exponential-tail distribution (76) and/or the alternative cutoff function (144) differ by about 1%.) For the quark masses and the scale parameter we adopt the values $m_u \simeq m_d \simeq 0.005$ GeV and $\Lambda_{\text{QCD}} = 0.2$ GeV, while the IOPE renormalization scale is set to $\mu = 0.5$ GeV. Note that both the screening and direct-instanton-induced subtraction constants are proportional to the instanton density $\bar{n}$ and therefore equally attenuated by renormalization (recall that $F_{\eta,\eta'}, m_{\eta,\eta'}^2 \propto \bar{n}$),

$$\Pi_P^{(\text{scr})}(0) \rightarrow \zeta \Pi_P^{(\text{scr})}(0), \quad (183)$$

$$\Pi_{S/P}^{(I+\bar{I})}(0) \rightarrow \zeta \Pi_{S/P}^{(I+\bar{I})}(0). \quad (184)$$

Finally, we recall the masses and couplings

$$F_{\eta'}^2 = 0.543 \text{ GeV}^6, \qquad F_\eta^2 = 0.0886 \text{ GeV}^6, \quad (185)$$

$$m_\eta = 0.55 \text{ GeV}, \qquad m_{\eta'} = 0.96 \text{ GeV}, \quad (186)$$

which determine the topological charge screening contributions (172).

B. Qualitative behavior of the Borel moments

In Figs. 3 and 4 we plot all four IOPE Borel moments (175) in both spin-0 glueball channels. The direct instanton contributions were calculated on the basis of the Gaussian-tail size distribution (85) and renormalized according to Eq. (142) with $\beta = 3$. These Borel moments will be the theoretical input for our sum rule analysis in Sec. VI E. For instructive purposes, i.e., to exhibit several qualitative features more prominently, the plots cover a region of the $\tau - s_0$ plane which extends beyond the limits in which the sum rule analysis is reliable.

An obvious feature of all Borel moments is that they are monotonically increasing with s_0 and monotonically decreasing with τ in their physically sensible domains. This behavior stabilizes multiparameter sum rule fits since the minimization routine is unlikely to get trapped in a local minimum of the deviation measure (cf. Sec. VI D). Furthermore, the monotonic increase of the τ slope with s_0, especially at small τ, ensures that the largest resonance mass squared remains below the duality continuum threshold, as it should be.

Another general property of all Borel moments is their increasing s_0 independence for $\tau \gg s_0^{-1}$. This is a consequence of the Laplace suppression factor $\exp(-\tau s)$ in the dispersion integrals (27) (which therefore have practically no support at $s \sim s_0$) and the damping of the instanton contributions at large s by realistic instanton size distributions (cf. Sec. IV E).

All Borel moments show an approximately exponential decay with increasing τ (for $s_0 \gtrsim 6$ GeV^2 in the lowest 0^{-+} moments, which includes the physical region). Thus, all of them provide resonance signals in the sum rules (28). After normalizing the moments to a common scale, the τ slopes of the 0^{-+} Borel moments are consistently larger than those of their 0^{++} counterparts in the region $\tau \lesssim 0.8$ GeV^{-2} where the heaviest isolated resonance dominates. Thus the glueball mass scale is considerably larger in the 0^{-+} than in the 0^{++} channel, in agreement with lattice results [28,43]. The same conclusion can be drawn independently from the ratios $\mathcal{R}_{G,k+1}/\mathcal{R}_{G,k}$ of adjacent moments in each channel. For $k \geq 0$ and if one pole dominates, they are about equal to the square of the resonance mass and indeed consistently larger in the 0^{-+} channel.

The pseudoscalar moments (especially those with $k \geq 0$) flatten out rather suddenly in the τ direction for $\tau \gtrsim 1$ GeV^{-2}. The visibly slower decay in the large-τ region is a qualitative indication for the appearance of a second
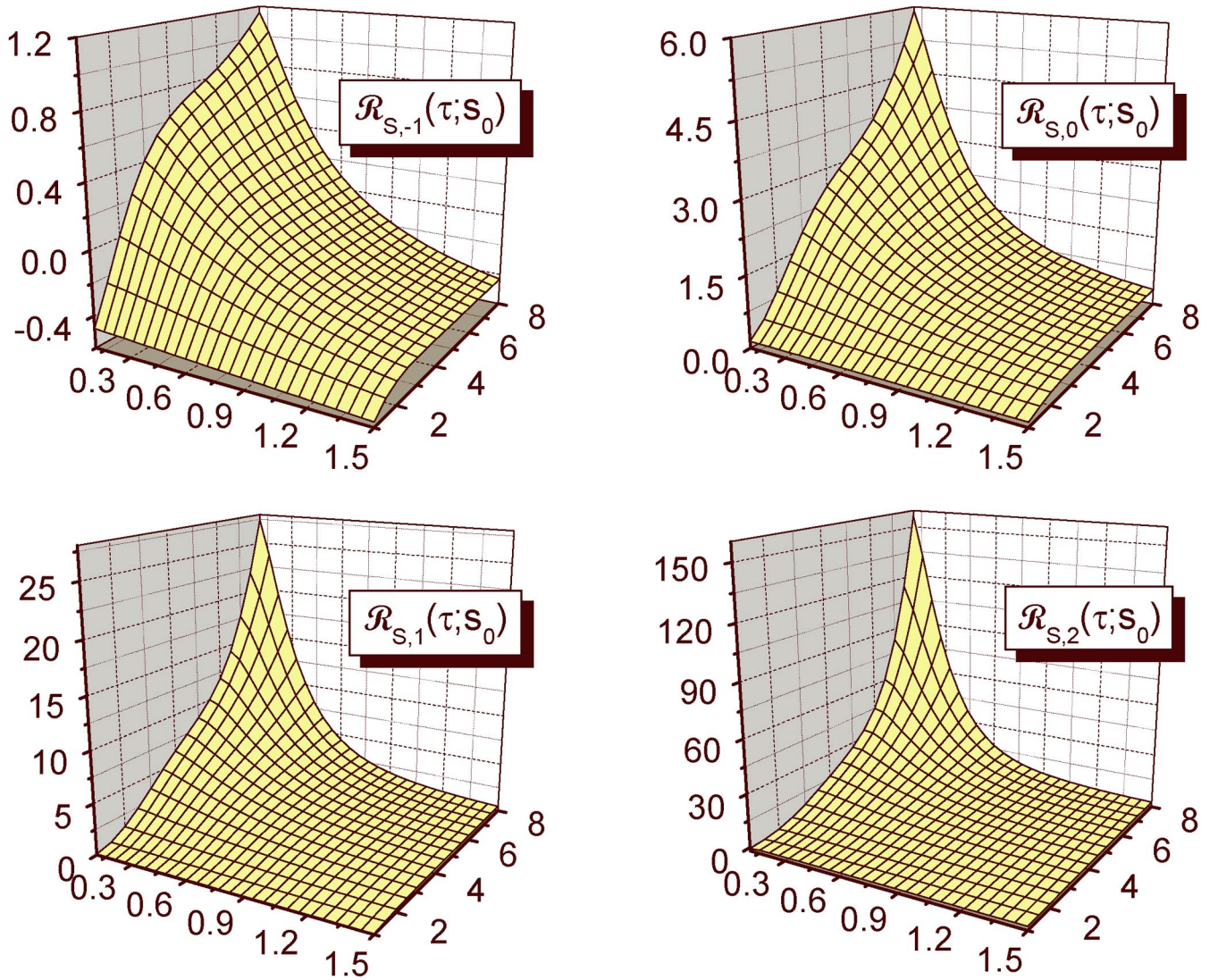
FIG. 3 (color online). The continuum-subtracted IOPE Borel moments of the scalar glueball correlator (calculated on the basis of the Gaussian-tail distribution and renormalized at the operator scale) as a function of τ (x axis) and s_0 (y axis). All units are appropriate powers of GeV.

resonance with a clear mass scale separation. The quantitative sum rule analysis below will confirm that the screening contributions have produced an additional signal for the η', as expected from unquenching the instanton contributions.

Several qualitative features of the Borel moments can be traced to the impact of finite-width distributions and renormalization on the direct instanton contributions. To exhibit them, we compare the $k = 0$ moments of Figs. 3 and 4 with those obtained from the traditional spike distribution, plotted in Fig. 5. Clearly, the neglect of interference between contributions from instantons of similar size in the spike distribution distorts the moments at small τ: positivity and monotonic rise with s_0 disappear. Moreover, the negative τ slope of $\mathcal{R}_{S,0}$ at small τ turns positive at larger s_0 and creates a "mountain ridge." In addition, $\mathcal{R}_{S,0}$ itself turns negative in the latter region while $\mathcal{R}_{P,0}$ becomes

negative mostly in the small-s_0 (and small-τ) region. In both channels, the maximal τ slope and consequently an upper bound on the glueball mass predictions is reached at intermediate s_0.

The positivity violations generated by the spike distribution can be traced to the large-s oscillations in the instanton-induced imaginary part. As discussed in Sec. IV E, these oscillations affect mostly the small-τ behavior of the moments and are a conceptually worrisome artifact. Their practical impact is moderate, however, since the positivity violations occur mostly outside of the fiducial τ and s_0 domains in which the sum rule analysis takes place. This is in marked contrast to the impact of the positivity violations which we have discussed in Sec. V, i.e., those which arise in the pseudoscalar Borel moments when the screening contributions are ignored. Indeed, a glance at Fig. 2(a) shows that these occur mostly at
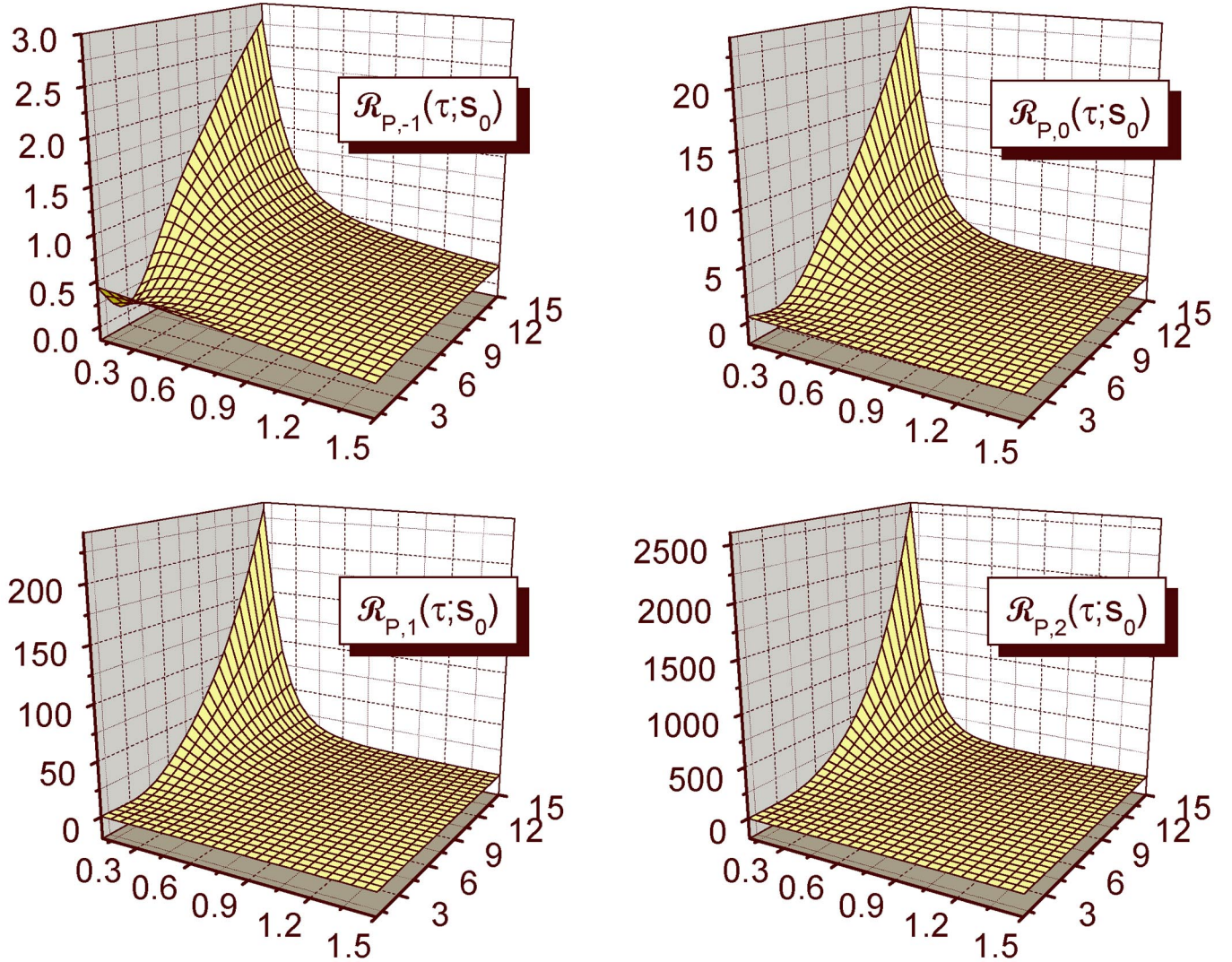
FIG. 4 (color online). The continuum-subtracted IOPE Borel moments of the pseudoscalar glueball correlator (calculated on the basis of the Gaussian-tail distribution and renormalized at the operator scale) as a function of τ (x axis) and s_0 (y axis). All units are appropriate powers of GeV.

intermediate and large τ, i.e., exactly in the region where the sum rules are matched. They would make a meaningful sum rule analysis impossible and once more underline the necessity of the topological charge screening contributions.

The renormalization of the direct instanton contributions generally increases the size of the moments at small τ (due to the enhanced imaginary part at large s, cf. Fig. 1(b)) and reduces it at the upper end of the fiducial τ domain (due to the effectively reduced instanton density $\bar{n} \to \zeta \bar{n}$). Both effects tend to increase the resonance mass predictions of the IOPE sum rules [cf. Eq. (28)]. Another effect of the improved treatment of the nonperturbative Wilson coefficients is a substantial reduction in the overall size of the direct instanton contributions. In addition, the perturbative contributions are enhanced by the 3-loop corrections (and additionally by the now favored, larger values for $\Lambda_{\rm QCD}$ cf. Sec. III A). Hence the previous dominance of the instanton-

induced coefficients, found in Ref. [13] on the basis of the 2-loop radiative corrections and the spike distribution, is considerably weakened. As a side effect, the derivation of the scaling relations between glueball and instanton properties [13] is obscured since the latter relied on the dominance of the instanton contributions at intermediate and large τ. Nevertheless, these relations remain suggestive, especially because they are consistent with large-N_c counting.

A semiquantitative upper bound on the sum rule predictions for the glueball masses can be obtained from the moment ratios considered above. Its derivation starts from the expressions

$$m_G^{(k)}(\tau; s_0) \equiv \sqrt{\frac{\mathcal{R}_{G,k}(\tau; s_0)}{\mathcal{R}_{G,k-1}(\tau; s_0) + \delta_{k,0}\Pi_G^{\rm (ph)}(0)}} \qquad (187)$$

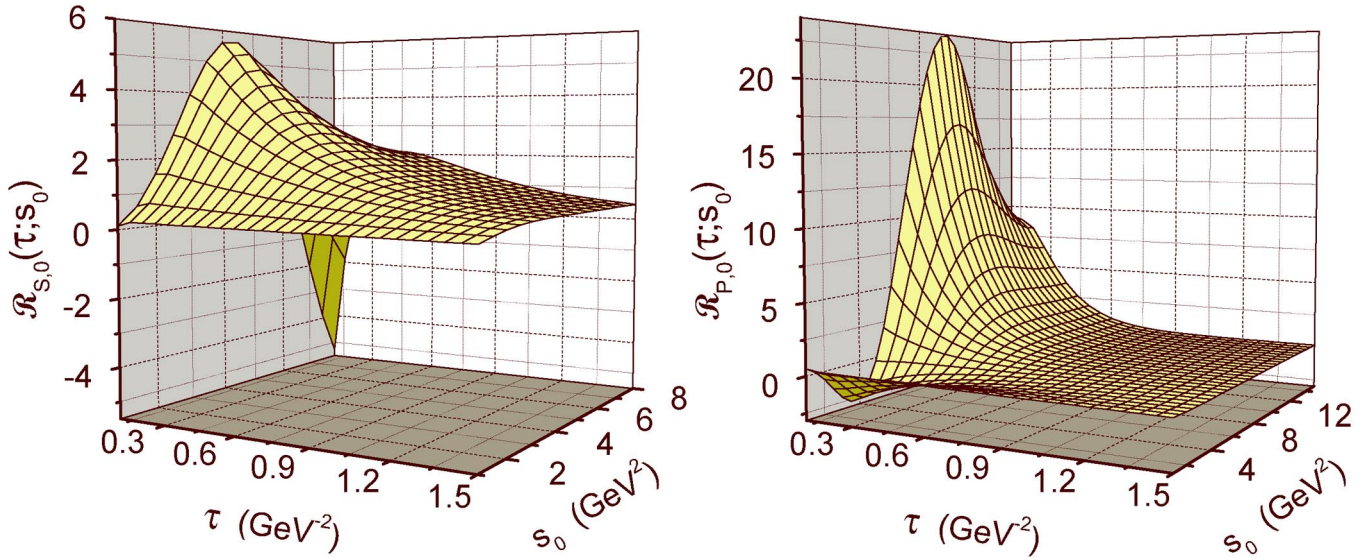($k = 0 - 2$) which are obtained by setting $f_{G2} = 0$ in the

FIG. 5 (color online).   The $k = 0$ continuum-subtracted IOPE Borel moments of the 0^{++} (left panel) and 0^{-+} (right panel) glueball correlators, as obtained from the spike distribution.

sum rules (28) and solving for m_{G1}. (An alternative approach would be to take logarithmic τ derivatives of the Borel moments.) Upper bounds for the glueball masses are then found by searching for the position in the (τ, s_0) plane where $m_G^{(k)}$ is least sensitive to variations in both τ and s_0. These are either extrema or inflection points of Eq. (187). Estimates of this type [7] are often used instead of a full sum rule matching analysis although they can accommo-

date only one resonance pole and are of limited reliability. To give a specific example of this approach, we will use $m_S^{(2)}$ to establish a bound on the scalar glueball mass. From our Borel moments we obtain $m_S^{(2)}$ as plotted in Fig. 6. One reads off an extremum (maximum) in τ at $\tau^* \sim 0.2$ GeV^{-2} for $s_0 \lesssim 6.5$ GeV^2 and an inflection point in s_0 at $s_0^* \sim 4.5$ GeV. (In the analysis based on purely perturbative Wilson coefficients, one finds instead an inflection point
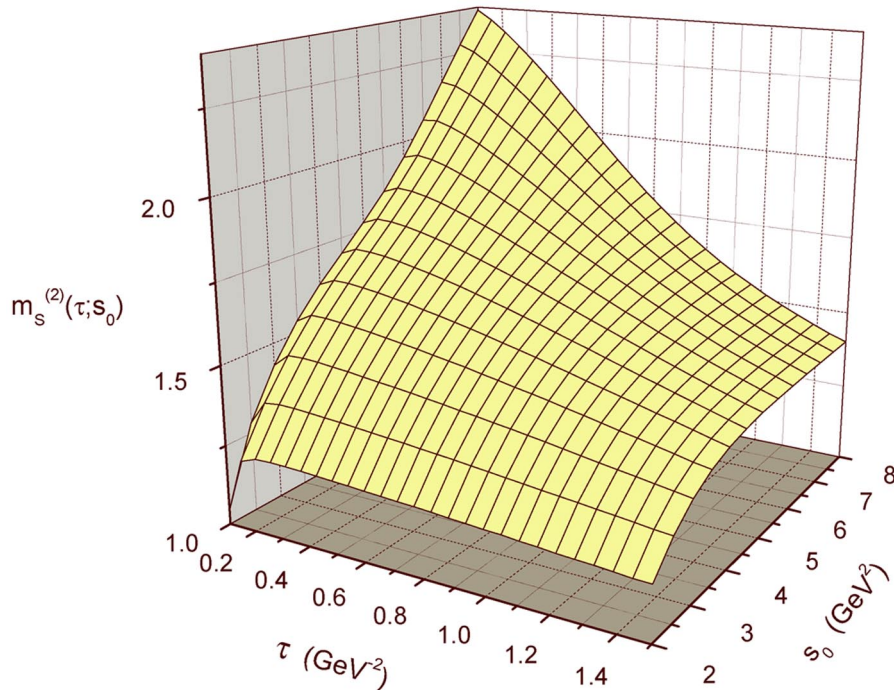

FIG. 6 (color online).   The square root of the ratio between the $k = 2$ and $k = 1$ continuum-subtracted IOPE Borel moments of the scalar glueball correlator.

of $m_S^{(2)}$ in τ and an extremum (minimum) in s_0 [7].) Together, they yield the upper bound

$$m_S \lesssim m_S^{(2)}(\tau^*; s_0^*) \simeq 1.7 \text{ GeV}, \qquad (188)$$

for the scalar glueball mass. The analogous estimates from $m_S^{(0,1)}$ result in somewhat smaller bounds. Nevertheless, these bounds should not be considered as a substitute for the sum rule results. Indeed, our quantitative sum rule analysis in Sec. VI E will show that they overestimate the 0^{++} glueball mass prediction by about 35%.

Figure 6 furthermore reveals that $m_S^{(2)}$ has a stronger τ dependence than the analogous expression for the spike size distribution (cf. Ref. [13], Fig. 3). This might indicate that a one-resonance sum rule analysis is somewhat less favored if realistic instanton size distributions and renormalization of the instanton-induced coefficients are taken into account.

Finally, the Figs. 3 and 4 show that the $k = -1$ Borel moments have a τ-independent offset which becomes visible at large τ. It is rather large and negative in $\mathcal{R}_{S,-1}$ while smaller and positive in $\mathcal{R}_{P,-1}$. These offsets are due to the subtraction terms which the nonperturbative IOPE coefficients generate. (For this reason, $\mathcal{R}_{G,-1} < 0$ does not imply positivity violations.) Their match to the subtraction constants on the phenomenological side of the sum rules is an important consistency criterion which we are going to discuss in the next section.

C. Subtraction constants

By design, the $k = -1$ Borel moment includes first-principle information provided by the low-energy theorem (10) into the 0^{++} glueball sum rule analysis [6]. As pointed out in Sec. II A, an equally useful low-energy theorem (14) exists in the pseudoscalar channel and suggests to analyze the analogous 0^{-+} sum rule, based on the moment $\mathcal{R}_{P,-1}$, as well. In order to prepare for this analysis, the present section investigates the conceptual and quantitative impact of the involved subtraction constants.

Since the perturbative UV contributions to the subtraction constants are removed by definition in the low-energy theorems (cf. Sec. II A) and by renormalization in the perturbative IOPE coefficients, it remains to clarify the role and treatment of the nonperturbative contributions. The direct instanton-induced subtraction terms

$$\Pi_{S/P}^{(I+\bar{I})}(0) = \pm 2^7 \pi^2 \bar{n}_{\text{dir}} \simeq \pm \zeta \times 0.95 \text{ GeV}^4 \qquad (189)$$

are part of the $k = -1$ Borel moments (105) and (128). Their size is significant but smaller than the size of the τ-dependent contributions (in particular, those due to direct instantons at small and intermediate τ). Moreover, for $\zeta = 1$ (i.e., for the spike distribution) the instanton-induced subtraction constant in the scalar channel is more the 50% larger than (and of the same sign as) the phenomenological LET value [cf. Eq. (10)]

$$\Pi_S^{(\text{ph})}(0) = \frac{32\pi}{b_0}\langle\alpha_s G^2\rangle \simeq 0.61 \text{ GeV}^4. \qquad (190)$$

It would remain larger even when the largest available value for the gluon condensate, $\langle\alpha_s G^2\rangle \sim 0.07 \text{ GeV}^4$, is used. In the pseudoscalar channel the discrepancy is yet more pronounced: the value (189) is more than an order of magnitude larger than the LET value (14)

$$\Pi_P^{(\text{ph})}(0) = (8\pi)^2 \frac{m_u m_d}{m_u + m_d}\langle\bar{q}q\rangle \simeq -0.022 \text{ GeV}^4 \qquad (191)$$

(and again of the same sign).

The impact on the $k = -1$ sum rules results from the fact that $\mathcal{R}_{G,-1}$ has to be fitted to the decaying resonance exponentials and the "phenomenological" subtraction constants (190) and (191). As a general rule, the smaller the difference between the IOPE subtraction constants and the LET values, which makes up the remaining offset, the better will be the fit quality to the resonances (which is the only intrinsic reliability measure for QCD sum rules). The impact of the remaining imbalance can be rather subtle since it is largest towards the upper boundary of the fiducial τ domain where the match to the exponential resonance contributions becomes delicate.

A glance at the above scales confirms that such a match is ruled out in the 0^{-+} channel, with its extreme discrepancy between LET and direct instanton-induced subtraction constants, if the nonperturbative IOPE coefficients arise exclusively from direct instantons. As we have shown in Sec. V C, however, this inconsistency is overcome by the crucial topological charge screening correction

$$\Pi_P^{(\text{scr})}(0) = \zeta\left(\frac{F_{\eta'}^2}{m_{\eta'}^2} + \frac{F_\eta^2}{m_\eta^2}\right) \simeq \zeta \times 0.89 \text{ GeV}^4, \qquad (192)$$

which cancels most of the direct instanton contribution (189) and brings the total IOPE subtraction constant in line with the small LET value (191). Previous analyses of 0^{-+} sum rules have discarded the $k = -1$ moment and therefore missed valuable first-principle information from the low-energy theorem as well as a useful consistency check.

One might wonder what happens to the rather delicate balance between the 0^{-+} subtraction constants in the $N_f = 0$ limit, i.e., in pure gauge theory or in the quenched approximation. In this case the above cancellation does not work since topological charge screening disappears. As is well known, however, the LET (14) and thus the phenomenological value for the zero-momentum correlator is strongly affected by the absence of light quarks, too. Indeed, it becomes

$$\Pi_P^{(\text{ph,qn})}(0) = -(8\pi)^2\chi_t^{(\text{qn})} \simeq -0.66 \text{ GeV}^4, \qquad (193)$$

where we have used the standard (quenched) lattice value $\chi_t^{(\text{qn})} \simeq (0.18 \text{ GeV})^4$ for the topological susceptibility [67], which is in agreement with the Witten-Veneziano formula

[80]. Thus we find again perfect consistency: the LET subtraction constant becomes much larger and cancels the direct instanton contributions by itself (assuming that the latter are not strongly affected by quenching).

A special situation arises if the difference between the IOPE and LET values of the subtraction constant becomes so strongly negative that even the τ-dependent contributions cannot prevent

$$\mathcal{R}_{G,-1}(\tau; s_0) + \Pi_G^{(ph)}(0) \qquad (194)$$

from turning negative inside the fiducial τ domain.[19] In this case the sum rule fit to the (always positive) resonance exponentials in Eq. (28) is substantially worsened even if the negative offset in (194) remains relatively small. Exactly this situation is encountered in the scalar $k = -1$ sum rule since

$$\Pi_S^{(ph)}(0) - \Pi_S^{(I+\bar{I})}(0) \simeq (0.61 - 0.95 \, \zeta) \, \text{GeV}^4 < 0.$$
$$(195)$$

For $\zeta = 1$ (spike distribution) the imbalance between the τ-independent terms is of about the same size with and without the direct instanton contribution. The main effect of the instanton contribution is to turn the sign negative, which causes the mentioned decline in sum rule consistency. One option to deal with this problem is to assume that unreliably calculated soft contributions dominate the instanton-induced subtraction constant (in particular when using the spike distribution), as discussed in Sec. IV C, and therefore to discard it completely. This strategy was adopted in Ref. [13] where the constant (189) was removed from the Borel moments (105) and (129). It strongly improves the sum rule quality and maintains the crucial mutual consistency with the predictions of the $k \geq 0$ sum rules and with the LET (10) (which is badly violated if nonperturbative contributions to the Wilson coefficients are ignored) [13]. This shows that the main reason for achieving a large glueball mass scale and LET consistency in the $\mathcal{R}_{S,-1}$ sum rule is the large overall size and slope of the τ-dependent direct instanton contributions (and not the relatively small, instanton-induced subtraction constant, as suggested in Ref. [81]).

Of course, discarding the instanton-induced subtraction constant completely is a very crude way of "renormalization." Our implementation of the IOPE renormalization scale on the basis of realistic size distributions accounts more accurately for the soft physics to be removed. Comparison of the above scales shows that this significantly improves the consistency with the LET: the difference between instanton- and LET-induced subtraction terms is reduced by $\zeta < 1$, and for realistic values $\zeta \simeq 2/3$ [cf. Eq. (182)] the sum (194) remains positive over

the whole fiducial τ domain.[20] Note that this renormalization maintains consistency with the LET in the pseudoscalar channel as well, while simply discarding the instanton-induced subtraction constant would leave the compensating screening corrections out of balance (cf. Sec. V C).

In the context of this section it might be useful to recall that the large phenomenological subtraction constant had caused serious problems in the 0^{++} glueball sum rule as long as the nonperturbative Wilson coefficients were ignored: the ensuing, weaker decay of the sum (194) generated a much smaller 0^{++} glueball mass "prediction" (well below 1 GeV) which was inconsistent with the predictions well beyond 1 GeV from the $k \geq 0$ sum rules. It was pointed out in Ref. [13] that the missing, strongly decaying τ dependence can only reside in the Wilson coefficients and that it should be of nonperturbative origin, suggesting (together with other indications) direct instantons as its main source. The inclusion of the direct instanton contributions indeed overcame the mutual inconsistencies among the 0^{++} sum rule predictions and restored the consistency with the LET.

In summary, the direct-instanton-induced subtraction terms and their renormalization play a rather complex role in the $k = -1$ glueball sum rules. In both channels they are essential for achieving consistency with the underlying low-energy theorems. In the pseudoscalar sum rules, this additionally requires strong cancellations with the indispensable topological charge screening contributions. These cancellations explain, in particular, how the equal size of the instanton-induced subtraction constants in both spin-0 glueball channels can be reconciled with the conspicuous difference between the LET values.

D. Sum rule analysis setup

In order to extract glueball properties from the IOPE Borel moments by means of a QCD sum rule analysis, the parametrization of the phenomenological spectral functions and the matching criteria have to be specified. Of course, the complexity of the phenomenological side (measured by the number of parameters to be predicted) is limited by the information content and resolution power of the truncated short-distance expansion. Therefore, judicious decisions are required about the amount of detail to include, e.g., about the number of isolated resonances, their individual widths and shapes, specific assumptions on quarkonium admixtures or even explicit multihadron continua (beyond the local-duality approximation). Guided by

---

[19]When $\tau \to \infty$ this will eventually happen for any negative difference (and does, of course, not imply that the spectral function violates the positivity bound).

[20]Although their numerical values are quite close, one should keep in mind that the physics entering $\Pi_S^{(I+\bar{I})}(0)$ and $\Pi_S^{(ph)}(0)$ is mostly complementary: as part of a Wilson coefficient, $\Pi_S^{(I+\bar{I})}(0)$ receives dominantly (semi-) hard contributions while $\Pi_S^{(ph)}(0)$ is renormalized by subtracting the hard (perturbative) fluctuations and therefore dominated by soft modes [note the appearance of the gluon condensate in the LET (10)].

the asymptotic nature of the spacelike IOPE (i.e., the factorial and not Borel-summable growth of the higher Wilson coefficients [82]) and its truncation, we restrict ourselves in the following analysis to at most two resonance poles in zero-width approximation[21] and the local-duality continuum, as anticipated in Eq. (28).

Any quantitative sum rule analysis requires a numerical measure δ for the deviation between both sides over the discretized fiducial τ domain (whose boundaries $\tau_{\min}$, $\tau_{\max}$ will be determined below). The iterative minimization of δ up to the desired accuracy is then performed numerically. We will adopt the Belyaev-Ioffe measure [33]

$$\delta = \frac{1}{N} \sum_{i=0}^{N} \ln\left(\frac{\max[\mathcal{R}_{G,k}^{(\mathrm{pole})}(\tau_i) - \delta_{k,-1}\Pi_G^{(\mathrm{ph})}(0), \mathcal{R}_{G,k}(\tau_i)] + \xi}{\min[\mathcal{R}_{G,k}^{(\mathrm{pole})}(\tau_i) - \delta_{k,-1}\Pi_G^{(\mathrm{ph})}(0), \mathcal{R}_{G,k}(\tau_i)] + \xi}\right), \tag{196}$$

with $N = 100$ grid points and $\tau_i = \tau_{\min} + i(\tau_{\max} - \tau_{\min})/N$.[22] The constant ξ is an offset to be added if otherwise the argument of the logarithm would become negative. An important requirement on reliable sum rule fits is that they should be stable, i.e., that the resulting hadron properties should be—inside the other typical errors of the analysis—independent of the starting values for the iterative minimization of δ. As mentioned above, the monotonic behavior of the IOPE Borel moments generally improves stability by reducing the likelihood for less than optimal local minima of δ. We have tested several alternative expressions for δ (with, e.g., different weights for the deviations in the large- and small-τ regions) and found them to change predictions of stable fits maximally at the 1% level.

The fiducial τ domain, in which the sum rule analysis takes place, is designed to optimally exploit the physical information in the IOPE without leaving the region of validity of the involved approximations. Hence, one seeks the maximal τ interval in which the sum rules can be expected to be both reliable and predictive. Towards small τ, the duality continuum in the Borel moments (25) increasingly dominates the glueball signal. In order to ensure that the sum rules remain sensitive to the glueball properties, we therefore fix $\tau_{\min}(k, s_0)$ by the standard requirement that the continuum contributions to the Borel moments must not exceed the resonance contributions, i.e.,

$$\frac{\mathcal{R}_{G,k}^{(\mathrm{cont})}(\tau_{\min}; s_0)}{\mathcal{R}_{G,k}(\tau_{\min}; s_0)} = 0.5. \tag{197}$$

Generally, the higher Borel moments require larger values of $\tau_{\min}$. The above criterion therefore also helps to assure consistency among sum rule predictions from different

moments. Furthermore, it typically reduces the fiducial domain of the higher-k sum rules and thereby renders their fits somewhat less stable. (The results for s_0, in particular, become less reliable with increasing k since the s_0 dependence of the Borel moments is largest at small τ.)

The standard sum rule criterion for determining the upper limit of the fiducial domain, $\tau_{\max}$, is to restrict the contribution of the highest-dimensional operator to maximally 10% of the total OPE contribution, i.e.,

$$\frac{\tilde{C}_8^{(G)}(\tau_{\max}; \mu)\langle\hat{O}_8\rangle_\mu}{\sum_{d=0,4,6,8} \tilde{C}_d^{(G)}(\tau_{\max}; \mu)\langle\hat{O}_d\rangle_\mu} = 0.1. \tag{198}$$

The neglected contributions from $d > 8$ operators should therefore remain small up to the onset of the asymptotic IOPE region. The above criterion is more stringent at smaller k where the condensates contributions have a relatively larger impact. (The size of the topological charge screening contributions also decreases with increasing k.)

In the presence of nonperturbative IOPE coefficients, the criterion for $\tau_{\max}$ requires some additional thought. Even for exclusively perturbative Wilson coefficients, the condition (198) is not too restrictive in the spin-0 glueball channels since the power corrections are unusually small. When the large direct instanton contributions to the unit-operator are added, it can become almost ineffective. (In the pseudoscalar channel their impact is reduced by cancellations with the screening contributions and the larger s_0 values.) Another constraint on $\tau_{\max}$, arising from the requirement that multi-direct-instanton corrections to the Wilson coefficients should remain negligible, will then become more stringent. In order to formulate this criterion quantitatively, we adopt the rough estimate

$$\tau \leq \tau_{\max} \simeq \frac{1}{2}(\bar{R} - 2\bar{\rho})^2 \sim 1.5 \text{ GeV}^{-2}. \tag{199}$$

For the higher Borel moments this criterion is typically more restrictive than (198) since the relative impact of the power corrections at large τ decreases with increasing k. In view of its approximate nature, however, it is reassuring that the sum rule results are rather insensitive to variations in $\tau_{\max}$. (The sensitivity to $\tau_{\min}$ is larger, as expected.)

Under the phenomenological parameters to be determined by the sum rule analysis, the duality threshold s_0

---

[21]Finite resonance widths require exponential resolution and are therefore in principle inaccessible to the standard OPE [83]. The situation is more complex when including nonperturbative Wilson coefficients which themselves introduce exponential contributions. In any case, the zero-width approximation in QCD sum rules does not require the corresponding, physical resonances to be particularly narrow.

[22]Because of the generally monotonic decrease of the glueball Borel moments with τ, scale-invariant measures favor an improved matching in the large-τ region. In two-resonance fits this favors the smaller-mass resonance.

plays a special role. It is not associated with a glueball property but rather corresponds roughly to the squared mass gap between ground state and first radially excited state. Indications for a delayed onset of duality [84] suggest, however, that this rule of thumb is invalid in the scalar glueball channel. (These indications could be tested on the lattice when reliable unquenched glueball spectra become available.) Hence, our only robust expectation for s_0 is that it should be larger than the squared mass of the highest-lying isolated resonance.

Below, we will determine s_0 together with the glueball parameters from the sum rule fits, which turns out to be possible even in the presence of two isolated resonances. Nevertheless, it might be instructive to briefly comment on alternative strategies for obtaining the duality threshold. One alternative would be to divide the fitting procedure into two steps, by first constraining $\sqrt{s_0}$ to exceed the largest resonance mass by a constant amount Δs,

$$\sqrt{s_0} = m_G + \Delta s, \qquad (200)$$

and by subsequently minimizing δ as a function of Δs. Such a constant splitting is probably not an unreasonable assumption since the τ slopes of the IOPE Borel moments at small τ increases rather monotonically with $\sqrt{s_0}$ (cf. Figs. 3 and 4) in the sum-rule-relevant τ region. (The couplings f_S are much less s_0 dependent.) Although this two-step procedure can accelerate the minimization procedure (in particular in the two-resonance case), we did not find it necessary even in the pseudoscalar channel. Another strategy, adopted, e.g., in Ref. [36], determines s_0 by analyzing a related finite-energy sum rule which roughly expresses a duality constraint. In view of the likely delayed onset of local duality this procedure might be misleading, however, in the scalar glueball channel. In Refs. [7,16], furthermore, s_0 is required to render specific combinations of Borel moments minimally τ sensitive. In Ref. [7], finally, an upper limit on the finite-energy sum rule value for s_0 is obtained by locating the extrema or inflection points of moment ratios like (187).

E. Results and discussion

After having done the groundwork, we now proceed to the quantitative sum rule analysis. This amounts to matching the continuum-subtracted IOPE Borel moments (175) to either one or two isolated resonances and, if $k = -1$, to the phenomenological subtraction constant [cf. Eq. (28)]. The decision about how many resonances to include will be made in the scalar and pseudoscalar channels individually, based on a comparative quantitative analysis. Of course, the more flexible two-resonance parametrization is almost bound to reduce the nominal fit errors at least slightly. Since this comes at the price of two more parameters to be determined, however, we will resort to the two-resonance parametrization only if it leads to a clear improvement of the fits. This is a necessary requirement for stable and physically meaningful predictions of additional resonance parameters.

1. Scalar glueball

The analysis of the 0^{++} glueball Borel sum rules on the basis of the spike distribution [with perturbative coefficients up to $O(\alpha_s)$] showed that a one-pole fit could almost perfectly match the IOPE moments [13]. This result left little room for improvement and therefore no indication for the presence of a second low-lying resonance with strong coupling to the scalar gluonic interpolator (2).

An extensive numerical survey of all four improved 0^{++} Borel sum rules, based on the IOPE (175), reveals that they can be well fitted by only one 0^{++} glueball pole, too. Again, there is no conclusive evidence for the presence of another low-lying, strongly coupled 0^{++} resonance. A sufficiently exhaustive analysis of the scalar sum rules can therefore be based on the traditional one pole plus duality continuum parametrization. The main part of the following discussion will deal with the results of this ''benchmark'' analysis. Nevertheless, there seems to be some indication for additional low-lying strength, as foreshadowed in the analysis of the moment ratio in Sec. VI B. We will come back to this issue at the end of this section.

The numerical results of the one-resonance analysis of all four Borel-moment sum rules are collected in Table I. They can be summarized in the overall prediction

$$m_S = 1.25 \pm 0.2 \text{ GeV}, \qquad f_S = 1.05 \pm 0.1 \text{ GeV}, \qquad (201)$$

for the scalar glueball mass and coupling. The error assignment includes the estimated uncertainties in the input parameter values. The corresponding sum rule fits, in their individual fiducial τ domains, are shown in Fig. 7.

TABLE I. The fiducial domain, fitting error, and predictions of the scalar glueball sum rule based on the kth Borel moment.

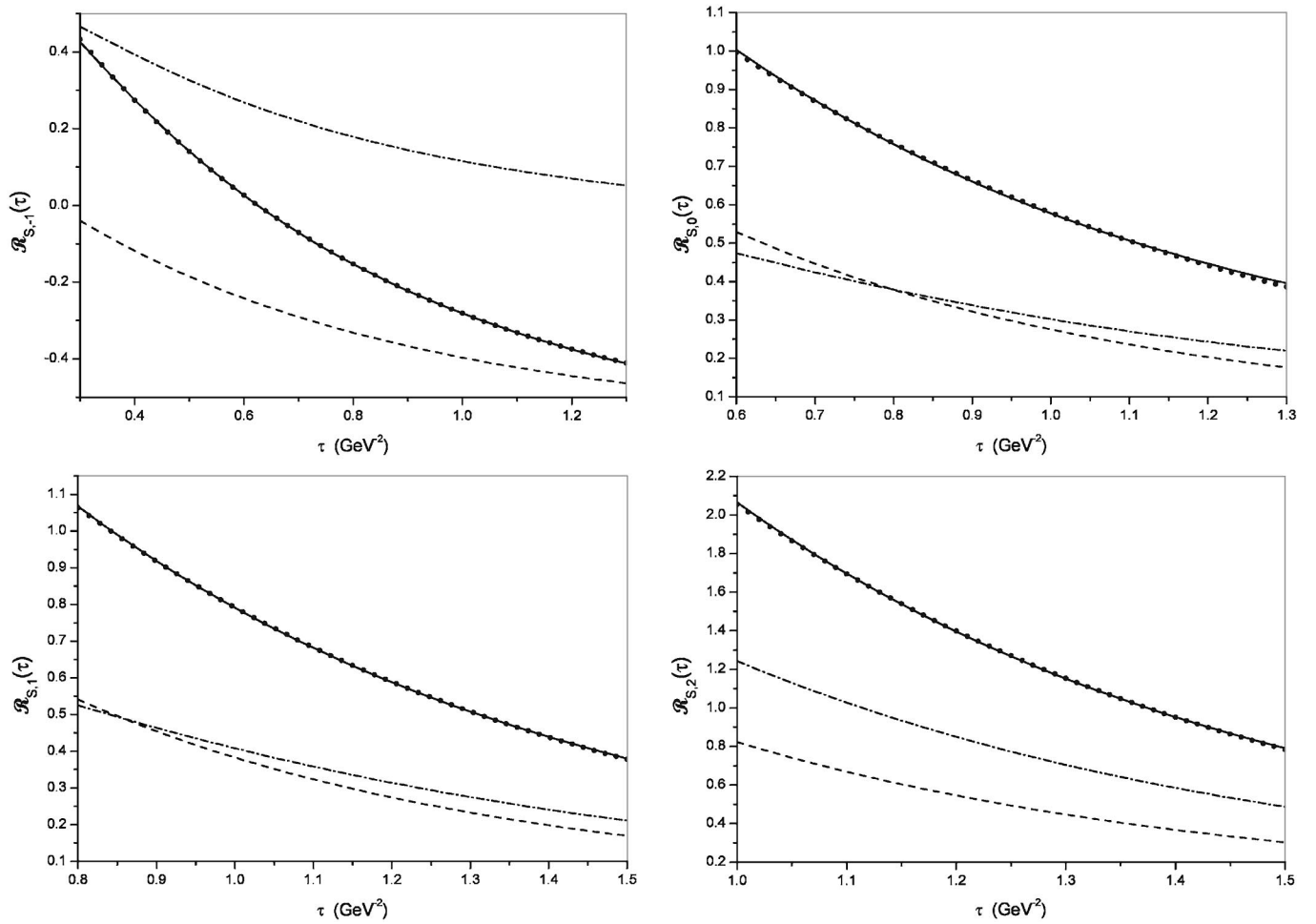| k	$\tau_{\min}$ (GeV^{-2})	$\tau_{\max}$ (GeV^{-2})	m_S (GeV)	f_S (GeV)	$\sqrt{s_0}$ (GeV)	$\delta \times 10^{-3}$
-1	0.3	1.3	1.28	1.02	2.22	1.06
0	0.6	1.3	1.16	1.11	1.75	5.70
1	0.8	1.5	1.22	1.04	1.63	1.63
2	1.0	1.5	1.39	1.01	1.82	2.13

FIG. 7. The individual contributions to the optimized Borel sum rules in the scalar glueball channel: the continuum-subtracted IOPE moments (solid line), the 0^{++} glueball pole (and subtraction constant, for $k = -1$) contributions (bulleted line), the direct instanton contributions (dashed line), and the contributions of the perturbative Wilson coefficients (dashed-dotted line).

Clearly, the overall fit quality is more than satisfactory. As anticipated, there seems to be no need for a second isolated (and rather narrow) resonance. The 3-parameter fits are inside typical errors independent of the starting values and also quite independent of the upper border of the τ domain. (Nevertheless, far-off starting values for the threshold s_0 can significantly slow down the minimization procedure since the s_0 dependence is rather shallow.) The instanton continuum contributions decisively improve the individual and mutual consistency of the sum rules (including the one associated with $\mathcal{R}_{S,-1}$) and of their results. As expected, we find little sensitivity to details of the instanton size distribution as long as its overall scales are kept fixed. The sum rule consistency noticeably worsens, however, when finite-width distributions are used without subtracting the large-ρ contributions.

The $\mathcal{R}_{S,-1}$ sum rule, singled out by the presence of subtraction terms (cf. Sec. VI C), has played a notorious role in previous glueball sum rule analyses and deserves some more specific comments. Since the phenomenologi-

cal subtraction constant is of significant size, the contributions of the perturbative Wilson coefficients alone were unable to generate a glueball mass of more than a few hundred MeV. As explained before, the direct instanton contributions with their large slope (cf. Fig. 7) resolve this problem [13]. The instanton-induced subtraction term, however, is overestimated by the spike approximation to the instanton size distribution: it so strongly overcompensates the phenomenological subtraction constant that the sum rule becomes inconsistent (the matching error increases by about 2 orders of magnitude).[23] As anticipated in Sec. VI C, this problem is resolved by realistic ρ distributions and renormalization of the instanton contributions. Indeed, Fig. 7 shows that the fit quality of the improved $\mathcal{R}_{S,-1}$ sum rule matches that of its higher-

----

[23]The same should probably hold for the corresponding Gaussian sum rule which, perhaps for this reason, was excluded in the analysis of Ref. [16].

moment counterparts, and all sum rules yield mutually consistent predictions for the glueball properties.

The impact of the subtraction constants on the sum rule analysis increases towards larger τ since the dominant τ-dependent contributions decrease. The sum rule fit in Fig. 7 shows that the residual discrepancy between LET- and IOPE-induced subtraction terms can be comfortably compensated by the small condensate contributions which are enhanced in the $k = -1$ sum rule. Even larger discrepancies, encountered, e.g., when using smaller values of the gluon condensate, could be accommodated. The $k = 1$ sum rule would then predict a larger value of s_0 and a marginally larger glueball mass.

In addition to the sum rule fits for the total IOPE Borel moments, Fig. 7 also shows the contributions from perturbative and nonperturbative Wilson coefficients separately. Comparison with the analogous figures in Ref. [13] (based on the spike distribution) confirms the discussion of Sec. VI B: the perturbative contributions are somewhat enhanced by the $O(\alpha_s^2)$ corrections while the direct instanton contributions are significantly reduced in the improved IOPE. (The duality continuum threshold decreases somewhat, too.) As a result, perturbative and nonperturbative coefficients are now of comparable size. Moreover, the slopes of the instanton contributions are reduced. Both effects manifest themselves in a 20% smaller prediction for the scalar glueball mass. However, the about threefold increase of the glueball decay constant f_S predicted in Ref. [13] (relative to previous sum rule analyses) remains intact. This implies that the reduced size of the Borel moments on the left-hand side of the sum rules (28) is compensated by the increased perturbative contributions and, in particular, by the smaller glueball mass factors on the right-hand side.

Our large result for f_S predicts strongly increased partial widths for the radiative decay of the heavy quarkonia J/ψ and Υ (and others) into scalar glueballs and therefore has relevance for experimental glueball searches [85]. In particular, it allows for an improved analysis of the existing $\Upsilon \rightarrow \gamma f_0$ decay data of the CLEO collaboration [86] and the forthcoming larger samples from CLEO-III. It will also be interesting to compare our prediction to the first calculation of f_S on the (quenched) lattice which is in progress [87]. Since f_S is related to the glueball wave function (or Bethe-Salpeter amplitude) at the origin, our large value predicts a strongly concentrated wave function and thus an unusually small size of the scalar glueball. Similar results have been found in the instanton liquid model [15] and on the lattice [14].

Our prediction for the central value of the scalar glueball mass is about 10%–20% smaller than the results of our previous analysis [13] based on the spike distribution, and lies 10%-40% below the quenched lattice results $m_S^{(q)} = 1.4 - 1.8$ GeV [28]. [All raw lattice data agree within statistical errors (about 40 MeV). The much larger range

quoted above reflects the ambiguities in setting the mass scale in the absence of direct experimental input (cf. the talk of Bali under Ref. [43]).] A similar reduction (25%) of the 0^{++} glueball mass was found in unquenched lattice simulations (on still rather small lattices with very limited statistics and quark masses of about 70 MeV) [43], although this might be dominantly a lattice artifact. On general grounds, however, one would expect light-quark effects and quarkonium admixtures to lower the quenched masses at least somewhat. Because of its smaller size, furthermore, the scalar glueball should be particularly susceptible to the momentum dependence of the sea-quark-induced vacuum polarization which modifies the color-dielectric properties of the vacuum at short distances [88]. Since this part of the vacuum polarization is neglected in the quenched approximation, one would expect the quenched mass predictions to be less reliable in the scalar channel. This expectation is supported, e.g., by the recent analysis of the radial excitation and Regge trajectories of the known isoscalar mesons [89], including those newly established by the Crystal Barrel Collaboration in proton-antiproton annihilation. The standard 0^{++} glueball candidates above 1 GeV, i.e., the $f_0(1300)$, $f_0(1500)$, and $f_0(1750)$ resonances, are found to lie solidly on $q\bar{q}$ trajectories and to fit well into a flavor nonet classification. Instead, the K matrix analysis predicts a light and broad scalar glueball state in the 1200–1600 MeV region [89], compatible with our result. An even lighter (and similarly broad) glueball state, centered around 1 GeV or a bit larger, is expected in mixing schemes which assume only one 0^{++} multiplet below 1.8 GeV [90].

The k dependence of our predictions for the scalar glueball properties in Table I shows a certain systematics. While the results for the coupling are practically k independent (within sum rule accuracy), the predictions for the mass increase with k for $k \geq 0$. Since f_S is associated with the integrated strength of the glueball, it enters all sum rules (28) in the same (i.e., k-independent) power. The k dependence of f_S in Table I thus gives an idea of the typical uncertainties of the matching analysis. The variations in the mass predictions, on the other hand, are larger and systematically increase with k. This suggests that the glueball strength is distributed over a rather broad s region: since the higher moments weight the spectral function more strongly at larger s, they will then predict a larger pole mass [cf. Eq. (28)]. (The $k = -1$ sum rule result is not conclusive in this regard since it receives additional contributions from the subtraction terms.) Our predicted mass range can therefore be regarded as a rough lower bound on the width of the scalar glueball, i.e., $\Gamma_S \gtrsim 0.3$ GeV, similar to the width found in the K matrix analysis [89].

The gap Δs between glueball mass and continuum threshold, as defined in Eq. (200), is relatively constant among the $k \geq 0$ sum rule results,

$$\Delta s = 0.5 \pm 0.1 \text{ GeV}, \tag{202}$$

while it is about twice as large in the $k = -1$ sum rule ($\Delta s = 0.94$ GeV), due to the subtraction term. The assumption of a common shift Δs for all sum rules in a simplified analysis (cf. Sec. VI D) would therefore fail in the lowest moment. The relatively early onset of the continuum may indicate, incidentally, that the first excited scalar glueball state lies around 2 GeV. Although the quenched lattice spectrum predicts this excitation well beyond 2 GeV and beyond the lowest 0^{-+} glueball state, its mass might again be lowered by quarkonium admixtures.

We had argued above that the quality of the one-pole sum rule fits leaves little room for physically significant improvement and provides no clear evidence for an additional low-lying resonance with strong coupling to the gluonic interpolating field. Nevertheless, a residual τ dependence of the Borel-moment ratio $m_S^{(2)}$ was found in Sec. VI B, and the fit quality of the $\mathcal{R}_{S,0}$ sum rule is somewhat lower than that of the other ones (cf. Table I and Fig. 7). Since this sum rule is probably most sensitive to low-lying strength, especially at large τ where it would be hidden in $\mathcal{R}_{S,-1}$ by the subtraction constants, it is tempting to attribute its reduced fit quality to some broad, low-lying structure missing on the phenomenological side. Amusingly, this would be consistent with the K matrix analysis of the 0^{++} meson data [89] which tentatively identifies the broad "σ resonance" $f_0(600)$ as a probably gluon-rich exotic state. Alternatively, this trace of low-lying strength might be interpreted as the Goldstone-boson pair continuum since it contributes considerably less strength than the glueball pole.

Unfortunately, a two-resonance analysis of the $\mathcal{R}_{S,0}$ sum rule does not help to settle this issue: due to the high quality of the one-pole fits, it can hardly reduce the deviation measure further and thus becomes unstable. (If nevertheless performed, it seems to favor an only somewhat smaller mass $m_{S1} \sim 0.8$–1.2 GeV of the lowest-lying resonance and a heavier glueball at $m_{S2} \sim 1.8$ GeV.) We conclude that significant low-lying 0^{++} strength with a sufficiently strong coupling to the gluonic interpolator (2), if it exists, is probably too broadly distributed to be resolved by a sum rules analysis.

2. Pseudoscalar glueball

As in the scalar channel, we start by surveying the quantitative behavior of all four sum rules in order to determine how many isolated resonances are required. The result is opposite to that in the scalar channel: all sum rules, especially those derived from the lower Borel moments, clearly favor two resonances, with a large separation between their masses. The improvement over the one-pole fits is substantial. In fact, the latter do not only produce significantly larger errors but also tend to destabilize the sum rules since either the stronger decay at small τ or the weaker one at large τ, but not both, can be matched to one resonance.

The emergence of a second, relatively low-lying isolated resonance is of course expected. In fact, its traces were already visible in the qualitative decay behavior of the Borel moments (cf. Sec. VI B). Moreover, our discussion in Sec. V anticipated the emergence of large η' intermediate-state contributions to the 0^{-+} glueball correlator, as a consequence of the anomaly-induced η' coupling to the topological charge. The results of the quantitative sum rule analysis, listed in Table II, indeed confirm this expectation: the central mass value of the lighter resonance reproduces the η' mass. Our central value for the coupling $f_{\eta'}$ is somewhat larger than its phenomenological value 0.82 GeV [78], likely because of η admixtures. (Note that we treat $f_{\eta'}$ on the same footing as the glueball decay constant, i.e., we do not extract the conventional factor $1/\sqrt{2N_f}$.) In any case, the result for $f_{\eta'}$ is probably our least accurate sum rule prediction since it originates from the small residue of the large-τ tail.

A two-resonance analysis, with five independent hadronic parameters to be determined, generally stretches the sum rule resolution to its limits. In fact, there is no guarantee that such an analysis will be stable. The large separation between the resonance masses in the 0^{-+} channel, however, improves the situation decisively since it assigns mutually almost exclusive roles to the two poles: the heavier 0^{-+} glueball has to fit the small-τ region and consequently decays so fast that it cannot significantly "contaminate" the large-τ tail, which is mostly generated by the η'. This scenario is corroborated by the fact that the predicted η' properties are, in contrast to the glueball properties, almost s_0 independent. A glance at Fig. 4 shows that the small-τ behavior of the moments indeed varies much more strongly with s_0 than the tails. It turns out that the clear mass separation renders the five-parameter fits stable and makes a quantitative sum rule analysis possible.

As another consequence of the large gap between the resonance masses, the relative strength of the η' and glue-

TABLE II. The fiducial domain, fitting error, and predictions of the pseudoscalar glueball sum rule based on the kth Borel moment.

k	$\tau_{\min}$ (GeV^{-2})	$\tau_{\max}$ (GeV^{-2})	$m_{\eta'}$ (GeV)	$f_{\eta'}$ (GeV)	m_P (GeV)	f_P (GeV)	s_0 (GeV^2)	$\delta \times 10^{-3}$
-1	0.2	1.2	0.97	0.88	2.12	0.43	6.79	3.22
0	0.25	1.3	0.81	1.31	2.32	0.76	9.14	3.89
1	0.55	1.4	1.05	0.84	2.08	0.72	6.63	1.59
2	0.55	1.5	1.08	1.10	2.20	0.79	7.31	4.86

ball signals, $\propto (m_{\eta'}/m_P)^{4+2k}$, decreases strongly with k since the Borel moments weight the large-s region of the spectral function by a factor s^k. For this reason, the glueball predictions of the higher-moment sum rules become more stable and the quality of one-pole fits improves with k, reflecting the diminishing impact of the η'. Nevertheless, the one-pole analysis remains inherently unstable since the resonance exponential can either match the IOPE moments at large or small τ, but not over the whole fiducial region. Hence the two-pole fits continue to be superior even for $k = 2$. The impact of the condensate contributions, incidentally, also decreases with k since the higher k moments are obtained by derivatives with respect to $-\tau$ and thus decrease the size of the power corrections at large τ.

The four 0^{-+} sum rule fits are displayed in Fig. 8 and produce the results contained in Table II. Their central values yield the predictions

$$m_P = 2.2 \pm 0.2 \text{ GeV}, \qquad f_P = 0.6 \pm 0.25 \text{ GeV}, \quad (203)$$

$$m_{\eta'} = 0.95 \pm 0.15 \text{ GeV}, \qquad f_{\eta'} = 1.05 \pm 0.25 \text{ GeV}, \tag{204}$$

again including an additional error due to estimated input parameter uncertainties. (One should keep in mind that the η' pole probably receives some strength from η admixtures.) As in the scalar channel, the figures also show the contributions from the perturbative and nonperturbative IOPE coefficients separately.

In the graph for $\mathcal{R}_{P,-1}$, we have additionally plotted the topological charge screening contribution alone (dotted line). Its negative sign is a consequence of the screening-induced subtraction term. Nevertheless, the total nonperturbative unit-operator coefficient (dashed line) is positive, due to the (positive) instanton-induced subtraction term. The balance between these subtraction constants is instrumental in reconciling the $k = -1$ sum rule with the low-energy theorem (14), as argued in Sec. VI C. Without the topological charge screening contributions this sum rule
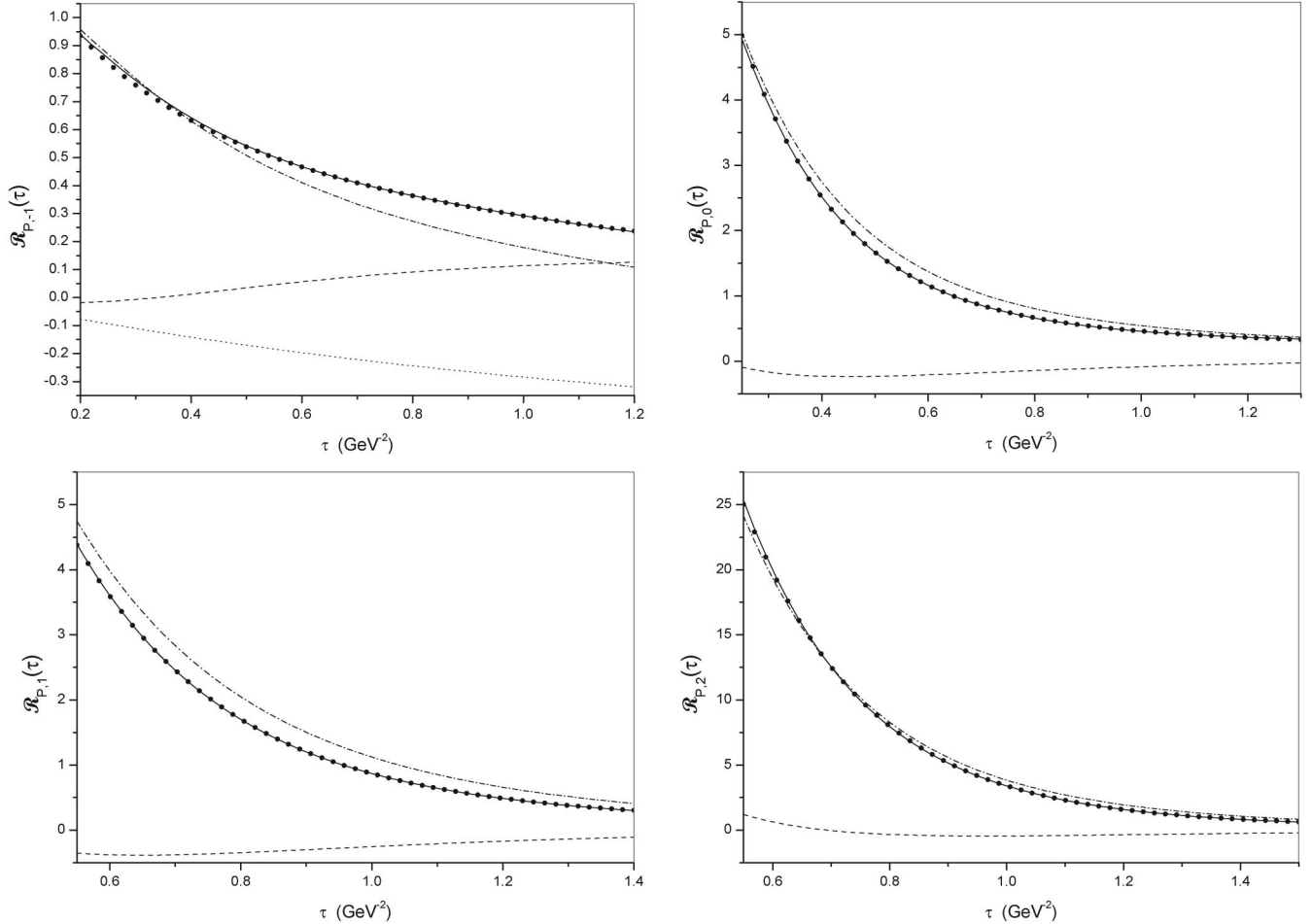

FIG. 8.   The individual contributions to the optimized Borel sum rules in the pseudoscalar glueball channel: the continuum-subtracted IOPE moments (solid line), the 0^{-+} glueball and η' (and subtraction constant, for $k = -1$) contributions (bulleted line), the contributions of the nonperturbative Wilson coefficients (due to both direct instantons and topological charge screening) (dashed line), and the contributions of the perturbative Wilson coefficients (dashed-dotted line). The figure for $k = -1$ additionally shows the screening contributions by themselves (dotted line).

would obviously be inconsistent and impossible to fit. The dependence on the LET parameters (quark masses and condensate), incidentally, is much weaker than in the scalar $k = -1$ sum rule since the phenomenological subtraction constant is an order of magnitude smaller. The cancellation between the individually much larger IOPE contributions is therefore a highly nontrivial consistency requirement of the anomalous axial Ward identity (cf. Sec. V).

In the higher-moment sum rules, the screening contributions remain essential and generate, besides the η' resonance, a clear 0^{-+} glueball signal. The plots of the nonperturbative Wilson coefficients in Fig. 8 contain the cancellations with the direct instanton contributions and demonstrate why it would be detrimental to ignore the topological charge screening contributions (cf. Sec. VI B). The screening contributions affect the behavior of the moments mostly at $\tau > 0.5$ where their impact becomes comparable to that of the perturbative and direct instanton contributions. Positivity violations due to the direct instantons and the dissolution of the glueball signal would manifest themselves in this τ region if the screening contributions were ignored [42].

Despite the larger values of s_0, the size of the direct instanton contributions is not much smaller than in the scalar channel. Our discussion of the finite-width distribution and renormalization effects in the previous section applies to the most part here, too. However, due to the cancellations among the nonperturbative contributions, their overall impact on the pseudoscalar sum rules is much more moderate. [The conventional criterion (198) therefore determines $\tau_{\max}$ only in the $k = 2$ sum rule.] As a consequence, one expects the results to become closer to those of the older 0^{-+} glueball sum rule analyses which neglected nonperturbative Wilson coefficients altogether. Indeed, Ref. [36] found $m_P = 2.3 \pm 0.2$ GeV which is compatible with our result.

Our prediction for the glueball pole residue, however, is about twice as large as the value $f_P = 0.30 \pm 0.05$ GeV of Ref. [36]. This enhancement is due to the remaining non-perturbative contributions, the higher-order perturbative corrections and the additional η' pole. Since f_P is related to the scale of the light-cone distribution amplitude for the pseudoscalar glueball, our result can be used, e.g., to determine the $\gamma\gamma \to G_P \pi^0$ cross section at large momentum transfer [91]. As in the scalar channel, the increased prediction for the coupling f_P and the consequently larger partial width of radiative J/ψ decays into pseudoscalar glueballs [92] are of relevance for experimental glueball searches.

Our prediction for the 0^{-+} glueball mass lies inside the range of quenched lattice results, $m_P^{(q)} = 2.1$–2.5 GeV [28]. (The range of values again reflects scale-setting ambiguities.) Unquenched simulations are still at an exploratory stage, with correspondingly large errors for the higher-lying glueball masses [43]. The pseudoscalar

mass, however, is close to that for the lowest tensor glueball and in the same range as the quenched results. The fact that our prediction for the 0^{-+} glueball mass is close to the quenched lattice results while that for the 0^{++} glueball mass is significantly smaller may be related to the smaller 0^{++} glueball size. Since sea-quark-induced vacuum polarization, which is missing in the quenched approximation, affects mainly the short-distance properties of the glueball wave functionals, one might expect the quenched mass predictions to be subject to larger dynamical-quark corrections in the scalar channel.

The K matrix analysis of Ref. [89] cannot identify narrow-resonance candidates for a 0^{-+} glueball in the above mass range since both $\eta(1295)$ and $\eta(1440)$ are found to lie on linear quark-antiquark trajectories. The Gaussian sum rule analysis of [42] gives an about 20% larger 0^{-+} mass than ours, outside of the range of lattice results. Because of the absence of the crucial screening contributions the underlying IOPE is inconsistent with the axial Ward identity, however, and these results cannot be trusted.

In contrast to the results in the scalar channel, the k dependence of the pseudoscalar glueball mass shows no particular systematics, although the coupling is again practically k independent for $k \geq 0$. It might be tempting to speculate that this implies a less homogeneous distribution of the 0^{-+} glueball strength, perhaps generated by two (or more) neighboring resonances. In any case, it seems that no useful estimate for (or bound on) the width of the pseudoscalar glueball can be delineated from the variation of the pseudoscalar glueball properties with k. (The monotonic increase in the predictions for the η' mass with k, as well as the larger fluctuations in the coupling, are probably due to contaminations by the increasingly dominant glueball signal.)

The derivative of the topological charge correlator at $Q^2 = 0$ has played an important role in the analysis of the proton spin content and the related structure function [34]. The strong cancellations among the nonperturbative contributions to the pseudoscalar IOPE might explain why QCD sum rule estimates of χ' on the basis of purely perturbative Wilson coefficients seem to be sufficiently stable [93]. Nevertheless, this analysis should be repeated on the basis of the full IOPE.

VII. SUMMARY AND CONCLUSIONS

The central themes of this paper are the derivation of nonperturbative short-distance contributions to the spin-0 glueball correlators and a comprehensive sum rule analysis of their predictions for glueball properties. The dominant nonperturbative contributions to the operator product expansion of these correlators turn out to be (semi-) hard, i.e., to reside in the Wilson coefficients. Their soft counterparts, contained in the condensates, play a comparatively minor role. Both sources of hard nonperturbative physics consid-

ered in this paper, direct instantons and topological charge screening, are associated with the topology of the vacuum gluon fields or, equivalently, of the QCD gauge group. The main benefit of analyzing the hard nonperturbative contributions by means of a short-distance expansion is that it allows an analytical and model-independent treatment. The complementary bulk information on the soft physics, which enters through a few condensates and the instanton size distribution, can be straightforwardly imported from other sources.

Direct-instanton contributions to other hadron correlators were calculated previously, and several important effects with diverse physical impact were found in the corresponding QCD sum rules (including those for the 0^{++} glueball). However, their evaluation was restrained by three major approximations: (i) all instantons were taken to be of the same size, (ii) the renormalization of the instanton-induced Wilson coefficients was ignored and (iii) the contributions of only the instanton nearest to the interpolator arguments were taken into account explicitly. The first of these approximations becomes exact in instanton vacuum models at large N_c and the third can be regarded as the leading term in an expansion in the instanton density.

An important point on our agenda was to assess the validity of these approximations and to improve upon them. We have removed restriction (i) by implementing a realistic, finite-width instanton size distribution which incorporates all currently available information on its scales, overall shape, and limiting behavior. To improve upon approximation (ii), we have devised a simple renormalization procedure which explicitly restricts the contributing instantons to the direct ones, i.e., to those which are smaller than the inverse operator scale. These developments are channel independent and will be useful in other hadron correlators as well.

The improvements in the direct instanton sector have several notable effects on the glueball sum rule analysis and its results. Finite-width distributions considerably slow the asymptotic decay of the instanton contributions at large momentum transfer, which reduces the glueball mass predictions. They furthermore resolve artifacts in the IOPE which previously distorted the Borel moments and contaminated the results for the scalar glueball. As an additional benefit, realistic instanton size distributions tend to enlarge the fiducial τ domain of the sum rule analysis. The gauge-invariant renormalization of the instanton-induced Wilson coefficients significantly improves the consistency with the underlying low-energy theorem in the scalar channel—and sum rule consistency in general. Renormalization also reduces the overall size of the instanton contributions. The analysis of the new IOPE sum rules in the scalar glueball channel shows that the impact of the direct instanton contributions is enhanced by the above improvements. The consistency among different Borel moments

and with the low-energy theorem is consolidated and the previously deficient and usually discarded lowest-moment sum rule becomes one of the most reliable.

In the pseudoscalar channel the emerging pattern is more complex: the sum rules with purely perturbative Wilson coefficients are found to be consistent with the corresponding low-energy theorem (which had not been appreciated before since the pertinent $\mathcal{R}_{P,-1}$ sum rule was not analyzed). However, this consistency is lost entirely when direct instanton corrections are included and additional physics, both (semi-) hard and nonperturbative, is needed to restore it.

Our third improvement of the IOPE consists in identifying this missing physics as due to topological charge screening and in implementing the screening contributions. This is our conceptually farthest-reaching extension of the OPE since it introduces for the first time nonperturbative physics beyond single instantons into the IOPE coefficients. This physics turns out to be highly channel selective: it almost exclusively affects the 0^{-+} glueball correlator (and the related η' correlator) which is proportional to the topological charge correlator and thus specifically tuned to those light-quark-induced correlations which produce topological charge screening. Under the suggestive (but not necessary) assumption that the topological vacuum charge is mostly due to instantons, the implementation of its screening can be regarded as an improvement upon approximation (iii) mentioned above: the small instanton packing fraction does not suppress the exceptionally strong and short-ranged correlations between opposite topological charges as strongly as others. Therefore, in this specific case the nearest-instanton approximation is insufficient and the screening corrections have to be added in the 0^{-+} glueball (and η') channel.

We have found compelling evidence for the screening contributions to be an indispensable complement to the direct instanton contributions. They restore consistency with the axial Ward identity and thereby overcome, in particular, the above-mentioned problem with the low-energy theorem. This manifests itself, e.g., in the screening contribution to the subtraction constant in the lowest-moment sum rule which cancel most of the direct instanton contribution. In the chiral limit, this cancellation becomes exact. It also explains in a natural way how the equal size of the instanton-induced subtraction constants in both spin-0 glueball channels can be reconciled with the order-of-magnitude difference in the sizes of their phenomenological counterparts. (In the absence of light quarks this difference would practically disappear together with the screening contributions, so that the sum rules would remain intact.)

The topological charge screening corrections lead to the emergence of a strong η' resonance signal and necessitate a two-resonance analysis of the 0^{-+} sum rules. Remarkably, the large gap between the η' and 0^{-+} glueball

masses allows for a simultaneous prediction of all associated resonance and threshold parameters. The impact of the direct instanton contributions differs strongly in both spin-0 glueball channels. In addition to their opposite sign (a consequence of the instanton's self-dual field strength), the larger continuum threshold and the strong cancellations with the screening corrections drastically modify the role of the instantons in the 0^{-+} channel and counterbalance their repulsion. In fact, ignoring the screening contributions would, besides violating the anomalous Ward identity, lead to spectral positivity violations and the disappearance of the 0^{-+} glueball signal. Pseudoscalar glueball sum rules with unscreened direct instanton contributions are therefore invalid.

Our comprehensive numerical analysis of all eight Borel sum rules in both spin-0 glueball channels reveals a rather diverse pattern of glueball properties. The hard topological physics in the IOPE coefficients turns out to strongly affect the sum rule results and to generate several new predictions. In the scalar channel, the improved treatment of the direct instanton sector reduces our earlier (spike distribution based) result for the 0^{++} glueball mass by about 20%, to $m_S = 1.25 \pm 0.2$ GeV. Although still consistent within errors, our new central mass prediction is smaller than the quenched lattice result. However, light-quark effects and especially quarkonium admixtures are expected to reduce the quenched masses, and the first unquenched simulations indeed show a tendency towards smaller scalar glueball masses. Moreover, our mass prediction is consistent with the broad glueball state found in a recent K matrix analysis of the scalar meson spectrum which includes the new states recently identified in the Crystal Barrel data. The systematics in our results from different Borel-moment sum rules indicates a rather large width of the scalar glueball, $\Gamma_S \gtrsim 0.3$ GeV. A similarly large width is found in K matrix and mixing analyses and could also be expected from unquenched lattice simulations with realistic quark masses, due to the increased number of open decay channels.

Our prediction for the glueball decay constant $f_S = 1.05 \pm 0.1$ GeV is several times larger than the value obtained when ignoring the nonperturbative Wilson coefficients. This result implies an exceptionally small glueball size, in agreement with some lattice and instanton liquid model evidence. The strong concentration of the 0^{++} glueball (Bethe-Salpeter) wave function is therefore at least partially explained by the strong instanton-induced attraction between gluons in the scalar channel. Moreover, its small size makes the scalar glueball more susceptible to the momentum dependence of the color-dielectric constant arising from sea quarks. Since this part of the vacuum polarization is missing in the quenched approximation, one would expect larger errors in the quenched predictions for the 0^{++} glueball properties than for their 0^{-+} counterparts. This might explain why our mass prediction deviates more strongly from the quenched results in the scalar

channel. Furthermore, our enhanced prediction for f_S implies substantially larger partial widths of radiative J/ψ and Υ decays into scalar glueballs. It is therefore of importance for experimental glueball searches, especially for the interpretation of the recent CLEO and forthcoming CLEO-III data on $\Upsilon \to \gamma f_0$ and other decay branches, and for related measurements of scalar glueball properties.

Although hints of some gluon-rich spectral strength in the 0^{++} channel well below 1 GeV can be detected in the sum rule analysis, we find no clear evidence for a low-lying and sufficiently narrow glueball resonance in the region of the $f_0(600)$. (The $\mathcal{R}_{S,-1}$ sum rule would "predict" a spurious low-lying resonance if the direct instanton contributions were ignored. However, this result is inconsistent with both the low-energy theorem and the higher-moment sum rules and therefore obsolete.)

In the pseudoscalar glueball channel, the topological charge screening contributions do not only resurrect the sum rules but also have a strong impact on their quantitative predictions. Because of the cancellations with the direct instanton contributions, the overall size of the nonperturbative IOPE coefficients remains below about 20% of their perturbative counterparts and the detrimental problems encountered when ignoring the screening contributions are resolved. Although the origin of the individual nonperturbative contributions is more diverse and complex than in the scalar channel, their overall impact is therefore smaller. This is one of the reasons for the considerably weaker binding of the 0^{-+} glueball. Nevertheless, the hard nonperturbative contributions modify qualitative features of the 0^{-+} Borel moments to which the matching analysis is particularly sensitive, and they are vital for achieving consistency among all moment sum rules and with the axial anomaly. The strong cancellations among the nonperturbative contributions to the pseudoscalar IOPE may also explain why QCD sum rule estimates of the derivative of the topological susceptibility, which plays an important role in the analysis of the proton spin content, seem to be sufficiently consistent without nonperturbative Wilson coefficients. Their reanalysis on the basis of the full IOPE is in progress.

The quantitative sum rule analysis results in the values $m_P = 2.2 \pm 0.2$ GeV for the pseudoscalar glueball mass and $f_P = 0.6 \pm 0.25$ GeV for the decay constant. Our mass prediction lies inside the range obtained from quenched and unquenched lattice data. The coupling is again enhanced by the nonperturbative Wilson coefficients, but less strongly than in the scalar channel. The consequently larger partial width of radiative quarkonium decays into pseudoscalar glueballs and the enhanced $\gamma\gamma \to G_P \pi^0$ cross section at high momentum transfers will be relevant for the experimental identification of the lowest-lying 0^{-+} glueball and help in measuring its properties.

Our extended IOPE should be useful for the calculation of other spin-0 glueball properties as well. Quantitative

estimates of the already mentioned production rates in gluon-rich channels (including J/ψ and Υ decays) and characteristic glueball decay properties and signatures, including $\gamma\gamma$ couplings, OZI suppression, and branching fractions incompatible with $q\bar{q}$ decay, would be particularly interesting.

APPENDIX A: BOREL MOMENTS FROM PERTURBATIVE WILSON COEFFICIENTS

In this appendix we list the contributions from the perturbative OPE coefficients to the Borel moments $\mathcal{L}_k(\tau, s_0)$ with $k \in \{-1, 0, 1, 2\}$ for both spin-0 glueball correlators (before RG improvement). In terms of the continuum factors ρ_k and the exponential integral E_1, defined as

$$\rho_k(x) = e^{-x} \sum_{n=0}^{k} \frac{x^n}{n!}, \tag{A1}$$

$$E_1(x) = \int_1^{\infty} dt \frac{e^{-xt}}{t}, \tag{A2}$$

one obtains ($\gamma = 0.5772$ is Euler's constant and the coefficients $A_i - D_i$ are given in Sec. III A)

$$\mathcal{L}_{G,-1}^{(pc)}(\tau, s_0) = -\frac{A_0}{\tau^2}[1 - \rho_1(s_0\tau)] + \frac{2A_1}{\tau^2}\left[\ln(\tau\mu^2) + \gamma - 1 + E_1(s_0\tau) + e^{-\tau s_0} + \ln\left(\frac{s_0}{\mu^2}\right)\rho_1(s_0\tau)\right] - B_0 + B_1[\ln(\tau\mu^2)$$
$$+ \gamma + E_1(s_0\tau)] - C_0\tau + C_1\tau\left[\ln(\tau\mu^2) + \gamma - 1 - \frac{e^{-\tau s_0}}{\tau s_0} + E_1(s_0\tau)\right] - \frac{D_0}{2}\tau^2, \tag{A3}$$

$$\mathcal{L}_{G,0}^{(pc)}(\tau, s_0) = -\frac{2A_0}{\tau^3}[1 - \rho_2(s_0\tau)] + \frac{4A_1}{\tau^3}\left[\ln(\tau\mu^2) + \gamma - \frac{3}{2} + E_1(s_0\tau) + \rho_0(s_0\tau) + \frac{1}{2}\rho_1(s_0\tau) + \ln\left(\frac{s_0}{\mu^2}\right)\rho_2(s_0\tau)\right]$$
$$- \frac{B_1}{\tau}[1 - \rho_0(s_0\tau)] + C_0 - C_1[\ln(\tau\mu^2) + \gamma + E_1(s_0\tau)] + D_0\tau, \tag{A4}$$

$$\mathcal{L}_{G,1}^{(pc)}(\tau, s_0) = -\frac{6A_0}{\tau^4}[1 - \rho_3(s_0\tau)] + \frac{12A_1}{\tau^4}\left[\ln(\tau\mu^2) + \gamma - \frac{11}{6} + E_1(s_0\tau) + \rho_0(s_0\tau) + \frac{1}{2}\rho_1(s_0\tau) + \frac{1}{3}\rho_2(s_0\tau)\right.$$
$$\left. + \ln\left(\frac{s_0}{\mu^2}\right)\rho_3(s_0\tau)\right] - \frac{B_1}{\tau^2}[1 - \rho_1(s_0\tau)] + \frac{C_1}{\tau}[1 - \rho_0(s_0\tau)] - D_0, \tag{A5}$$

$$\mathcal{L}_{G,2}^{(pc)}(\tau, s_0) = -\frac{24A_0}{\tau^5}[1 - \rho_4(s_0\tau)] + \frac{48A_1}{\tau^5}\left[\ln(\tau\mu^2) + \gamma - \frac{25}{12} + E_1(s_0\tau) + \rho_0(s_0\tau) + \frac{1}{2}\rho_1(s_0\tau) + \frac{1}{3}\rho_2(s_0\tau)\right.$$
$$\left. + \frac{1}{4}\rho_3(s_0\tau) + \ln\left(\frac{s_0}{\mu^2}\right)\rho_4(s_0\tau)\right] - \frac{2B_1}{\tau^3}[1 - \rho_2(s_0\tau)] + \frac{C_1}{\tau^2}[1 - \rho_1(s_0\tau)]. \tag{A6}$$

APPENDIX B: INSTANTON INTEGRALS

An explicit expression for $\Pi_S^{(I+\bar{I})}(x^2)$ can be obtained by Fourier transforming its dispersive representation (118):

$$\Pi_S^{(I+\bar{I})}(x^2) = \int \frac{d^4Q}{(2\pi)^4} e^{-iQx} \Pi^{(I+\bar{I})}(Q^2) = \frac{1}{\pi} \int_0^{\infty} ds \text{Im}\Pi^{(I+\bar{I})}(-s) \int \frac{d^4Q}{(2\pi)^4} \frac{e^{-iQx}}{s + Q^2} \tag{B1}$$

$$= \frac{1}{4\pi^3} \frac{1}{x} \int_0^{\infty} ds \text{Im}\Pi^{(I+\bar{I})}(-s)\sqrt{s}K_1(\sqrt{s}x) \tag{B2}$$

$$= -4\pi \int d\rho n(\rho)\rho^4 \frac{1}{x} \int_0^{\infty} ds s^{5/2} J_2(\sqrt{s}\rho)Y_2(\sqrt{s}\rho)K_1(\sqrt{s}x) \tag{B3}$$

$$= \frac{2^8 3}{7} \int d\rho \frac{n(\rho)}{\rho^4} {}_2F_1\left(4, 6, \frac{9}{2}, -\frac{x^2}{4\rho^2}\right), \tag{B4}$$

as anticipated in Eq. (92). The hypergeometric function $_2F_1(a, b, c, z)$ [54,57] is defined as the analytical continuation of Gauß's hypergeometric series (except if c is a nonpositive integer $-n$ and neither b nor a equal an integer $-m$ with $m < n$)

$$_2F_1(a, b, c, z) = \frac{\Gamma(c)}{\Gamma(a)\Gamma(b)} \sum_{n=0}^{\infty} \frac{\Gamma(a + n)\Gamma(b + n)}{\Gamma(c + n)} \frac{z^n}{n!}. \tag{B5}$$

For convenience, we recall the limits

$$_2F_1\left(4, 6, \frac{9}{2}, -\frac{x^2}{4\rho^2}\right) \rightarrow \begin{cases} 1 - \frac{4}{3}\frac{x^2}{\rho^2} + O\left(\left(\frac{x^2}{\rho^2}\right)^2\right) & \text{for } x^2 \ll \rho^2 \\ 14\left(\frac{\rho^2}{x^2}\right)^4 + O\left(\left(\frac{\rho^2}{x^2}\right)^5\right) & \text{for } \rho^2 \ll x^2 \end{cases}, \tag{B6}$$

which imply, in particular,

$$\Pi_S^{(I+\bar{I})}(x^2 = 0) = \frac{2^8 3}{7} \int d\rho \frac{n(\rho)}{\rho^4}. \tag{B7}$$

The integral (B1) can alternatively be done by several other methods, e.g., by introducing Feynman parameters, which leads to [9]

$$\Pi_S^{(I+\bar{I})}(x^2) = -2^{11} \int d\rho n(\rho)\rho^8 \left(\frac{\partial}{\partial x^2}\right)^3 \frac{\xi^6}{x^6}\left[\frac{3}{\xi} \text{arctanh}(\xi)\right.$$
$$\left. + \frac{5 - 3\xi^2}{(1 - \xi^2)^2}\right] \text{ where } \xi^2 = \frac{x^2}{x^2 + 4\rho^2}, \tag{B8}$$

but is generally less convenient for practical calculations and for the study of analyticity properties.

A straightforward way to calculate the Fourier transform of $\Pi_G^{(I+\bar{I})}(x^2)$ starts from the original integral

$$\Pi_S^{(I+\bar{I})}(x^2) = \frac{2^9 3^2}{\pi^2} \int d\rho n(\rho)$$
$$\times \int d^4 x_0 \frac{\rho^8}{[(x - x_0)^2 + \rho^2]^4[x_0^2 + \rho^2]^4}, \tag{B9}$$

and makes use of the fact that (in Euclidean space-time)

$$\Pi_S^{(I+\bar{I})}(Q^2) = \frac{2^9 3^2}{\pi^2} \int d\rho n(\rho) \int d^4 x e^{iQx}$$
$$\times \int d^4 x_0 \frac{\rho^8}{[(x - x_0)^2 + \rho^2]^4[x_0^2 + \rho^2]^4} \tag{B10}$$

$$= \frac{2^9 3^2}{\pi^2} \int d\rho n(\rho) \left(\int d^4 x e^{iQx} \frac{\rho^4}{(x^2 + \rho^2)^4}\right)^2. \tag{B11}$$

With

$$\int d^4 x \frac{e^{iQx}}{(x^2 + \rho^2)^4} = \frac{4\pi^2}{Q} \int_0^{\infty} dx \frac{x^2 J_1(Qx)}{(x^2 + \rho^2)^4}$$
$$= \frac{\pi^2}{12} \frac{Q^2}{\rho^2} K_2(Q\rho), \tag{B12}$$

one then immediately obtains

$$\Pi_G^{(I+\bar{I})}(Q^2) = 2^5 \pi^2 \int d\rho n(\rho)(\rho Q)^4 K_2^2(Q\rho). \tag{B13}$$

In order to perform the Borel transform of (B13), it is convenient to start from an integral representation ([57], Eq. 8.486.15) for the McDonald function,

$$Q^2 K_2(Q\rho) = 2\rho^2 \int_0^{\infty} d\alpha \alpha e^{-(Q^2/4\alpha) - \alpha\rho^2}. \tag{B14}$$

For the calculation of the lowest ($k = -1$) Borel moment we then write

$$\frac{\Pi_S^{(I+\bar{I})}(Q^2)}{-Q^2} = -2^5 \pi^2 \int d\rho n(\rho)\rho^4 Q^2 K_2^2(Q\rho) \tag{B15}$$

$$= -2^7 \pi^2 \int d\rho n(\rho)\rho^8 \int_0^{\infty} d\alpha \alpha \int_0^{\infty} d\beta \beta$$
$$\times \int_0^{\infty} d\gamma e^{-(Q^2/4)[(1/\alpha) + (1/\beta) + 4\gamma] - (\alpha + \beta)\rho^2}, \tag{B16}$$

and make use of

$$\hat{B}e^{-aQ^2} = \delta(a - \tau), \tag{B17}$$

to obtain

$$\mathcal{L}_{-1}^{(I+\bar{I})}(\tau) = \hat{B}\left[\frac{\Pi_S^{(I+\bar{I})}(Q^2)}{-Q^2}\right] \tag{B18}$$

$$= -2^7 \pi^2 \int d\rho n(\rho)\rho^8 \int_0^{\infty} d\alpha \alpha \int_0^{\infty} d\beta \beta$$
$$\times \int_0^{\infty} d\gamma e^{-(\alpha + \beta)\rho^2} \delta\left(\frac{\alpha + \beta}{4\alpha\beta} + \gamma - \tau\right). \tag{B19}$$

The three remaining parameter integrals are elementary. Their evaluation leads to

$$\mathcal{L}_{-1}^{(I+\bar{I})}(\tau) = -2^6 \pi^2 \int d\rho n(\rho)\xi^2 e^{-\xi}\left[(1 + \xi)K_0(\xi)\right.$$
$$\left. + \left(2 + \xi + \frac{2}{\xi}\right)K_1(\xi)\right], \tag{B20}$$

where we have defined the dimensionless variable

$$\xi = \frac{\rho^2}{2\tau}. \tag{B21}$$

The higher moments with $k \geq -1$ follow, as previously, by differentiation with respect to $-\tau$,

$$\mathcal{L}_{k+1}^{(I+\bar{I})}(\tau) = -\frac{\partial}{\partial \tau} \mathcal{L}_{k}^{(I+\bar{I})}(\tau), \tag{B22}$$

and generate the expressions (107)–(109).

---

[1] M. Gell-Mann, Acta Phys. Austriaca Suppl. **9**, 733 (1972); H. Fritzsch and M. Gell-Mann, ''Proceedings of the Sixteenth International Conference on High-Energy Physics, Chicago, 1972,'' Vol. 2, p. 135.

[2] For recent reviews see, e.g., M. R. Pennington, hep-ph/9811276; W. Toki, in *Proceedings of BNL Workshop on Glueballs, Hybrids and Exotic Hadrons, New York, 1988*, edited by Suh-urk Chung AIP Conf. Proc. No. 185 (AIP, New York, 1989) p. 692; S. Spanier, Phys. At. Nucl. **59**, 1291 (1996); Yad. Fiz. **59**, 1352 (1996).

[3] Review of Particle Properties, K. Hagiwara *et al.*, Phys. Rev. D **66**, 010001 (2002).

[4] K. G. Wilson, Phys. Rev. **179**, 1499 (1969).

[5] V. A. Novikov, M. A. Shifman, A. I. Vainsthein, and V. I. Zakharov, Phys. Lett. **86B**, 347 (1979); Nucl. Phys. **B165**, 55 (1980).

[6] V. A. Novikov, M. A. Shifman, A. I. Vainsthein, and V. I. Zakharov, Nucl. Phys. **B165**, 67 (1980).

[7] S. Narison, Nucl. Phys. **B509**, 312 (1998).

[8] V. A. Novikov, M. A. Shifman, A. I. Vainsthein, and V. I. Zakharov, Nucl. Phys. **B191**, 301 (1981).

[9] T. Schaefer and E. V. Shuryak, Rev. Mod. Phys. **70**, 323 (1998); D. I. Diakonov, Prog. Part. Nucl. Phys. **51**, 173 (2003). For an elementary introduction to instantons see H. Forkel, hep-ph/0009136.

[10] E. V. Shuryak, Nucl. Phys. **B203**, 116 (1982).

[11] T. DeGrand and A. Hasenfratz, Phys. Rev. D **64**, 034512 (2001); M. G. Perez, O. Philipsen, and I.-O. Stamatescu, Nucl. Phys. **B551**, 293 (1999); D. A. Smith and M. Teper, Phys. Rev. D **58**, 014505 (1998); A. Hasenfratz and C. Nieter, Phys. Lett. B **439**, 366 (1998); P. de Forcrand, M. G. Perez, and I.-O. Stamatescu, Nucl. Phys. **B499**, 409 (1997); R. C. Brower, T. L. Ivanenko, J. W. Negele, and K. N. Orginos, Nucl. Phys. B, Proc. Suppl. **53**, 547 (1997).

[12] A. Ringwald and F. Schremmp, Phys. Lett. B **459**, 249 (1999).

[13] H. Forkel, Phys. Rev. D **64**, 034015 (2001).

[14] N. Ishii, H. Suganuma, and H. Matsufuru, Phys. Rev. D **66**, 94506 (2002); P. de Forcrand and K.-F. Liu, Phys. Rev. Lett. **69**, 245 (1992); R. Gupta *et al.*, Phys. Rev. D **43**, 2301 (1991).

[15] T. Schaefer and E. V. Shuryak, Phys. Rev. Lett. **75**, 1707 (1995).

[16] D. Harnett and T. G. Steele, Nucl. Phys. **A695**, 205 (2001).

[17] H. Forkel and M. K. Banerjee, Phys. Rev. Lett. **71**, 484 (1993).

[18] P. Di Vecchia and G. Veneziano, Nucl. Phys. **B171**, 253 (1980); see also K. Kawarabayashi and N. Ohta, Nucl. Phys. **B175**, 477 (1980).

[19] V. A. Novikov, M. A. Shifman, A. I. Vainshtein, and V. I. Zakharov, Nucl. Phys. **B191**, 301 (1981); M. A. Shifman, Phys. Rep. **209**, 341 (1991).

[20] I. Halperin and A. Zhitnitski, Mod. Phys. Lett. A **13**, 1955 (1998).

[21] M. A. Shifman, A. I. Vainshtein, and V. I. Zakharov, Nucl. Phys. **B166**, 493 (1980); H. Leutwyler and A. Smilga, Phys. Rev. D **46**, 5607 (1992); for two degenerate flavors see also R. J. Crewther, Phys. Lett. **70B**, 349 (1977).

[22] G. 't Hooft, Phys. Rev. Lett. **37**, 8 (1976); Phys. Rev. D **14**, 3432 (1976); **18**, 2199(E) (1978).

[23] E. V. Shuryak, Rev. Mod. Phys. **65**, 1 (1993).

[24] H. Forkel, *Instantons, OPE and Hadron Structure*, (to be published).

[25] H. Forkel and K. Schwenzer, Phys. Rev. C **67**, 035205 (2003).

[26] C. A. Dominguez and N. Paver, Z. Phys. C **31**, 591 (1986); **32**, 391 (1986).

[27] V. A. Novikov, M. A. Shifman, A. I. Vainshtein, and V. I. Zakharov, Nucl. Phys. **B174**, 378 (1980).

[28] W. Lee and D. Weingarten, Phys. Rev. D **61**, 014015 (2000); C. Morningstar and M. Peardon, Phys. Rev. D **60**, 034509 (1999).

[29] M. C. Chu, J. M. Grandy, S. Huang, and J. W. Negele, Phys. Rev. D **48**, 3340 (1993).

[30] S. J. Hands, P. W. Stephenson, and A. McKerrell, Phys. Rev. D **51**, 6394 (1995).

[31] M. A. Shifman, A. I. Vainshtein, and V. I. Zakharov, Nucl. Phys. **B147**, 385 (1979).

[32] M. Shifman, Z. Phys. C **9**, 347 (1981).

[33] V. M. Belyaev and B. L. Ioffe, Sov. Phys. JETP **56**, 493 (1982).

[34] G. M. Shore and G. Veneziano, Nucl. Phys. **B381**, 23 (1992).

[35] B. Chibisov, R. D. Dikeman, M. A. Shifman, and N. Uraltsev, Int. J. Mod. Phys. A **12**, 2075 (1997).

[36] D. Asner, R. B. Mann, J. L. Murison, and T. G. Steele, Phys. Lett. B **296**, 171 (1992).

[37] S. Narison, N. Pak, and N. Paver, Phys. Lett. **147B**, 162 (1984).

[38] K. G. Chetyrkin, B. A. Kniehl, and M. Steinhauser, Phys. Rev. Lett. **79**, 2184 (1997).

[39] E. Bagan and T. G. Steele, Phys. Lett. B **234**, 135 (1990); **243**, 413 (1990).

[40] A. I. Kataev, N. V. Krasnikov, and A. A. Pivovarov, Nucl. Phys. **B198**, 508 (1982).

[41] A. I. Kataev, N. V. KrasnikovA. A. Pivovarov, Nucl. Phys. **B490**, 505(E) (1997).

[42] A. Zhang and T. G. Steele, Nucl. Phys. **A728**, 165 (2003).

[43] A. Hart and M. Teper, Phys. Rev. D **65,** , 034502 (2002); G. Bali, hep-ph/0110254; SESAM-TxL Collaborations, G. Bali *et al.*, Phys. Rev. D **62**, 054503 (2000).

[44] H. Forkel and M. Nielsen, Phys. Rev. D **55,**, 1471 (1997); M. Aw, M. K. Banerjee, and H. Forkel, Phys. Lett. B **454,**, 147 (1999).

[45] A. A. Belavin *et al.*, Phys. Lett. **59B**, 85 (1975).

[46] A. E. Dorokhov, S. V. Esaybegyan, N. I. Kochelev, and N. G. Stefanis, J. Phys. G **23**, 643 (1997).

[47] M. Garcia Perez, T. Kovacs, and P. van Baal, Phys. Lett. B **472**, 295 (2000).

[48] C. G. Callen Jr., R. Dashen, and D. J. Gross, Phys. Rev. D **17**, 2717 (1978).

[49] E. M. Ilgenfritz and M. Müller-Preussker, Nucl. Phys. **B184**, 443 (1981).

[50] D. I. Diakonov and V. I. Petrov, Nucl. Phys. **B245**, 259 (1984).

[51] C. Kamp and G. Münster, Eur. Phys. J. C **17**, 447 (2000).

[52] E. V. Shuryak, hep-ph/9909458.

[53] L. S. Brown, R. D. Carlitz, D. B. Creamer, and C. Lee, Phys. Rev. D **17**, 1583 (1978).

[54] M. Abramowitz and I. A. Stegun, *Handbook of Mathematical Functions*, National Bureau of Standards' Applied Mathematics Series—55, (U.S. GPO, Washington, DC, 1972).

[55] H. Forkel, hep-ph/0112357.

[56] E. V. Shuryak, Nucl. Phys. **B214**, 237 (1983); H. Forkel and M. Nielsen, Phys. Lett. B **345,**, 55 (1995).

[57] I. S. Gradshteyn and I. M. Ryzhik, *Table of Integrals, Series and Products*, (Academic Press, New York, 1965).

[58] A. B. Migdal, *Qualitative Methods in Quantum Theory*, (Benjamin, Reading, 1977).

[59] V. A. Novikov, M. A. Shifman, A. I. Vainshtein, and V. I. Zakharov, Nucl. Phys. **B249**, 445 (1985).

[60] M. Beneke, Phys. Rep. **317**, 1 (1999).

[61] A. V. Smilga, Yad. Fiz. **35**, 473 (1982) [Sov. J. Nucl. Phys. **35**, 271 (1982)]; B. L. Ioffe and A. V. Smilga, Nucl. Phys. **B232**, 109 (1984); S. L. Wilson, J. Pasupathy, and C. B. Chiu, Phys. Rev. D **36**, 1451 (1987).

[62] M. S. Dubovikov and A. V. Smilga, Nucl. Phys. **B185**, 109 (1981).

[63] S. Moch, A. Ringwald, and F. Schrempp, Nucl. Phys. **B507**, 134 (1997).

[64] Ph. Boucaud, F. De Soto, A. Donini, J. P. Leroy, A. Le Yaouanc, J. Micheli, H. Moutarde, O. Pène, and J. Rodríquez-Quintero, Nucl. Phys.B, Proc. Suppl. **114**, 117 (2003).

[65] S. Kovacs, Nucl. Phys. **B684**, 3 (2004).

[66] S. L. Adler, Phys. Rev. **177**, 2426 (1969); J. S. Bell and R. Jackiw, Nuovo Cimento A **60**, 47 (1967);

[67] M. Teper, Nucl. Phys. B, Proc. Suppl. **83**, 146 (2000).

[68] P. W. Debye and E. Hückel, Phys. Z. Sowjetunion **24**, 185 (1923).

[69] G. 't Hooft, Phys. Rep. **142**, 357 (1986).

[70] N. J. Dowrick and N. A. McDougall, Phys. Lett. B **285**, 269 (1992); see also S. Samuel, Mod. Phys. Lett. A **7**, 2007 (1992).

[71] H. Kikuchi and J. Wudka, Phys. Lett. B **284**, 111 (1992).

[72] E. V. Shuryak and J. J. M. Verbaarschot, Phys. Rev. D **52**, 295 (1995).

[73] M.-C. Chu, S. M. Ouellette, S. Schramm, and R. Seki, Phys. Rev. D **62**, 094508 (2000).

[74] A. Hasenfratz, Phys. Lett. B **476**, 188 (2000).

[75] P. Faccioli and T. A. DeGrand, Phys. Rev. Lett. **91**, 182 001 (2003).

[76] T. Schäfer and E. V. Shuryak, Phys. Rev. D **54**, 1099 (1996).

[77] A. M. Polyakov, Nucl. Phys. **B120**, 429 (1977).

[78] T. Feldmann, Int. J. Mod. Phys. A **15**, 159 (2000).

[79] H. Panagopoulos and E. Vicari, Nucl. Phys. **B332**, 261 (1990); A. DiGiacomo, K. Fabricius, and G. Paffuti, Phys. Lett. **118B**, 129 (1982).

[80] E. Witten, Nucl. Phys. **B156**, 269 (1979); G. Veneziano, Nucl. Phys. **B159**, 213 (1979).

[81] D. Harnett, T. G. Steele, and V. Elias, Nucl. Phys. **A686**, 393 (2001).

[82] M. A. Shifman, in *Particles, Strings and Cosmology*, edited by J. Bagger *et al.*, (World Scientific, Singapore 1996).

[83] M. A. Shifman, Prog. Theor. Phys. Suppl. **131**, 1 (1998);

[84] A. Vainshtein, in *Handbook of QCD*, edited by M. Shifman, (World Scientific, Singapore 2002).

[85] M. B. Cakir and G. R. Farrar, Phys. Rev. D **50**, 3268 (1994).

[86] CLEO Collaboration, A. Anastassov *et al.*, Phys. Rev. Lett. **82**, 286 (1999); S. Richichi *et al.*, *ibid.***87**, 141 801 (2001); G. Masek *et al.*, Phys. Rev. D **65**, 072002 (2002).

[87] Y. Chen *et al.*, Nucl. Phys. B, Proc. Suppl. **129**, 203 (2004).

[88] D. Weingarten, Phys. Lett. **109B**, 57 (1982).

[89] V. V. Anisovich, AIP Conf. Proc. **717**, 441 (2004).

[90] W. Ochs, AIP Conf. Proc. **717**, 295 (2004).

[91] K. Passek-Kumericki, Fiz. B **13**, 513 (2004); A. B. Wakely and C. E. Carlson, Phys. Rev. D **45**, 338 (1992); Phys. Rev. D **45**, 1796 (1992).

[92] G. J. Gounaris, R. Kogerler, and J. E. Paschalis, Phys. Lett. **186B**, 107 (1987).

[93] G. M. Shore, S. Narison, and G. Veneziano, Nucl. Phys. **B546**, 235 (1999).